

NATIONAL ACADEMY OF SCIENCES  
NATIONAL RESEARCH COUNCIL

of the

UNITED STATES OF AMERICA  
UNITED STATES NATIONAL COMMITTEE

International Union of Radio Science



**1975 Meeting**  
**June 3-5**

Held Jointly With The  
Institute of Electrical and Electronics Engineers  
Antennas and Propagation Society

University of Illinois  
at Urbana-Champaign  
Urbana, IL 61801

1975 Meeting  
Condensed Program

Monday June 2

0900-1210	II-1	EM Propagation in the Earth	136P
1400-1700	II-2	EM Propagation in Random Media	158P

Tuesday June 3

0900-1130	Joint	Special AP-S/URSI Session	141P
0900-1150	VI-2	Optics	143P
1200		Lunch, Holography Demonstration	Illini Rm. A,B
1400-1710	I-2	Measurement I	198CSL
	II-3	Radio Oceanography	158P
	III-1	General Topics in Ionospheric Radio	144P
	VI-1	HF Diffraction	136P
1830		Reception	Ramada Inn
1930		Banquet	Ramada Inn

Wednesday June 4

0900-1210	I-1	Infrared and Submillimeter	147P
	II-4	Remote Sensing	158P
	III-2	Satellite Beacon Experiment	136P
	VI-3	Transient I	141P
	VI-4	Arrays	144P
	VI-10	Ray Techniques	151P
1400-1710	I-3	Measurement II	136P
1400-1710	II-5	Acoustics and EM Sounding	158P
1400-1530	III-3	Scintillation and Irregularity	280MRL
1600		Business Meeting (III)	280MRL
1400-1712	VI-5	Antennas	144P
1400-1715	VI-11	EM Pulse	151P
1715		Business Meeting (II)	158P
1715		Business Meeting (VI)	151P
2030		Panel Discussions on Transients	151P

Thursday June 5

0900-1210	II-6	Polarization, Radiometry	158P
	III-4	E-Region and Below	280MRL
	VI-6	EM Theory	151P
	VI-8	Biological Effects	136P
1400-1710	II-7	ATS-6 Experiments	158P
	VI-7	Numerical Methods	144P
	VI-9	Transients II	151P

CSL: Coordinated Science Laboratory  
 Illini: Illini Union  
 MRL: Materials Research Laboratory  
 P: Physics Building

United States National Committee  
INTERNATIONAL UNION OF RADIO SCIENCE

PROGRAM AND ABSTRACTS

1975 Meeting  
June 3-5

Sponsored by USNC-URSI in cooperation  
with IEEE

Antennas and Propagation Society

Urbana, Illinois

NOTE

Programs and Abstracts of the USNC-URSI Meetings are available from:

USNC-URSI  
National Academy of Sciences  
2101 Constitution Avenue, N.W.  
Washington, DC 20418

The full papers are not published in any collected format, and requests for them should be addressed to the authors who may have them published on their own initiative. Please note that these meetings are national and are not organized by international URSI, nor are these programs available from the international Secretariat.

MEMBERSHIP

United States National Committee

INTERNATIONAL UNION OF RADIO SCIENCE

Chairman F. S. Johnson, University of Texas, Dallas  
Vice Chairman J. V. Evans, Lincoln Laboratory, MIT  
Secretary C. G. Little, Environmental Res. Labs, NOAA  
Editor T. B. A. Senior, University of Michigan

Immediate Past  
Chairman A. T. Waterman, Jr., Stanford University

Commission Chairmen

Commission I: Radio Measurements and Standards  
George Birnbaum  
Science Center of Rockwell International  
1049 Camino dos Rios  
Thousand Oaks, CA 91360

Commission II: Radio and Non-ionized Media  
Isadore Katz  
Applied Physics Laboratory  
The Johns Hopkins University  
8621 Georgia Avenue  
Silver Spring, MD 20910

Commission III: On the Ionosphere  
John M. Kelso  
ITT Electro-physics Laboratories, Inc.  
9140 Old Annapolis Road  
Columbia, MD 21043

Commission IV: On the Magnetosphere  
Andrew F. Nagy  
Dept. of Electrical Engineering  
University of Michigan  
Ann Arbor, MI 48104

Commission V: Radio and Radar Astronomy  
Alan H. Barrett  
Research Laboratory of Electronics (26-457)  
Massachusetts Institute of Technology  
Cambridge, MA 02139

Commission VI: Radio Waves and Transmission of Information  
Aharon A. Ksienski  
ElectroScience Laboratory  
Ohio State University  
1320 Kinnear Road  
Columbus, OH 43212

Commission VII: Radio Electronics  
Peter L. Bender  
Joint Institute for Laboratory Astrophysics  
University of Colorado  
Boulder, CO 80302

Commission VIII: On Radio Noise and Interference  
George H. Hagn  
Assistant Director, Program Development  
SRI Washington  
1611 North Kent Street  
Arlington, VA 22209

Members at Large

P.M. Banks	E.E. Gossard
C.I. Beard	A. Ishimaru
W.C. Erickson	J.S. Nisbet
L.B. Felsen	W.F. Utlaut

Officers of URSI resident in the United States

Honorary President	S. Silver
Vice President	H.G. Booker
Chairman, Commission III	S.A. Bowhill
Chairman, Commission IV	F.L. Scarf
Chairman, Commission VI	K.M. Siegel
Vice Chairman, Commission I	H.M. Altschuler
Vice Chairman, Commission V	G. Westerhout

American Geophysical Union  
IEEE

A.J. Dessler  
E. Weber

United States Government  
Department of Commerce  
Department of Defense  
Air Force  
Army  
Navy  
FCC  
NASA  
NSF  
OTP

A.H. Shapley  
E. Paroulek  
C.J. Sletten  
A.R. Rasmussen  
A.H. Schooler  
H. Fine  
E.R. Schmerling  
R. Fleischer  
W. Dean, Jr.

Foreign Secretary, NAS  
Chairman, NRC Division of  
Physical Sciences

G.S. Hammond  
R. Smoluchowski

Honorary Members

H.H. Beverage  
A.H. Waynick

## DESCRIPTION OF

### INTERNATIONAL UNION OF RADIO SCIENCE

The International Union of Radio Science is one of 14 world scientific unions organized under the International Council of Scientific Unions (ICSU). It is commonly designated as URSI (from its French name, Union Radio Scientifique Internationale). Its aims are (1) to promote the scientific study of radio communications; (2) to aid and organize radio research requiring cooperation on an international scale and to encourage the discussion and publication of the results; and, (3) to facilitate agreement upon common methods of measurement and the standardization of measuring instruments. The International Union itself is an organizational framework to aid in promoting these objectives. The actual technical work is largely done by the National Committees in the various countries.

The officers of the International Union are:

President	W.J.G. Beynon (UK)
Immediate Past President:	W. Dieminger (West Germany)
Vice Presidents:	H.G. Booker (USA) W.N. Christiansen (Australia) V.V. Migulin (USSR) J. Voge (France)
Secretary General:	C.M. Minnis (Belgium)
Honorary Presidents:	B. Decaux (France) C. Manneback (Belgium) J.A. Ratcliffe (UK) S. Silver (USA) R.L. Smith-Rose (UK)

The Secretary's office and the headquarters of the organization are located at 7, Place Emile Danco, 1180 Brussels, Belgium. The Union is supported by contributions (dues) from 37 member countries. Additional funds for symposia and other scientific activities of the Union are provided by ICSU from contributions received for this purpose from UNESCO.

The International Union has seven permanent bodies called Commissions for centralizing studies in the principal technical fields. In addition, Commission VIII has been established on a provisional basis. The names of the Commissions and the chairmen are as follows:

- I Radio Standards and Measurements  
P.O. Lundbom (Sweden)
- II. Radio and Non-ionized Media  
P. Misme (France)
- III. On the Ionosphere  
S.A. Bowhill (USA)
- IV. On the Magnetosphere  
F.L. Scarf (USA)
- V. Radio Astronomy  
J.L. Locke (Canada)
- VI. Radio Waves and Circuits  
K.M. Siegel (USA)
- VII. Radio Electronics  
A.L. Cullen (UK)
- VIII. On Radio Noise of Terrestrial Origin  
N.C. Clarence (South Africa)

Every three years, the International Union holds a meeting called the General Assembly. The next General Assembly, the XVIII, will be held in Lima, Peru, in August 1975. The Secretariat prepares and distributes the Proceedings of these General Assemblies. The International Union arranges international symposia on specific subjects pertaining to the work of one Commission or to several Commissions. The International Union also cooperates with other Unions in international symposia on subjects of joint interest.

Radio is unique among the fields of scientific work in having a specific adaptability to large-scale international research programs, for many of the phenomena that must be studied are world-wide in extent and yet are in a measure subject to control by experimenters. Exploration of space and the extension of scientific observations to the space environment is dependent on radio for its communication link and at the same time expands the scope of radio research. One of its branches, radio astronomy, involves cosmos-wide phenomena. URSI has in all this a distinct field of usefulness in furnishing a meeting ground for the numerous workers in the manifold aspects of radio research; its meetings and committee activities furnish valuable means of promoting research through exchange of ideas.

JOINT SPECIAL AP-S/URSI SESSION

(Joint AP-S 10)

0900 Tuesday, June 3

141 Physics

Chairman: E. C. Jordan, University of Illinois

(Invited Papers)

1. THE MANY FACES OF THE INSULATED ANTENNA  
(0900) R. W. P. King, Harvard University
2. ELECTROMAGNETIC WAVE TRANSMISSION WITHIN THE EARTH  
(0930) J. R. Wait, U.S. Department of Commerce, Boulder
3. MAGNETIC SUSPENSION OF HIGH-SPEED VEHICLES  
(1000) J. R. Reitz, Ford Motor Company
  
- (1030) COFFEE BREAK
  
4. RECENT DEVELOPMENTS IN HOLOGRAPHY  
(1100) T. H. Jeong, Lake Forest College
- (1200) LUNCH followed by Holography demonstration

COMMISSION I

RADIO MEASUREMENTS AND STANDARDS

George Birnbaum, Chairman

<u>Session</u>	<u>Page</u>
1. FAR INFRARED AND SUBMILLIMETER TECHNIQUES (0900 Wednesday, June 4, 147 Physics) Chairman: Paul D. Coleman University of Illinois	3
2. /AP-S 15. MEASUREMENT I (1400 Tuesday, June 3, 198 CSL) Chairman: E. S. Gillespie California State University at Northridge	4
3. /AP-S 20. MEASUREMENTS II (1400 Wednesday, June 4, 136 Physics) Chairman: R. C. Baird National Bureau of Standards	5

COMMISSION I

0900 Wednesday, June 4

147 Physics

Session I-1

FAR INFRARED AND SUBMILLIMETER TECHNIQUES

Organizer and Chairman: Paul D. Coleman, University of Illinois

- 1-1. ATMOSPHERIC PROPAGATION IN THE FAR INFRARED  
(0900) V. J. Corcoran, Institute for Defense Analyses
- 1-2. JOSEPHSON EFFECT DETECTORS  
(0920) P. L. Richards, University of California, Berkeley
- 1-3. ELECTRON TUNNELING DIODE DETECTORS  
(0940) T. K. Gustafson, University of California, Berkeley
- 1-4. FREQUENCY AND LINE WIDTH MEASUREMENTS IN FAR IR  
(1000) J. Gallagher, Georgia Tech

(1020) COFFEE BREAK

- 1-5. CW FAR IR WAVEGUIDE LASERS  
(1050) D. T. Hodges, Aerospace Corporation
- 1-6. OPTICAL PUMPING OF FAR IR LASERS  
(1110) F. Brown, Williams College
- 1-7. HIGH POWER FAR IR LASERS  
(1130) T. A. DeTemple, University of Illinois
- 1-8. FAR IR PROBLEMS OF INTEREST TO THE ARMY  
(1150) Charles M. Bowden, Redstone Arsenal

COMMISSION I.

1400 Tuesday, June 3

198 CSL

Session I-2 (Joint AP-S 15)

MEASUREMENT I

Chairman: E. S. Gillespie, California State University  
at Northridge

- 2-1. CAVITY METHOD FOR EXPERIMENTAL DETERMINATION  
(1400) OF SCATTER CHARACTERISTICS  
J. R. Christian, U.S. Army Electronics Command, Fort  
Monmouth, and S. Fich, G. Goubau, Rutgers University
- 2-2. PRECISION POLARIZATION MEASUREMENT TECHNIQUES  
(1420) FOR CIRCULARLY POLARIZED ANTENNAS  
W. J. English and R. W. Gruner, COMSAT Laboratories
- 2-3. IMPROVED POLARIZATION MEASUREMENTS USING A MODIFIED  
(1440) THREE ANTENNA TECHNIQUE  
A. C. Newell, National Bureau of Standards
- 2-4. DIPOLE MEASUREMENT IN SMALL ANECHOIC CHAMBER  
(1500) Y. Naito and K. Horie, Tokyo Institute of Technology
- (1520) COFFEE BREAK
- 2-5. MEASUREMENTS ON COUPLED LEAKY COAXIAL CABLES  
(1540) S. C. Dass and J. C. Beal, Queen's University
- 2-6. PERFORMANCE OF A COMPACT ANTENNA RANGE  
(1610) R. C. Johnson, Georgia Institute of Technology and  
D. W. Hess, Scientific-Atlantic, Inc.
- 2-7. MOTION STABILITY MEASUREMENTS OF SUBMARINE-TOWED  
(1630) ELF RECEIVING PLATFORM  
J. Goldstein and R. Dinger, Naval Research Laboratory
- 2-8. MEASUREMENT OF CURRENT AND CHARGE ON A THIN  
(1650) STEPPED RADIUS MONOPOLE  
B. M. Duff and S. Singarayar, University of Mississippi

COMMISSION I

1400 Wednesday, June 4

136 Physics

Session I-3 (Joint AP-S 20)

MEASUREMENT II

Chairman: R. C. Baird, National Bureau of Standards

- 3-1. G/T MEASUREMENT ERRORS WITH RADIO STARS  
(1400) W. C. Daywitt and M. Kanda, National Bureau of Standards
- 3-2. A METHOD OF MEASURING THE SURFACE SHAPE OF  
(1420) REFLECTOR ANTENNAS  
J. M. Payne, J. M. Hollis and J. W. Findlay,  
National Radio Astronomy Observatory
- 3-3. A TECHNIQUE FOR SIMULTANEOUS MEASUREMENT OF  
(1440) ATTENUATION AND BISTATIC SCATTER DUE TO  
RAINFALL AT MILLIMETER WAVES  
J. W. Mink, U.S. Army Electronics Command
- 3-4. ELECTROOPTIC MEASUREMENT OF PULSED ANTENNA NEAR FIELD  
(1500) R. S. Kasevich and C. Harris, Raytheon Company
- (1520) COFFEE BREAK
- 3-5. STUDY OF ERRORS IN PLANAR NEAR-FIELD MEASUREMENTS  
(1540) A. C. Newell and A. D. Yaghjian,  
National Bureau of Standards
- 3-6. A STUDY OF CURRENT AND CHARGE DISTRIBUTIONS ON  
(1610) ELECTRICALLY THICK AND THIN RADIATING STRUCTURES  
IN THE VICINITY OF EDGES AND DRIVING POINTS  
L. J. Cooper, Emerson Electric Company
- 3-7. MEASUREMENT OF CURRENT AND CHARGE ON THIN  
(1630) BENT-WIRE AND V-CROSS SCATTERERS  
B. M. Duff and S. Singarayar, University of Mississippi
- 3-8. SOME COMPARATIVE HF AND LF MEASUREMENTS OF  
(1650) GROUND CONDUCTIVITY AND PERMITTIVITY  
A. F. Lyle Rocke, 3613 Queen Mary Drive, Olney, Maryland

COMMISSION II

RADIO AND NON-IONIZED MEDIA

Isadore Katz, Chairman

<u>Session</u>	<u>Page</u>
1. EM PROPAGATION IN THE EARTH; WAVEGUIDE AND DUCT PROPAGATION (0900 Monday, June 2, 136 Physics) Chairman: A. H. LaGrone University of Texas	7
2. EM PROPAGATION IN RANDOM MEDIA (1400 Monday, June 2, 158 Physics) Chairman: W. S. Ament Naval Research Laboratory	12
3. RADIO-OCEANOGRAPHY (1400 Tuesday, June 3, 158 Physics) Chairman: I. Katz Johns Hopkins University	16
4. REMOTE SENSING (0900 Wednesday, June 4, 158 Physics) Chairman: C. I. Beard Naval Research Laboratory	22
5. ACOUSTICS AND EM SOUNDING (1400 Wednesday, June 4, 158 Physics) Chairman: J. W. Rouse, Jr. Texas A and M University	26
6. PRECIPITATION: POLARIZATION AND STATISTICS; RADIOMETRY (0900 Thursday, June 5, 158 Physics) Chairman: L. J. Ippolito NASA/Goddard Space Flight Center	30
7. ATS-6 MILLIMETER WAVE EXPERIMENTS; ATS-6 13/18 GHz EXPERIMENT (1400 Thursday, June 5, 158 Physics) Chairman: C. W. Bostian Virginia Polytechnic Institute	34

COMMISSION II

0900 Monday, June 2

136 Physics

EM PROPAGATION IN THE EARTH; WAVEGUIDE AND DUCT PROPAGATION

A. H. LaGrone, Chairman

- II. 1-1 DETERMINATION OF THE PHYSICAL PROPERTIES OF A COAL SEAM BY USING ELECTRICAL METHODS. R. J. Lytle, E. F. Laine, and D. L. Lager, Lawrence Livermore Laboratory

The demand for low cost energy has dictated that the feasibility of various energy conversion methods be investigated. One alternative to presently used energy conversion techniques is in-situ coal gasification. Knowledge of the physical properties of the coal seam are of prime importance for in-situ coal gasification experimental design and evaluation. Parameters of significance include the coal porosity, the coal permeability for fluids, the location and extent of fractures, the seam thickness and orientation, and the location of anomalies within the seam. High frequency (1-100 MHz) and low frequency (20 Hz) electrical measurements conducted on the surface, in a single drill hole, and between drill holes have been conducted to determine these parameters for a site near Kemmerer, Wyoming.

The radius of investigation for low frequency probes in a drill hole was enlarged. These results indicate the thickness and degree of uniformity of the coal seam. The high frequency results provide a detailed subsurface electrical profile. Good resolution was obtained both vertically and horizontally by using sophisticated data inversion algorithms. Results were obtained before and after fracturing induced by high explosives.

Electrical methods show much promise as a monitoring tool for coal-field experiments.

- II. 1-2 TRANSMISSION OF ELECTROMAGNETIC WAVES DOWN A MINE HOIST SHAFT. David A. Hill and James R. Wait,\* Office of Telecommunications, Institute for Telecommunication Sciences, U.S. Department of Commerce, Boulder, Colorado, 80302

In many mines, there is a need to communicate from the surface to the interior of the mine by direct transmission of electromagnetic waves down a hoist shaft. In this analysis, the hoist shaft is modelled as a vertical circular tunnel in a lossy half-space. A metal hoist cable, located at the center of the tunnel, permits propagation of a TEM mode as well as higher

order evanescent modes. The propagation constants of these modes are determined by a numerical solution of the mode equation. The transmitting antenna, which could be a toroidal coil, is modelled as an annular slot in a finite circular ground plane at the surface. Using a half-space model of the earth, we derive the amplitudes of the tunnel modes. Numerical results are obtained for the attenuation rate of the dominant TEM mode, the input conductance as seen by the annular slot, and the overall transmission efficiency. Finally, we consider various schemes to effectively receive the downward propagated signal in the cage suspended by the mine hoist "rope" (i.e., cable). Some unresolved questions here are pointed out.

---

\*ERL/NOAA, U.S. Department of Commerce, Boulder, Colorado, 80302.

- II. 1-3 EFFECT OF THE FREQUENCY DEPENDENCE OF EARTH ELECTRICAL PARAMETERS ON EM PROBING OF THE EARTH'S CRUST. Charles H. Stoyer and James R. Wait, Cooperative Institute for Research in Environmental Sciences, University of Colorado, Boulder, Colorado, 80302

Both in-situ and laboratory studies indicate that naturally occurring earth materials are electrically dispersive. Comparisons are made in this paper among synthetic field data from non-dispersive, semi-dispersive, and dispersive electrical structures. Structures under the influence of natural and artificial sources are considered for various degrees of dispersion. Admittivities of the form  $\sigma' = A + B \log(\omega/\omega_0) + jK$  and other frequency dependent forms are used in the calculations. The results indicated that interpretation of electromagnetic field data, in terms of non-dispersive layered structures, can lead to significant errors in the estimation of sub-surface structure. Thus, there may be an important limitation in the use of variable frequency or transient data in the currently popular inversion schemes.

- II. 1-4 LONG RANGE ULF PROPAGATION IN THE EARTH LITHOSPHERE. Hsi-Tien Chang\* and Mario D. Grossi, Raytheon Company, Sudbury, Massachusetts, 01776

Low-loss lithospheric propagation paths are expected to exist in the low conductivity sublayer that has been hypothesized to extend from the bottom of the high conductivity overburden layer at the earth's surface (or from the bottom of the ocean) down to the Moho discontinuity. A study of ULF propagation in the lithosphere, taking into account the influence of the earth-ionosphere waveguide, is given in this paper. It is found that the field modes can be separated into air modes and lithospheric modes. Field strength in the atmosphere obtained from

the air modes agrees well with previous investigations on atmospheric propagation inside the earth-ionosphere waveguide. The lithospheric modes show a strong geometric guidance and the absorption rates are low in the presence of realistic conductivity profiles of the sublayer. Effects of various factors such as different locations of the transmitter and receiver, changes in the air or sublayer conductivity, variations in the thickness of the sublayer, presence of a mud layer at the sea bottom, and the earth curvature are also considered.

---

\*Presently at Tamkang College of Arts and Sciences, EE Department, Tamsui, Taipei Hsien, Taiwan 251, China.

II. 1-5 MICROWAVE OPTICS IN A PERTURBED ATMOSPHERIC BOUNDARY LAYER. Lewis Wetzel, Naval Research Laboratory, Washington, D.C., 20375

In propagation through an inhomogeneous medium containing small perturbations in refractivity, the resulting phase changes "focus" the incident radiation into corresponding amplitude changes a suitable distance away. If the propagation takes place at very small grazing angles in the quasi-stratified atmospheric boundary layer, perturbations in this boundary layer should accordingly give rise to observable variations in the illumination field measured along the earth. Some features of this illumination field should be visible in records of microwave backscatter from the sea at extended ranges.

The literature contains abundant evidence from high resolution radar and acoustic sounders that a variety of waves appear on elevated layers within the atmospheric boundary layer (0 - 1 km), while buoy measurements have disclosed periodic variations in water vapor pressure in the evaporative layer over the sea (0 - 10 m).

This paper will show 1) fine-grained ray tracings through both elevated and surface perturbations of the atmospheric boundary layer, thereby establishing credence in the hypothesis that such perturbations can produce observable optical effects, and 2) radar evidence of such effects in the form of time history (falling raster) displays of sea backscatter at extended ranges. The spatial and temporal scales of the backscatter variations are commensurate, respectively, with the thickness and Brunt-Väisälä period of the atmospheric boundary layer.

II. 1-6 PHASE INTEGRAL CALCULATIONS FOR A DUCTING ENVIRONMENT  
AT VHF THROUGH MICROWAVES. R. A. Pappert, Naval  
Electronics Laboratory Center, San Diego, California

A recent phase integral formulation<sup>1</sup> which allows for the transition between locked and leaky modes is used to calculate mode properties associated with ground based elevated layers. Although the method is restricted to specialized refractivity profiles, the profile selected is sufficiently general to allow for comparison with some experimental height gain measurements at 65 and 620 MHz. Approximate agreement is found between measurements and calculations.

Field strength dependence upon layer parameters and frequency is also discussed.

1. Hayes, M. G. W., The transition from locked to leaky modes in tropospheric radio propagation, Journal of Physics A, Vol. 6, 177-191, 1973.

II. 1-7 RADIATION FROM THE INNER SURFACE OF A BEND CONNECTING  
TWO STRAIGHT SECTIONS OF DIELECTRIC SLAB WAVEGUIDE.  
S. W. Maley, University of Colorado, Boulder,  
Colorado, 80302

The radiation from the outer surface of a bend in a dielectric slab waveguide has previously been studied. The results have some application to the study of radiation from ground waves incident upon obstacles on the surface of the earth. Radiation from the inner surface of a bend in a dielectric slab waveguide can have similar applications. Such radiation has been analyzed. The configuration studied consists of two straight sections of slab waveguide joined by a circular bend. The radius of curvature of the bend is assumed to be many wavelengths. The technique used to study radiation from the outer surface of the bend can be adapted to this problem. It is assumed that the power radiated from the bend is a small fraction of the power carried by the waveguide. The results of the analysis show that the power radiated decreases with increasing radius of curvature of the bend and that the radiation pattern consists of a number of closely spaced narrow lobes. The bend in the waveguide causes power to be reflected back along the waveguide, but for the range of values of radius of curvature under consideration (100 wavelengths or more), the reflection was small.

II. 1-8 RADIATION FROM A DISCONTINUITY IN A PLANAR, SURFACE-  
WAVE GUIDING STRUCTURE. S. W. Maley, University of  
Colorado, Boulder, Colorado, 80302

A planar surface wave-guiding structure (this could be an approximation to the surface of the earth) with a simple discontinuity in the electrical parameter of the structure along a line

perpendicular to the direction of propagation has been analyzed. The discontinuity causes a reflected wave, which has been analyzed previously; but it also causes some power to be lost by radiation away from the waveguiding structure. This analysis concentrates on the latter problem. A perturbation type of analysis is employed; it is the same type of analysis that has been used in the study of radiation from bends in surface waveguiding structures. The assumption is made that the power lost at the discontinuity is small; then the character of the propagating surface wave can be approximated to a high order of accuracy. The radiated field is formulated in terms of integrals over a set of equivalent currents on the plane. The characteristics of the radiated field are found by evaluation of the integrals. The results indicate that a cylindrical type of wave is radiated from the discontinuity and its pattern is strongest at low angles of elevation above the plane in the direction of propagation of the surface wave.

- II. 1-9 EFFECT OF A VERTICAL BURIED CONDUCTOR ON THE SUB-SURFACE ELECTRIC FIELD FOR HORIZONTAL ELECTRIC DIPOLE EXCITATION. M. Caeterman, P. DeGauque, R. Gabillard, Lille University, Electronics Department, 59650 - Villeneuve d'Ascq - France, and J. Grimoud, Franlab, Informatique, 4 Av. Bois-Préau, 92500 - Rueil - France.

Some geophysical prospecting techniques use the measurement in a borehole of the vertical electric field  $E_z$  radiated by an electric horizontal dipole situated on the earth surface. The electrodes fixed on a carrier are lowered into a well on the end of a non-insulated cable.

In order to evaluate the influence of this wire on the  $E_z$  measurement, we develop a theoretical approach of the electromagnetic response of this heterogeneity in a conducting half-space. We assume a low frequency emission to use the quasi-static approximation.

The solution is in the form of an integral equation which is reduced to a matrix equation and solved numerically. The electric field component in the heterogeneity is determined. One advantage of this numerical technique is that it is not necessary to find the scattering currents throughout the half-space.

The response of the cable is studied in some detail. Numerical results are given for different values of the emitter-borehole distance and also, as a function of the length between the electrodes and the non-insulated cable.

1400 Monday, June 2

158 Physics

## EM PROPAGATION IN RANDOM MEDIA

W. S. Ament, Chairman

- II. 2-1 SOME NEW RESULTS ON PROPAGATION IN STRONG TURBULENCE.  
 Ronald L. Fante, AFCRL (LZP), Hanscom AFB,  
 Massachusetts, 01731

In this paper we will present some new results for the variance and covariance of the intensity of a wave propagating in a strongly turbulent medium. The results are obtained by solving the "Markov approximation" equation for the fourth moment of the electric field, in the limit when the turbulence is strong. We shall present the solution and show that it compares very well with the recent (1973) experimental data of Gracheva et al. in the Soviet Union.

We shall also examine the consequences of the solution, including the temporal frequency spectrum of the intensity fluctuations, the phase structure and angle of arrival fluctuations, and aperture averaging. In short we find that the expression for the phase structure function (and consequently the angle of arrival fluctuations) in strong turbulence does not differ greatly from the weak turbulence result. However, the nature of the aperture averaging and the intensity scintillation spectrum is considerably altered.

- II. 2-2 WAVE PROPAGATION IN INHOMOGENEOUS RANDOM MEDIA.  
 P. C. Lam, C. S. Gardner, Raj Mittra, Department  
 of Electrical Engineering, University of Illinois

Most of the theoretical work on wave propagation in random media has been concerned with homogeneous isotropic media. Unfortunately, the statistical characteristics of the earth's atmosphere are at best only locally homogeneous. We have begun to investigate wave propagation in inhomogeneous media using the parabolic equation method (PEM). The refractive index covariance is assumed to be given as the product of a function depending on the difference coordinate and another function depending on the average coordinate.

$$\langle n_1(\mathbf{r}_1) n_1(\mathbf{r}_2) \rangle = B_n^v \left( \frac{\mathbf{r}_1 + \mathbf{r}_2}{2} \right) B_n^o(\mathbf{r}_1 - \mathbf{r}_2). \quad (1)$$

$B_n^0$  measures the correlation between the fluctuations at points  $\underline{r}_1$  and  $\underline{r}_2$  while  $B_n^v$  measures the strength (variance) of fluctuations. Woo and Ishimaru\* have used this description of the refractive index and the Rytov method to study radio occultation of planetary atmospheres. The parabolic equation for the second order mutual coherence function (MCF),  $\Gamma_2$ , is given by

$$2ik \frac{\partial \Gamma_2(x, \underline{r}_c, \underline{r}_d)}{\partial x} + 2\sqrt{\underline{r}_c \cdot \nabla} \cdot \nabla_{\underline{r}_d} \Gamma_2(x, \underline{r}_c, \underline{r}_d) + ik^3 H(x, \underline{r}_c, \underline{r}_d) \Gamma_2(x, \underline{r}_c, \underline{r}_d) = 0 \quad (2)$$

where

$$\underline{r}_c = \frac{\underline{r}_1 + \underline{r}_2}{2} \quad \underline{r}_d = \underline{r}_1 - \underline{r}_2$$

$$H(x, \underline{r}_c, \underline{r}_d) = B_n^0(0) B_n^v(x, \underline{r}_c + \frac{\underline{r}_d}{2}) + B_n^v(x, \underline{r}_c - \frac{\underline{r}_d}{2}) - 2 B_n^0(\underline{r}_d) B_n^v(x, \underline{r}_c).$$

We have obtained solutions of (2) and are studying the behavior of  $\Gamma_2$  for various types of random media. Results are presented for plane, spherical and beam wave propagation through turbulent layers and turbulent "balls." These results indicate that the MCF is highly dependent on  $B_n^v$ .

\*R. Woo and A. Ishimaru, "Remote sensing of turbulence characteristics of a planetary atmosphere by radio occultation of a space probe," Rad. Sci., Vol. 8, p. 103-108, February 1973.

II. 2-3 REFLECTION AND TRANSMISSION FROM A LOSSY ONE DIMENSIONAL RANDOM SLAB. Roger H. Lang and Robert F. Nelson, George Washington University, Washington, C.C., 20052

The problem of a plane wave normally incident on a lossy one-dimensional random medium is investigated in the regime where backscattering is important. It is assumed that refractive index variations are small, however large slab widths are considered so that multiple scattering effects appear. The invariant embedding technique and the Markov approximation are used to obtain an approximate equation for the probability density function of the amplitude and phase of the reflection and transmission coefficients. This probability density function is then used to compute the average reflected power and its variance as well as the average and variance of the transmitted power. These statistics are then examined as functions of the

medium loss, correlation length and slab width. It is seen that as medium loss increases, the effects of multiple scattering become smaller.

II. 2-4 PROBABILITY DISTRIBUTION OF IRRADIANCE FLUCTUATION PROPAGATING THROUGH THIN TURBULENT SLABS.

Y. Furuhashi,\* National Oceanic and Atmospheric Administration, Environmental Research Laboratories, Boulder, Colorado, 80302

The general solution of irradiance fluctuations of a plane wave for a strongly turbulent thin slab is derived by the parabolic-equation method. This solution reduces to the same expression as that derived by the phase-screen theory. For a power-law spectrum of refractive-index irregularities, asymptotic values of the Nth-order moment of the irradiance fluctuation are obtained in the long-distance limit. The irradiance probability-density function, derived from its moments, turns out to be the well-known exponential distribution in the strong-turbulence limit and the distribution is independent of the slope and strength of the spectrum of the irregularities. The probability distribution for independent, multiple, thin turbulent layers, well separated from each other, is also exponential.

These results are applicable to many problems in atmospheric optics, e.g., stellar scintillation by the irregularities at the tropopause height; in radio wave propagation through the ionosphere; and in radio astronomy.

\*Permanent Address: Radio Research Laboratories, Tokyo 184, Japan.

II. 2-5 THE DIFFRACTION OF ELECTROMAGNETIC BEAMS BY PERIODICALLY-MODULATED MEDIA. Ruey-Shi Chu, Communication Systems Division, GTE Sylvania, Inc., Needham, Maryland, 02194; and Theodor Tamir, Polytechnic Institute of New York, Brooklyn, New York, 11201

Analytical results are given on the diffraction of optical beams by a periodically-modulated dielectric medium, which represents a thick hologram or an acoustic column. By using a rigorous representation for the field of an incident beam, this paper shows that, for an optical beam incident at a Bragg angle, a strong diffracted beam (denoted as the "Bragg-scattered" beam) occurs in addition to the reflected and refracted beams. The Bragg-scattered beam is formed by the continuous coupling of energy from the refracted beam into the Bragg-scattered wave. In the meantime, the Bragg-scattered wave also couples part of its energy back to the refracted wave. This continuous coupling of energy back and forth between these two waves results in a diffusion of these two beams

into an angular wedge, which extends between the axis of the refracted wave and the axis of the Bragg-scattered wave in the dielectric region. A numerical example to illustrate this beam diffusion process within the modulated region is presented. For a sufficiently thick modulated slab, both the refracted and the Bragg-scattered beams will split into two beams. Diffraction phenomena for the case when the optical beam is incident at an angle not in the vicinity of a Bragg angle are also given.

II. 2-6 LONG-RANGE ELECTROMAGNETIC RANDOM WAVE PROPAGATION USING THE PARABOLIC EQUATION METHOD: A WAVE-KINETIC APPROACH. Ioannis M. Besieris, Department of Electrical Engineering, Virginia Polytechnic Institute and State University, Blacksburg, Virginia

The theoretical development is based on the parabolic approximation to the reduced wave equation together with appropriate initial and boundary conditions. This parabolic equation automatically includes diffraction and all other full-wave effects, such as "transverse" and "range" dependence of the speed  $v$  and the "volume loss"  $\mu$ . In the course of this work it is assumed that  $v = \langle v \rangle + \delta v$  and  $\mu = \langle \mu \rangle + \delta \mu$ , where  $\langle v \rangle$ ,  $\langle \mu \rangle$  are the deterministic parts, and  $\delta v$ ,  $\delta \mu$  are the randomly fluctuating parts, respectively.

Using the wave-kinetic method developed by Besieris and Tappert, and within the framework of the long-range, Markovian approximation, expressions have been determined for the mean intensity, the transverse correlation, the longitudinal correlation, and the two-frequency correlation. (The last quantity is important in the study of propagation of pulse trains in a stochastic channel.) In the Markov-diffusion approximation, several of the aforementioned results specialize to those reported by Tatarskii and Klyatskin.

## COMMISSION II

1400 Tuesday, June 3

158 Physics

### RADIO-OCEANOGRAPHY

I. Katz, Chairman

- II. 3-1 SEA BACKSCATTER MEASUREMENTS USING A PULSE COMPRESSION RADAR. Dale L. Schuler, Naval Research Laboratory, Washington, D.C., 20375

Radar scatterometers have been developed into useful instruments for remotely sensing certain parameters which characterize the air-sea interface (e.g., surface wind magnitudes<sup>1</sup>). Extension of the scatterometer principle to frequency modulated high time-bandwidth transmitted signals has been investigated<sup>2</sup> in an effort to make dynamic, accurate measurements of the sea backscatter cross section  $\sigma$ . The results of the investigation show that a scatterometer built using a pulse compression radar would have a wider range of capabilities than a conventional scatterometer. A technique has been developed which allows use (on a pulse by pulse basis) of 1) the uncompressed backscattered video signal to accurately measure the mean cross section  $\sigma$  and number  $N_g$  of independent scatterers/(bandwidth x area) and, 2) the compressed, backscattered, high resolution signal to measure wave and ship profiles.

An accurate estimate of the mean cross section  $\sigma$  may be obtained using the uncompressed sea return because a number of independent subsignals, not present in conventional gated-CW signals, may be extracted from the return under certain conditions.

The number of subsignals, or degrees of freedom,  $N_f$  (proportional to the pulse compression ratio  $K^2$ ) may be combined to reduce the variance in the estimate of the mean value of the cross section  $\sigma$ . This smoothing technique is complimentary to existing smoothing procedures employing temporal, spatial or pure frequency smoothing to achieve a better estimate of  $\sigma$ .

Experimental measurements at L-band using the smoothing technique indicate a reduction  $\delta$  in the standard deviation to mean ratio for the return signals of greater than 3.7 dB for a pulse compression ratio of 200. Larger reductions are expected as the pulse compression ratio is increased. Results will be presented to show the sensitivity of the reduction  $\delta$  to changes in 1) grazing angle, 2) sea-state, 3) compression ratio  $K$ , and 4) resolution cell size.

Measurements of the number  $N_g$  of independent scatterers (the patches of composite sea-surface theory)/(bandwidth x area)

for a particular sea state have been taken for a range of sea conditions. The relevance of the magnitude of  $N_s$  to statistical models of composite sea surfaces will be discussed.

1. Daley, J. C., "Wind Dependence of Radar Sea Return," J. Geophysical Research, 78, p. 7823 (1973).
  2. Schuler, D. L., "Dynamic Measurement of Sea Backscatter Cross Section Using A Pulse Compression Radar," USNC-URSI Digest 1974 Symposium, Boulder, Colorado, p. 65 (1974).
- II. 3-2 NEAR-NADIR MEASUREMENTS OF  $\sigma^0$  FOR THE OCEAN SURFACE FROM THE SKYLAB RADAR ALTIMETER. G. S. Brown, Applied Science Associates, Inc., Apex, North Carolina, 27502

Accurate measurements of  $\sigma^0$  for near normal incidence and under varying ocean surface conditions are essential to the design of future microwave remote sensors. In addition, such measurements are required in order to verify current theoretical models of short wavelength rough surface scattering. The Skylab short pulse radar altimeter obtained such  $\sigma^0$  data over surface conditions ranging from near "glassy" to extremely rough ( $H_{1/3} \approx 7m$ ). Average cross section data (over the equivalent footprint of the system) are derived from the altimeter's AGC. However, since the average return waveform was also measured, it is possible to produce extremely high resolution data (as a function of incidence angle) out to about one degree off-nadir.

In this paper, we present a brief summary of the type of corrections that must be made to convert Skylab return power measurements into  $\sigma^0$  values. Data are also presented on the range of values of  $\sigma^0$  which were measured and on the correlation of surface roughness and  $\sigma^0$  (where surface truth data was available). Average return waveform results will be presented when they imply a marked departure of  $\sigma^0$  from expected behavior.

- II. 3-3 STUDIES OF BACKSCATTERED SEA RETURN WITH A DUAL FREQUENCY X-BAND RADAR. William J. Plant, Naval Research Laboratory, Washington, D.C., 20375

A correlation between the backscattered sea returns at two adjacent X-Band frequencies has been detected. The correlation is induced in the returns by the spatial modulation of the scattering properties of capillary waves caused by long gravity waves. The sea returns were obtained at low grazing angles using a coherent dual-frequency, C. W. radar. The frequency difference between the two transmitted signals was variable from 7 MHz to 150 MHz. The correlation was observed as a Doppler-shifted line in the spectrum of the product of the returns. The Doppler shift changed as the frequency difference was varied, thus allowing the dispersion relation of the long gravity waves to be

determined. The amplitude of the line varied with the gravity wave amplitude and the angle between the radar line of sight and the water wave vector.

II. 3-4 NEAR AND FAR FIELD HF RADAR GROUND WAVE RETURN FROM THE SEA. Irvin Kay, Institute for Defense Analyses, Arlington, Virginia, U.S.A.

This paper will be concerned with radar scattering from the sea when the wavelength is large compared to the amplitude of the sea surface disturbance and the antenna is located on the surface. It has been observed, both theoretically and experimentally, that under these conditions, for vertical polarization of the radiated field, the return is due primarily to a single spatial frequency component of the sea surface and is much larger than would be expected from an estimate based upon summing the returns which might be attributed to the individual water wave peaks.

D. E. Barrick and W. H. Peake, by integrating the effects predicted by a mathematical model, due to S. O. Rice, of scattering from a slightly perturbed surface, have calculated the average scattering cross section per unit area  $\sigma_0$  for the sea. Barrick has shown some agreement with experiment for his result using a statistical model of the sea surface given by O. M. Phillips. However, there appears to be some reason for concern about the validity of characterizing HF radar return from the sea by means of a scattering cross section since the distance between the illuminated area on the sea surface and the antenna will usually be too small for the validity of the radar range equation; i.e., while the scattering region may be in the far field of the antenna the antenna will often not be in the far field of the illuminated sea surface area at these wavelengths. A calculation of the radar return valid for shorter distances would, therefore, appear to be useful.

A variation of a method due to J. R. Wait is used to calculate the return from an arbitrary small antenna located at the sea surface at distances from the scattering region just large enough so that the scattering region lies in the far field of the antenna. Specifically, it is assumed that the distance between the scattering region and the antenna is large compared to the radar wavelength which is, itself, large compared to the sea surface disturbance amplitude, but not necessarily large compared to the width of the illuminated sea surface area. The formula for the radar return derived in this calculation shows that Barrick's result is essentially correct, modified slightly by the antenna pattern and the directional behavior of the spatial power spectrum of the sea surface, for very large distances compared to the width of the illuminated sea surface. However, when the width of the illuminated surface is large Barrick's result can be greatly in error.

- II. 3-5 FIRST-ORDER HF SEA-ECHO DOPPLER PEAK BROADENING FROM WAVE-WAVE INTERACTIONS. Donald E. Barrick and Robert L. Weber, Wave Propagation Laboratory, National Oceanic and Atmospheric Administration, Boulder, Colorado, 80302

The strongest HF radar echoes from the sea surface appear as two narrow spikes in the Doppler domain. These echoes are produced by first-order Bragg scatter, i.e., they originate from ocean waves exactly one-half the radar wavelength (for near-grazing backscatter) which move toward and away from the radar. Certain investigators (including ourselves) have observed that the widths of these spectral peaks appear at times to exceed the limits imposed by the system Doppler processing resolution, and some have suggested a possible relationship between this width and sea state. One postulated mechanism which could explain this broadening is a wave-wave interaction, i.e., the effect of one gravity wavetrain of finite height on the speed of a second wavetrain (in this case, the Bragg-scattering wavetrain) via the nonlinear boundary condition at the free water/air interface. This effect could pose a natural resolution limitation on radar systems designed to measure near-surface current.

Employing a perturbation analysis of the nonlinear surface boundary condition, an expression was derived for the gravity-wave dispersion relationship, correct to third order. While this expression indicates some expected broadening in the first-order Doppler peak, it is still at least an order of magnitude lower than the widths observed from our surface-wave radar experiments. Since the widths extracted from our experimental data show no clearcut correlation with sea state and/or frequency, we are inclined to eliminate nonlinear wave-wave interactions from the list of candidate mechanisms which might explain this broadening.

- II. 3-6 THE RECOVERY OF MICROWAVE SCATTERING PARAMETERS FROM SCATTEROMETRIC MEASUREMENTS WITH SPECIAL APPLICATION TO THE SEA. John P. Claassen and Adrian K. Fung, University of Kansas Center for Research, Inc., Lawrence, Kansas, 66045

Certain considerations from reception and scattering theories are combined to reveal the character of radar returns from a homogeneous non-coherent target. The polarization properties of the scene and scatterometer antenna are carefully observed to develop a complete (non-coherent) scatterometer equation. The resulting equation is significantly different from that commonly reported, particularly when the distinction between antenna and surface polarization is noted. Comparison of the equation with that derived for non-statistical targets shows that certain simplifications may not be realized for statistical targets. The meaning and significance of various scattering coefficients not commonly appearing in the scatterometer equation are examined within the

context of scattering theories applicable to the sea. The implication of these terms and others on the retrieval of the scattering properties is discussed in general.

A technique based on intensity measurements is developed to derive all the non-coherent scattering coefficients. Computer simulations based on the technique and on a scattering characteristic similar to that of the sea were conducted. The results of the simulations are used to demonstrate antenna requirements for accurate recovery of the coefficients and to evaluate whether the distinction between antenna and surface polarizations is important. The results clearly show the care with which an investigator must perform his measurements if he is to compare his measurements with theory or with other measurements.

II. 3-7 DETERMINATION OF SWH FROM AN AIRCRAFT USING A PULSE-LIMITED RADAR ALTIMETER. E. J. Walsh, NASA Wallops Flight Center, Wallops Island, Virginia, 23337

A digital computer program has been developed for extracting maximum likelihood estimates of significant wave height (SWH) from pulse-limited radar altimeter data. The program is described and its expected accuracy is discussed. The problems inherent in using an aircraft as an observation platform are discussed in reference to testing advanced altimetry concepts prior to putting an instrument in orbit and in gathering data with existing systems to serve as ground truth for orbiting experiments such as GEOS-C. A simulation of the sea surface for various wave spectra is used to develop estimates of the shape of the mean radar return and the portion of the standard deviation in the SWH estimate contributed by the inhomogeneities in the sea surface for various spatial averages and sea states.

II. 3-8 SURFACE MULTIPATH PREDICTIONS FOR A UHF MARINE LINK TO THE GOES SATELLITE. K. R. Carver, Department of Electrical and Computer Engineering, New Mexico State University, Las Cruces, 88003

A new surface multipath predictive model is presented with application to a UHF link between ocean-based data buoys or ships and the GOES satellite. Theoretical and experimental data are presented which point out that antenna height or lobing effects are of major importance in predicting short-term fading behavior, with maximum Rayleigh as well as oscillatory fading occurring at heights for which there is a pattern lobe minimum.

The effective coherent reflected field depends on the Fresnel reflection coefficients and the free-space vector effective height pattern of the marine-based antenna as well as sea surface roughness and antenna height. The interference lobe

structure thus produced becomes less pronounced as the sea roughness increases since more reflected power is transferred to the diffuse component. The model uses an approximate expression for the diffusely scattered component based on experimental measurements by Beard, although predicted fading ranges may be too high for high angles of arrival. Subsidiary parameters examined include buoy or ship motional effects, frequency shift effects, ocean salinity changes, antenna polarization and pattern shape.

Experimentally measured data taken in September, 1974 on Santa Catalina Island by total power 468 MHz reception from GOES (at 46° W longitude) confirm the low-angle periodic height dependence of both the median short-term power level as well as the fading range.

COMMISSION II

0900 Wednesday, June 4

158 Physics

REMOTE SENSING

C. I. Beard, Chairman

- II. 4-1 A GREEN'S THEOREM REMOTE SENSING STRATEGY. L. B. Dean, NOAA Post-Doctoral Fellow, U.S. Department of Commerce, National Oceanic and Atmospheric Administration, Environmental Research Laboratories, Boulder, Colorado, 80302

A remote sensing strategy is presented for determining the spatial variation of the complex conductivity within a volume from a knowledge of the fields on the surface of the volume. The method is based on an integral equation developed from Green's theorem which relates the surface fields to the current density within the volume. Purely formal methods are utilized to examine the solution of the integral equation to obtain the volume current density, the solution for the fields interior to the volume from the current density and the solution for the conductivity distribution from the relation  $J = \sigma E$ . Comments are offered concerning the application and possible extensions of the method.

- II. 4-2 ACTIVE MICROWAVE SENSING OF THE ATMOSPHERE FROM SATELLITES. Isadore Katz, Applied Physics Laboratory, Johns Hopkins University, Silver Spring, Maryland

This is a report on the work of the Atmospheric Panel of the Active Microwave Workshop sponsored by NASA in Houston, Texas during July 1974. The Panel was part of a larger study involving applications of satellite borne radar to land and ocean problems as well as the atmosphere.

The Panel concluded that a satellite radar is potentially useful in the following weather-related areas: tropical storms (their genesis, time development and vertical extent), global mapping of rainfall intensity, measurement of storm maximum echo heights, the height of the melting layer, cirrus clouds, drop size spectra, the wind field in precipitation regions, surface wind fields over oceans, sea ice, and surface atmospheric pressure.

II. 4-3 PRECIPITATION MEASUREMENTS BY OPTICALLY PROCESSED REFERENCE BEAM HOLOGRAPHIC METHODS. M. L. A. Gassend, D. K. Morland and W. M. Boerner, Department of Electrical Engineering, University of Manitoba, Winnipeg, Manitoba R3T 2N2 Canada

For more than ten years, holocameras for particle measurements have been designed using the basic in-line Fraunhofer configuration. Off-axis methods have been developed in order to overcome the limitations inherent to in-line Fraunhofer holography. However, for both fundamental configurations, an undisturbed path has to be provided for the illuminating beam in the in-line set-up and for the reference beam in the off-axis set-up.

The local reference beam holographic methods with optically processed reference beam would permit the design of an air-borne holocamera with an illuminating beam generated by a pulsed laser source located and operated from the ground, the resolution of the obtained images being unaffected by the disturbances that the illuminating beam may encounter. Thus, our main objective is to investigate the feasibility of particle measurement in remote sensing applications of considerable importance such as the study of particulate fields in atmospheric pollution control and natural occurring precipitations.

Advantages of the proposed methods over the others will be discussed in relation to the size, density and transparency of the particles. A theoretical analysis supported by experimental results based on the simulation of particle fields will be presented.

II. 4-4 REMOTE PROBING OF RAIN PARAMETERS BY USE OF OPTICAL SCINTILLATIONS. T-i Wang, CIRES, University of Colorado/NOAA, Boulder, Colorado; S. F. Clifford, K. B. Earnshaw and G. M. Lerfald, National Oceanic and Atmospheric Administration, Environmental Research Laboratories, Boulder, Colorado, 80302

We apply the theory of optical scattering by spheres to calculate the time-lagged covariance function of the irradiance fluctuations of a light wave passing through rainfall. The measurement of the time-lagged covariance function of two vertically spaced detectors contains the necessary information to evaluate the path-averaged terminal-velocity-distribution of various-sized raindrops. For a given monotonic relationship between the drop size and its associated terminal velocity, we can obtain the path-averaged rainfall rate and path-averaged-drop-size-distribution. The rainfall rate can be obtained from the time-lagged covariance function without assuming a size-distribution of raindrops. It should be possible to use this technique as a remote sensor of path-averaged rain parameters along a line-of-sight optical path up to several kilometers. Preliminary experimental results, obtained with a laser beam, agree with the theoretical predictions.

- II. 4-5 STATISTICS AMONG THE DOPPLER SPECTRUM COEFFICIENTS OF A WEATHER LIKE SIGNAL. D. S. Zrnic and F. T. Hules, Department of Electrical and Electronics Engineering, California State University, Northridge, California, 91324

Joint probability density between any two power spectrum coefficients is derived. The inphase and quadrature time series components are assumed to be jointly Gaussian with known autocorrelation function. Periodogram is computed using a discrete Fourier transform and the density is found to be Rician. This density reveals that correlation among spectral coefficients is partly due to correlation between time series samples and partly to the window effect.

The joint density between signal and noise power in a single spectrum coefficient is also Rician. It is used to find conditional probabilities of the random signal being above or below a threshold when the coefficient is above or below the same threshold. This information may be useful in the design of threshold detectors for broad spectra that indicate tornadoes or turbulences. Probability of false alarm (when receiver noise is mistaken for a signal) is a function of threshold setting and so is the probability of detection.

- II. 4-6 THE EFFECT OF SURFACE ROUGHNESS ON THE RADAR SENSITIVITY TO SOIL MOISTURE. Fawwaz T. Ulaby and Percy P. Batlivala, University of Kansas Center for Research, Inc., Remote Sensing Laboratory, Lawrence, Kansas, 66045

Using a 2-8 GHz radar spectrometer mounted atop a 20 meter truck-mounted boom, the backscatter from three bare fields was measured as a function of moisture content. By applying different management techniques to the soil, three different scales of roughness were produced: a RMS height of .88 cm for the smooth field, 2.6 cm for the medium rough and 4.3 cm for the very rough. After measuring the return with the fields dry, the three fields were sprinkled with water until saturation. The radar return was then observed as a function of time as the soil dried up. Soil samples were taken at several depths below the surface at each of eight locations on the field. The radar data included measurements at 12 frequencies between 2 GHz and 8 GHz at incidence angles between nadir and  $40^\circ$  (in  $10^\circ$  increments) for HH and VV polarizations. The results of this experiment indicate good correlation of the radar return with soil moisture for all roughnesses, the sensitivity to soil moisture variations, however, decreases with incidence angle and roughness. This paper will discuss the results and propose incidence angle ranges over which the effect of roughness on the radar soil moisture sensitivity is minimal.

- II. 4-7 OPTIMIZING RADAR SYSTEM PARAMETERS FOR THE REMOTE SENSING OF CROPLANDS. Thomas F. Bush and Fawwaz T. Ulaby, University of Kansas Center for Research, Inc., Remote Sensing Laboratory, Lawrence, Kansas, 66045

During the spring and summer (May through September) of 1974 the microwave backscattering properties of various crops were studied in the 8-18 GHz band. The targets studied were corn, milo, soybeans, alfalfa and winter wheat. Backscatter measurements were made at incidence angles of  $0^\circ$  through  $70^\circ$  in  $10^\circ$  increments for both like polarizations (HH and VV) at 800 MHz increments across the band. At the time of each measurement ground truth data were collected to provide records of soil and plant moisture, plant height and rainfall. A complex dependency of  $\sigma^0$  on the target variables is indicated by the data. However, with a prudent choice of system parameters it is possible to obtain good correlations of  $\sigma^0$  with plant height, plant moisture and underlying soil moisture. This paper will present the results of this analysis.

- II. 4-8 A TECHNOLOGY TRANSFER: X-RAY TOMOGRAPHY TO ELECTRO-MAGNETIC PROBING OF THE GROUND. D. L. Lager and R. J. Lytle, Lawrence Livermore Laboratory

The data inversion algorithms developed in the last few years by investigators in the field of x-ray tomography for producing 3-D reconstructions of the human head and torso from 2-D projections have been applied to the problem of determining the structure of the ground between a pair of drill holes. The "projections" are made by probing the ground at HF and recording the magnitude and phase of the received signal for various positions of transmit and receive antennas.

The region between the holes were divided into rectangular zones (around 50, a la checkerboard) and several algorithms were applied to assign appropriate values of electrical permittivity and skin depth to each zone. The three most successful algorithms so far have been modified versions of the tomographer's ART (Algebraic Reconstruction Technique), SIRT (Simultaneous Inter-active Reconstruction Technique) and the Back Projection Technique. Results are presented to show the ability of the algorithms to resolve various sized simulated anomalies analogous to voids and ore bodies. Finally the results of experimental measurements are presented.

COMMISSION II

1400 Wednesday, June 4

158 Physics

ACOUSTICS AND EM SOUNDING

J. W. Rouse, Jr., Chairman

- II. 5-1 A REVIEW OF NOAA WORK ON DEVELOPMENT AND APPLICATION OF ECHOSONDES. Freeman F. Hall, Wave Propagation Laboratory, NOAA Environmental Research Laboratories, Boulder, Colorado, 80302

In the short span of six years echosonde development has progressed from the initial studies of McAllister (1968) and Little (1969) to the point, today, of ready commercial availability. NOAA's Wave Propagation Laboratory has made major contributions, both to this development, and to the application of echosondes to commerce and the atmospheric sciences. The present time represents a turning point at which the scientific community will decide whether the echosonde is a limited tool used mainly for qualitative display of boundary layer structure or whether, to the contrary, the echosonde is essential for efficient and comprehensive quantitative measurements in the atmosphere. Since a review of the past will help to guide such a decision, we will cover briefly the development at WPL of echosonde hardware, experimental and theoretical atmospheric sound propagation studies, echosonde antenna design and measurement in the field, applications for the FAA of Doppler echosondes to the measurement of winds and wind-shears above airports, and studies of tropical marine-atmosphere structures during GATE. And, for a glimpse at one possible future, we will sketch the outlines of a study now under way on the feasibility of measuring boundary layer critical parameters by echosondes.

- II. 5-2 A FIELD OBSERVATION OF ATMOSPHERIC FREE CONVECTION USING AN ACOUSTIC SOUNDER. D. E. Fitzjarrald, NRC Resident Research Associate, NOAA Environmental Research Laboratories, Boulder, Colorado, 80302

Measurements during periods of atmospheric free convection have been made using acoustic echo sounders and instruments on a meteorological tower. Comparison of data from the two instrument systems shows good agreement. Fourier analysis of the data indicates that the predominant horizontal scales of motion are approximately six times the depth of the convecting layer, in good agreement with laboratory convection experiments.

- II. 5-3 USE OF ACOUSTIC ECHO SOUNDERS AND MICROBAROGRAPHS TO STUDY WAVE MOTIONS IN THE PLANETARY BOUNDARY LAYER. W. H. Hooke, B. Stankov, and J. T. Merrill, Cooperative Institute for Research in Environmental Sciences, NOAA/University of Colorado, Boulder, Colorado, 80302

In March of 1974, staff of the Wave Propagation Laboratory (NOAA) and CIRES (NOAA/CU) mounted a two-week experiment to study gravity-wave motion in the planetary boundary layer, using an acoustic echo sounder, an instrumented 150 m meteorological tower and arrays of sensitive microbarographs spread some 50 m to 2 km apart. The experiment provided data on several types of wave generation by shear instability: (a) wave generation in the shear flow of the steady-state nocturnal inversion itself, (b) wave generation in shear flows overlying the nocturnal inversion, and (c) wave generation in shear flows associated with frontal passage. The three types of events and their role in boundary-layer development and maintenance are discussed.

- II. 5-4 INFRASOUND FROM CONVECTIVE STORMS .... IS IT USEFUL FOR STORM WARNING? T. M. Georges and Gary E. Greene, Wave Propagation Laboratory, NOAA Environmental Research Laboratories, Boulder, Colorado, 80302

During the summer of 1973, we did an experiment to collect statistics on the observability of severe storm infrasound at three stations. The results have been evaluated with the help of four "indices of usefulness": (a) false-alarm rate, which tells how often infrasound from other sources is mistaken for that from storms; (b) miss rate (or failure-to-alarm rate), which tells how many severe storms go undetected; (c) timeliness, which tells how much advance warning the waves give; and (d) location accuracy, which tells how well the emissions can be used to locate and track storms. The answer to the title question is that the waves show promise as a supplement to the present warning system. The remaining question is whether it is cost-effective to do the additional research required to deploy an operational sensor network.

- II. 5-5 SIMULTANEOUS ACOUSTIC AND FM-CW RADAR SOUNDING. Juergen H. Richter and Douglas R. Jensen, Naval Electronics Laboratory Center, San Diego, California, 92152

An acoustic sounder and FM-CW radars have been operated simultaneously over a one year period in the San Diego area. A cross section of monostatic observations is presented which include multiple layer structures, wave motions, marine layer structure and its relation to fog formation, and drizzle. Similarities and dissimilarities between acoustic and FM-CW radar soundings are discussed and interpreted and the complementary nature of

simultaneous observations with the two remote sensing techniques is emphasized. The acoustic sounder used in these measurements also has provisions for bistatic operation to sense the vertical wind profile. Problems encountered in obtaining reliable wind profiles with this sounder are discussed.

II. 5-6 GROWTH OF THE CONVECTIVE LAYER AS OBSERVED BY TWO MICROWAVE RADARS AND A SODAR. V. R. Noonkester and D. R. Jensen, Naval Electronics Laboratory Center, San Diego, California, 92152

The depth  $h$  of the surface-based mixing layer is important for global weather forecasting and for mesoscale forecasts of clouds, turbulence, visibility and pollution. Measurements of the variation of  $h$  with surface heat flux  $F$  and atmospheric stability  $\gamma$  (vertical lapse rate of temperature) are needed to verify several recent theories on the mixing layer. Observations of  $h$  are difficult to make by direct sensing techniques. The development of certain remote sensors in recent years has provided an opportunity to monitor continuously the convective layer. An FM-CW radar, a high-power pulse radar, and a sodar have been used recently in an experiment to observe simultaneously the convective field in great detail. Radiosondes were used to provide vertical stability information. The changes in  $h$  revealed by each sensor show compatible features when the unique characteristics of each sensor are considered. In general  $|\Delta h/\Delta t|$  ( $t$  is time) was greater during the morning growth after the convective destruction of the nocturnal inversion than the decay in the afternoon. The depth  $h$  was more variable near and after the maximum  $h$  which was usually before the surface temperature maximized. The morning rise rate  $\Delta h/\Delta t$  increased as  $\gamma$  decreased at the top of the convective layer and was constant during the convective destruction of each stable layer. These results indicate that some theories relating  $h$ ,  $\gamma$  and  $F$  may need modification.

II. 5-7 SIMULTANEOUS MEASUREMENT OF RADAR REFLECTIVITY IN CLEAR AIR BY FM-CW RADAR AND PULSE RADAR. Thomas G. Konrad, Applied Physics Laboratory, Johns Hopkins University, Silver Spring, Maryland; and Douglas R. Jensen, Propagation Technology Division, Naval Electronics Laboratory Center, San Diego, California

The radar reflectivity of atmospheric processes in the clear air involving turbulent mixing, such as shear layers and convection, has been measured using both high power, narrow beam, pulse radars and ultra-high resolution FM-CW radars. Both types of radar are highly sensitive with the capability of detecting the returns from fluctuations in the radio refractive index due to turbulent mixing. However, the radar reflectivities measured by the two types of radars have differed on occasion by as much as several orders of magnitude. This difference in reflectivities may be real, since the observations by the two radars were made in

different locations on different atmospheric structures. On the other hand the apparent discrepancy may be due to the difference in resolution capability of the two types of radar, i.e., beam filling limitations. A basic assumption in the calculation of radar reflectivity for distributed targets is that the pulse volume is filled with scatterers. The observations by the high resolution FM-CW radar, however, have shown that the reflecting regions in layers and convection are generally quite thin, only a few tens of meters thick. In this case the pulse volume of the pulse radar may not be filled resulting in a calculated reflectivity which is too low.

A unique experiment was performed wherein an FM-CW radar, and a high power, pulsed radar simultaneously observed the same region of a convective field. Quantitative data were recorded by the FM-CW and pulse radar in the same volume of air on a number of occasions. Radar reflectivities for each radar were calculated and compared assuming beam filling for both. Using the patterns of the returns from the high resolution FM-CW radar, the thickness of the reflecting regions were measured and the reflectivities were recalculated using estimates of beam filling based on the observed thickness. Two types of targets were included, refractivity fluctuations in the clear air due to convective activity and insects.

- II. 5-8 SIMULTANEOUS MICROWAVE IRRADIATION AND SPECTROPHOTOMETRIC OBSERVATION USING A CROSSED-BEAM APPARATUS.  
John W. Allis, Environmental Protection Agency,  
Research Triangle Park, North Carolina; and  
David E. Janes, Jr., Environmental Protection Agency,  
Washington, D.C.

A spectrophotometer has been adapted for use as a simultaneous observation-exposure system for irradiation of samples by 1.7 to 2.6 GHz electromagnetic radiation. The quality of the absorption spectra is not measurably impaired and the flexibility of the spectrophotometric technique remains intact.

A waveguide applicator is mounted vertically in the sample compartment of a Cary 15 spectrophotometer such that the sample can be placed simultaneously in the light path and in a slot in the applicator. A standard 1 cm path square cuvette contains the sample which is irradiated through the open top of the cuvette. Temperature of the sample and an unirradiated reference are monitored continuously without measurable interference from the microwave field. Temperature can be controlled within a few tenths of a degree between 15°C and 40°C and an absorbed dose rate can be calculated using thermal measurement techniques.

Microwave generator output and reflected power are monitored at all times. The frequency can be changed easily and standing waves minimized by adjusting a waveguide tuning section. The microwave energy within the basic frequency range can be applied as continuous wave or modulated.

PRECIPITATION: POLARIZATION AND  
STATISTICS; RADIOMETRY

L. J. Ippolito, Chairman

- II. 6-1 DEPOLARIZATION OF ATS-6 SATELLITE 20 GHZ BEACON TRANSMITTED THROUGH RAIN. D. A. Gray, Bell Laboratories, Crawford Hill Laboratory, Holmdel, New Jersey, 07733

We present first measurements of depolarization of a linearly polarized wave transmitted through rain on an earth-space path. The radio receiver used for the measurements, which provides 62 and 75 dB signal-to-noise ratios in the principal and cross polarization channels, respectively, will be described. The data obtained are compared with theoretical predictions. The worst measured cross talk ratio, 13 dB, was simultaneous with a 39 dB path attenuation observed during a heavy rain shower. Ancillary measurements show the 20 GHz cross polarization discrimination of the satellite's pencil beam antenna to be good near axis (greater than 40 dB), but poorer in other regions.

- II. 6-2 PRECIPITATION DEPOLARIZATION MEASUREMENTS WITH THE ATS-6 20 GHZ DOWNLINK. R. E. Marshall, C. W. Bostian, W. L. Stutzman, E. A. Manus, and P. H. Wiley, Department of Electrical Engineering, Virginia Polytechnic Institute and State University, Blacksburg, Virginia, 24061

As part of the ATS-6 millimeter wave experiment, the authors are measuring precipitation depolarization at 20 GHz. The measurement system uses a linear dual polarized receiving antenna feeding a single-channel switched receiver and offers residual cross polarization isolation of better than 30 dB. This paper discusses the depolarizing effects of rain, snow, and clouds and presents some recent observations.

- II. 6-3 MEASUREMENTS OF THE BACKSCATTER MATRIX OF DIELECTRIC BODIES. L. E. Allan and G. C. McCormick, National Research Council of Canada, Ottawa, Ontario, Canada

The difference in the principle plane elements,  $S_{xx}$  and  $S_{yy}$ , of the scattering matrix of spheroids can be measured directly by various techniques. A method is described for obtaining the parameters  $\nu$  and  $\delta$  where

$$ve^{i\delta} = \frac{S_{xx} - S_{yy}}{S_{xx} + S_{yy}} \quad (1)$$

using circular polarization at a frequency of 2.86 GHz. Right-hand and left-hand senses provide independent determinations. Specimens have been supported by nylon threads so arranged that they can be rotated through all aspects. Spheres and dipoles have been used for calibration purposes.

Measurements have been made on bodies having dielectric constants 2.56, 3.17, and 6.5 with axial ratios 0.5, 0.6, and 0.8. For Rayleigh scatterers  $\delta = 0$  and  $v$  depends on the shape but not on the size of the body. As the dimensions of the scatterer are increased toward and beyond resonance  $\delta$  becomes increasingly negative and  $v$  varies with size as well as shape.

II. 6-4 ATTENUATION STATISTICS CALCULATED FROM RADAR REFLECTIVITY DATA OF RAIN. Julius Goldhirsh, Applied Physics Laboratory, Johns Hopkins University, Silver Spring, Maryland

Fade depth and diversity gain statistics associated with earth-satellite paths have been calculated from radar reflectivity data of rain using modeling procedures. The reflectivity data base was obtained during the summer of 1973 at Wallops Island, Virginia using a high resolution S band radar interfaced with a computer and digital processing system. Fade statistics have been calculated for earth-terminal path angles of 30°, 45°, and 60° at the frequencies of 13, 18, 25, and 30 GHz.

Within the frequency interval and path angle range considered, the results show with good approximation the following salient features: (1) The fade depth exceeded (at any given probability and path angle) is proportional to the carrier frequency taken to a given exponent. (2) The fade depth exceeded (at any given frequency and probability) varies with path angle,  $\theta$ , according to the CSC  $\theta$  variation. (3) The rates at which the diversity gains approach their respective optima (associated with given fade depths) are essentially frequency independent. At a site spacing of 15 km, 85 to 90 percent of the optimum diversity gains are achieved.

The first result demonstrates that given fade statistics at two frequencies, fade statistics at any other frequency (between 13 and 30 GHz) may be predicted. The second result implies that given fade statistics at one path angle, fade statistics at other elevation angles may be predicted. Furthermore, this result implies that a large sample size of fade statistics gives rise to a condition such that the rain environment may be assumed (statistically) to possess uniform reflectivities (or rain rates). The third result may be useful in establishing design criteria associated with locating earth terminals for the space diversity mode.

- II. 6-5 EQUIVALENT PRECIPITATION. Claudio M. Einloft and Mauro S. Assis, CETUC - Catholic University, Rua Marquês de São Vicente, 209 - Gávea, Rio de Janeiro, Brazil

When considering rain effects on attenuation, a problem arises from the fact that the precipitation rate is not uniform over the whole length of a radio path. One solution to this problem is to use the concept of equivalent precipitation which corresponds to a uniform rain producing the same attenuation as the real precipitation (non-uniform). This concept has been introduced by French workers a few years ago, based on a small number of experimental results. We have re-analyzed the question with data from 21 experimental radio links at frequencies from 11 to 30 GHz and distances ranging from 3 to 80 km. The final curves give the relation between the equivalent precipitation and the punctual precipitation as a function of distance and the considered percentage of time (frequency dependence is not important in the range 10-30 GHz). A comparison with the previous French results shows that these earlier curves are too optimistic.

- II. 6-6 REMOTE SENSING OF ATMOSPHERIC WATER CONTENT FROM SATELLITES USING MICROWAVE RADIOMETRY. Norman C. Grody, National Oceanic and Atmospheric Administration, National Environmental Satellite Service, Washington, D.C., 20233

Analysis is presented which substantiates the high correlation achieved in relating integrated water vapor and cloud liquid water to brightness temperatures at frequencies near the 22.235 GHz water vapor line. The influence of atmospheric and surface variability is shown to be minimized over low emissivity sea surfaces. In the case of non-scattering precipitable clouds, the integrated liquid water is the sum of cloud and precipitable liquid water. However, the effect of scattering due to precipitation, if not taken into account, results in an under-estimate of integrated liquid water. Satellite data from the Nimbus-E Microwave Spectrometer aboard Nimbus-5 is compared with radiosonde water vapor measurements and cloud images recorded by the Temperature Humidity Infrared Radiometer aboard Nimbus-5.

- II. 6-7 ATMOSPHERIC ATTENUATION AT 15 AND 35 GHz FOR SLANT PATHS NEAR THE HORIZON. L. E. Telford and E. E. Altshuler, Microwave Physics Laboratory, Air Force Cambridge Research Laboratories, Hanscom AFB, Massachusetts, 01731

Atmospheric attenuation was measured in the Boston area at frequencies of 15 and 35 GHz for elevation angles from  $1^{\circ}$  to  $20^{\circ}$  for a period of approximately one year on days during which

there was no precipitation. The attenuation was determined from a measurement of the brightness temperature of the sun during rise and set times using the AFCRL 29-foot antenna. Scatter plots of attenuation as a function of absolute humidity showed that the correlation of attenuation with humidity decreased significantly at low elevation angles. There was a corresponding decrease in the correlations between the attenuations at 15 GHz and 35 GHz at the lower angles. It was found that the attenuation was proportional to the cosecant of the elevation angle for angles above  $10^\circ$ . An expression for the angle dependence of attenuation for lower angles was derived and compared with the measured data. On the basis of the data that have been obtained, the accuracy with which attenuation can be determined from absolute humidity and elevation angle is estimated.

II. 6-8 LOCAL VARIATIONS IN RADIOMETRIC SKY TEMPERATURE USING RADIOSONDE DATA. K. R. Carver and W. K. Cooper, Physical Science Laboratory, New Mexico State University, Las Cruces, 88003; and J. F. Paris, Lockheed Electronics Corp., Houston, Texas, 77058

A spherically stratified atmospheric radiative transfer model is used to compute local geographical and temporal fluctuations in the sky brightness temperature at 10, 18, 22, and 37 GHz using radiosonde data from coordinated balloon flights from four separate sites in the Chihuahuan desert of southern New Mexico over the period Nov. 1 - Dec. 6, 1974. Variations in the radiometric sky temperature are then examined with respect to local high desert geography and related meteorological profiles as well as the uncertainty connected with the water vapor volume absorption coefficient used in the model. The sky temperature is used as a reference for calibration of NASA Multifrequency Microwave Radiometer (MFMR) and Passive Microwave Imaging System (PMIS) when a suitable reflecting enclosure is used to block the radiation from surrounding terrain.

The four radiosonde launch sites, dispersed over 100 km with a 2.74 km high mountain range in between, varied in altitude from 1.22-1.35 km above MSL. Sky temperature fluctuations were most evident at the 22 GHz water vapor absorption line, with fluctuations in the zenith temperature being found between simultaneous ascensions from the same site. These data have led to procedures for estimating the uncertainty in  $T_{sky}$  caused by local geographical and temporal interpolation of radiosonde data.

COMMISSION II

1400 Thursday, June 5

158 Physics

ATS-6 MILLIMETER WAVE EXPERIMENTS; ATS-6 13/18 GHz EXPERIMENT

C. W. Bostian, Chairman

- II. 7-1 ATTENUATION OF 20 AND 30 GHz SATELLITE SIGNALS BY RAIN. Wolfhard Vogel, Bob M. Fannin, Archie W. Straiton and Norman K. Wagner, The University of Texas at Austin, Austin, Texas, 78712

This paper describes the participation by The University of Texas at Austin in the ATS-6 satellite millimeter experiment. Two 30 GHz phase lock receivers monitored the transmission from the satellite at two locations separated by ten kilometers. In addition, two radiometers operating at 20 GHz measured the sky temperatures in the direction of the satellite at two locations.

The 30 GHz transmissions were measured during as many rain storms as their prediction and the availability of the satellite signal permitted.

After being activated, the two radiometers were operated continuously except for minor interruptions due to equipment problems.

The measured signal loss at 30 GHz and the loss at 20 GHz calculated from the sky temperature data permitted a direct comparison of the rain attenuation at the two frequencies. The ratio of the thirty to twenty GHz losses varied over a wide range of about 3 to 7.

The comparison of the simultaneous losses at the two sites provided a measurement of the space diversity gain.

Weather Bureau data and local observations of the cloud heights and horizontal extents were analyzed and the concurrent attenuation was related to the cloud features.

- II. 7-2 ATMOSPHERIC ATTENUATION MEASUREMENTS AND PREDICTION TECHNIQUES AT 20 & 30 GHz WITH THE ATS-6 SATELLITE. Louis J. Ippolito, NASA Goddard Space Flight Center, Greenbelt, Maryland

The ATS-6 (Applications Technology Satellite) Millimeter Wave Experiment has been providing direct rain attenuation measurements at 20 and 30 GHz since July 1974 at a number of locations

in the continental United States. Studies at the NASA stations at Rosman, North Carolina, and Greenbelt, Maryland, are directed at an evaluation of: rain attenuation statistics, attenuation ratio variations, scintillation effects, coherence bandwidth in a 1400 MHz band, and attenuation prediction techniques utilizing rain gauge, radar, and radiometer measurements coincident with the earth-space attenuation measurements.

Results of the first 10 months of measurements are presented with major emphasis on the impact of the results on earth-space system design.

Attenuation ratios were found to be slightly greater than those predicted from the Medhurst values. Scintillations in excess of 5 dB have been observed at both 20 and 30 GHz in clear sky conditions. Fade duration and fade depth statistics indicate a number of large fades in excess of 20 dB occurring for sustained periods, at both 20 and 30 GHz.

Power margin requirements for Rosman developed from direct attenuation, rain gauge and radar measurements are shown to have a significant impact on millimeter wave system design.

II. 7-3 MEASUREMENT OF ATS-6 20/30 GHz SIGNALS AT CLARKSBURG, MARYLAND. D. J. Fang, J. M. Harris, G. Hyde, Propagation Department, COMSAT Laboratories, Clarksburg, Maryland, 20734

These measurements are part of the NASA/GSFC Long Baseline Diversity Measurements using the ATS-6 20/30 GHz millimeter wave experiment. The measurement equipment includes: (1) A 10-foot diameter antenna-receiver system for accepting 20 GHz satellite CW signals and a radiometer system at 11.7 GHz for monitoring sky noise temperature. (2) A 15-foot diameter antenna-receiver system capable of receiving 20 and 30 GHz main CW signals plus sidetones within 54 MHz bandwidth, and another radiometer system at 15.3 GHz. (3) Six rain gauges along the boresight path toward the satellite for recording instantaneous rainfall rates. (4) A weather radar at 5.4 GHz for detecting the motion pattern of the rain cloud in large scale.

Data analysis is performed by using received satellite signals as basic reference for correlation with other information derived from the radiometers, the rain gauges and the radar. Statistical relationships between satellite attenuation level and various meteorological parameters are examined. Important physical characteristics for prominent individual events of heavy rain storms are also studied.

II. 7-4 INITIAL RESULTS OF OSU 20 AND 30 GHz ATS-6  
PROPAGATION MEASUREMENTS.\* D. B. Hodge and  
D. M. Theobald, The Ohio State University  
ElectroScience Laboratory, Department of  
Electrical Engineering, Columbus, Ohio, 43212

The initial results of propagation measurements on the 20 and 30 GHz ATS-6 downlinks will be presented. Simultaneous 20 and 30 GHz radiometric temperature measurements are made for correlation with attenuation data. One fixed and one transportable station, each consisting of a 15 ft. parabolic antenna and a 20 and 30 GHz receiver-radiometer pair, are employed to make path diversity measurements at a separation of 12 km as well as at an extremely small separation of 7 meters. A third ground terminal provides 20 GHz radiometric temperature data only. All attenuation and temperature data are digitized and recorded in real time. The receiver data are sampled at rates up to 200 samples/second in order to permit analysis for scintillation characteristics.

\*The work reported in this paper was supported in part by Contract NAS5-21983 between NASA/Goddard Space Flight Center, and The Ohio State University Research Foundation.

II. 7-5 DATA REDUCTION AND PROCESSING FOR THE ATS-6 13/18 GHz  
COMSAT PROPAGATION EXPERIMENT. A. Kaul, B. Moseley  
and J. Steinhorn, COMSAT Laboratories

The effects of satellite orbital motion, attitude and temperature changes on the signals in the ATS-6 13/18 GHz COMSAT propagation experiment are described. It is shown that these effects may be removed to provide corrected data for analysis of propagation impairments at 13/18 GHz.

Parameters entering into data reduction and processing include satellite orbit parameters (inclination, longitude, etc.), slant range to each ground transmit site, transmit antenna patterns and boresight direction, satellite 13/18 GHz receive antenna patterns and boresight direction, satellite attitude, satellite 4 GHz transmit antenna pattern, and satellite temperature. The satellite diurnal motion combined with the ground transmit antenna and spacecraft receive antenna pattern characteristics cause a diurnal variation of the clear sky signal level. As the satellite attitude is changed for other experiments (ranging from Alaska, to the eastern Atlantic Ocean and to sub-satellite point), the changing gain of the spacecraft antennas towards the transmit sites must be taken into account. The gain of the transponder is also monitored by telemetry of temperatures and power output.

In proving out the data reduction scheme it was discovered that the nominal 2.9°E offset of the S/C 13/18 GHz receive antenna

led to problems in data reduction. Shifting the boresight axis to 2.7°, 1.3°N led to a best fit. Subsequent in-orbit measurements verified this.

II. 7-6 AT5-6 13/18 GHz COMSAT PROPAGATION EXPERIMENT.  
G. Hyde, COMSAT Labs, J. L. King, NASA/GSFC, and  
J. P. Steinhorn, COMSAT Labs

The COMSAT Propagation Experiment at 13/18 GHz using the AT5-6 satellite is described. 40 discrete signals in bands near 13 and 18 GHz are transmitted from 25 ground transmit sites, through the atmosphere to the transponder on the AT5-6 satellite, which retransmits at about 4.15 GHz down to the ground receive and data acquisition terminal.

There are twenty-five 18 GHz and fifteen 13 GHz transmitters grouped into three diversity locations (one dual frequency site and three single frequency sites spaced over about 40 km) 12 dual frequency sites and one single frequency site all east of the Mississippi River and spaced at least 160 km apart. Transmit antennas have 4° beam widths.

The transponder has redundant 13 and 18 GHz chains which translate the 13 and 18 GHz frequencies received to 4 GHz. The spacecraft 13/18 GHz receive antenna has an elliptical beam offset east. The S/C transmit antenna is approximately earth coverage. The 4 GHz transmissions are received at Andover, Maine, by the receive and data acquisition system.

The receive system provides a G/T of 37 dB/K. The 40 signals are downconverted, channelized and processed through individual phase-locked loop narrow band carrier processors, to provide a D.C. voltage which is measured, digitized and taped every second. The receiver is calibrated every eight hours by injection of known signals at each 4 GHz frequency at the horn. The tapes are reduced and analyzed at COMSAT Labs at Clarksburg, Maryland.

II. 7-7 PRELIMINARY RESULTS FROM THE AT5-6 13/18 GHz  
PROPAGATION EXPERIMENT. G. Hyde, COMSAT Labs,  
J. L. King, NASA/GSFC, and J. Stein, COMSAT Labs

The preliminary results of analysis of corrected data from the AT5-6 13/18 GHz COMSAT Propagation Experiment are presented. The experiment consists of transmitting 40 signals at 13 and 18 GHz from 25 sites covering the U.S. east of the Mississippi River through the atmosphere to AT5-6 spacecraft where signals are translated to 4 GHz and relayed back to ground for receiving, recording, reduction, processing and analysis.

There are 15 dual frequency 13/18 GHz sites spaced at least 160 km apart, providing comparison of path loss at 13 and 18 GHz and attenuation statistics for the eastern U.S. Data is shown for

sites at Miami, Fla., Tampa, Fla., Atlanta, Ga., Fayetteville, N.C., Rosman, N.C., New Orleans, La., Starksville, Miss., Nashville, Tenn., Wallops Is., Va., Clarksburg, Md., Columbus, Ohio, Philadelphia, Pa., Detroit, Michigan, Boston, Mass., and Andover, Me.

There are 3 diversity locations (each with one dual frequency site and three 18 GHz sites spaced east-west over approximately 40 km) providing direct information on diversity improvement versus separation at 18 GHz, and by comparison of 13 and 18 GHz attenuation at 13 GHz. Data are presented for diversity locations at Starkeville, Miss., Columbus, Ohio, and Boston, Mass.

COMMISSION III

ON THE IONOSPHERE

John M. Kelso, Chairman

<u>Session</u>	<u>Page</u>
1. GENERAL TOPICS IN IONOSPHERIC RADIO (1400 Tuesday, June 3, 144 Physics) Chairman: J. M. Kelso ITT, Electro-Physics Labs, Inc.	40
2. SATELLITE BEACON EXPERIMENTS (0900 Wednesday, June 4, 136 Physics) Chairman: T. A. Seliga The Ohio State University	45
3. SCINTILLATION AND IRREGULARITY (1400 Wednesday, June 4, 280 MRL) Chairman: E. A. Mechtly University of Illinois	48
4. E-REGION AND BELOW (0900 Thursday, June 5, 280 MRL) Chairman: E. K. Smith OT/ITS	51

COMMISSION III

1400 Tuesday, June 3

144 Physics

GENERAL TOPICS IN IONOSPHERIC RADIO

J. M. Kelso, Chairman

III. 1-1 CCIR NEEDS IN IONOSPHERIC PROPAGATION.  
Ernest K. Smith.

At the URSI XVIII General Assembly in Lima in August of 1975, one of the topics of the Symposium on Radio Waves and the Ionosphere is Ionospheric Problems in Radio Communication. An effort has been made on the international front to solicit the views of URSI participants who are also active in the CCIR (International Radio Consultative Committee of the ITU) as to the important problems.

A US-CCIR organization exists (organized by the State Department) in rather analogous fashion to the domestic URSI structure. Study Group 6 of the CCIR deals with ionospheric propagation, and U.S. Study Group 6 has been struggling with the question of research priorities.

The purpose of this paper is to bring to the Members of IEEE/AP-S and of US-URSI the research priorities as seen by US-CCIR Study Group 6 (of which the author is chairman). This is felt to be in keeping with the emphasis of this meeting on radio propagation aspects. The current list of priorities encompassing VLF through SHF will be presented, and the rationale behind the list will be discussed.

III. 1-2 INVERSION OF OBLIQUE IONOGRAMS FOR ECCENTRIC QUASI-PARABOLIC LAYER PARAMETERS. N. Narayana Rao and Parviz Parhami, Department of Electrical Engineering, University of Illinois at Urbana-Champaign, Urbana, Illinois, 61801

A method is presented for the derivation of the parameters of an ionospheric layer model including horizontal gradients of electron density from sweep-frequency oblique ionogram data. The model employed is a quasiparabolic layer having its center of curvature displaced from the center of the earth. Briefly the method consists of an iterative procedure for obtaining a five-parameter solution for the eccentric layer model consistent with five points on the ionogram in a best fit sense. The method is illustrated with an example.

III. 1-3 ERROR ANALYSIS OF PROFILE INVERSION FOR IONOSPHERIC INHOMOGENEITIES BY THE REFLECTION COEFFICIENT METHOD. Saeyoung Ahn and Arthur K. Jordan, Naval Research Laboratory, Washington, D.C., 20375

The reconstruction of the electron density profile,  $N(x)$ , of an inhomogeneous ionosphere is discussed. If the reflection coefficient,  $r(k)$ , of the incident radio pulse is analyzed as a (complex) function of wave number,  $k$ , then improved resolution of ionospheric electron density profiles can be obtained. An exact mathematical procedure for ionospheric profile inversion is described which does not rely on approximate numerical integration; this procedure also provides the exact electromagnetic field which propagates through the medium described by that profile. The mathematical procedure is applied to a general third-order approximation for  $r(k)$  and a profile is obtained which closely approximates a typical ionospheric case. The error bounds on the electron density profile are obtained from the analysis of variations in the reflection coefficient for the third-order case.

III. 1-4 SYNTHESIS OF OPTIMUM RECTANGULAR APERTURES FOR HIGH FREQUENCY IONOSPHERIC PROPAGATION. R. L. Bell, C. H. Vandament, P. A. Mayer, C. G. Hood, Collins Radio Group/Rockwell International

An optimization algorithm has been combined with a high frequency ionospheric prediction program to synthesize optimum antenna apertures for coverage of a specified area over a given time period. The areas and time domain coverage are approximated by considering discrete points in the receive area at specified time intervals. Weighting factors were applied to these points to achieve weighted area coverage when desired. The path parameters were predicted using an HF ionospheric radio prediction program using an isotropic transmit antenna and actual patterns for the receive antenna. Seven modes were considered and the appropriate path parameters for each mode were stored on a disc file for later use in the optimization. During optimization, the isotropic antenna gain is replaced by the computed gain of the optimized aperture including effects of real ground. Signal to noise ratio or circuit reliability may be used as the significant parameter in the objective function. FSN and reliability are recomputed for each mode at each step in the optimization process.

- III. 1-5 A HIGH POWER METEOR RADAR SYSTEM WITH REAL TIME DATA PROCESSING. G. C. Hess, S. A. Bowhill and M. A. Geller, Aeronomy Laboratory, Department of Electrical Engineering, University of Illinois, Urbana, Illinois, 61801

The meteor radar system at the Aeronomy Laboratory of the University of Illinois uses a 5 Mw pulsed transmitter at 41 MHz frequency, together with a PDP15/40 computer for data collection and real time processing of upper atmosphere wind data. Integration of receiving hardware with software range, doppler, and angle algorithms is discussed. Preliminary results of N-S winds in the meteor region (80-120 km) are presented.

- III. 1-6 EXPERIMENTAL STUDIES OF VLF/LF PROPAGATION OVER DISTANCES OF APPROXIMATELY 1000 KM. C. P. Tou, Department of Electrical Engineering, Nova Scotia Technical College, Halifax, Nova Scotia, Canada; and D. B. Ross, Communications Research Centre, Department of Communications, Ottawa, Ontario, Canada

Experimental investigations of multi-frequency VLF/LF propagation have been carried out in Canada over the Ottawa-Halifax (west-to-east) and Ottawa-Great Whale River (south-to-north) paths during the past four years. The relative phase and amplitude of the total field have been measured at six different frequencies. The observed data have been processed and analyzed extensively by the technique of normal loop induction locus and partially by waveguide mode theory.

The analysis of the data is rather complicated because the groundwave may no longer be neglected if ray theory is applied and more modes must be considered when waveguide mode theory is used. However, over shorter propagation paths the propagation characteristics are more sensitive to changes of ionospheric conditions than in the case of very long propagation paths. Thus, the data would provide valuable information with regard to the propagation characteristics and the physical properties of the lower ionosphere.

This paper reports the results of both theoretical and statistical analysis of diurnal and seasonal variations of the signals under normal propagation conditions. In particular, the sunrise and sunset effects on propagation are treated in detail. It is believed that the results would provide a better understanding and more reliable prediction of regular diurnal and seasonal changes for a given path of the same order of distances.

III. 1-7 RESONANCE LINE SPLITTING AS A FUNCTION OF MEASUREMENT PARAMETERS AND RESONANCE BANDWIDTH. A. Paul, COMSAT Laboratories; and C. Polk, University of Rhode Island

This paper attempts to explain the pronounced "line splitting" in the "Schumann" extremely low frequency (ELF) earth-ionosphere cavity resonance spectrum which is occasionally observed during periods of high Solar activity. Experimental results indicated that the frequency of occurrence of "split" peaks is directly related to the width of the resonance peaks and is inversely proportional to the length of the data sample. The normalized standard error  $\epsilon$  in the evaluation of the power spectral density is also inversely proportional to the length of the data sample and the spectral resolution. It is possible to predict the probability of occurrence of "split" peaks as a function of measurement parameters, i.e., sample length and frequency resolution, and the characteristics of the true power spectrum (resonance bandwidth or Q). To do this, the probability of finding a "split" (i.e., two peaks and a valley of specified depth) in the experimental record of white noise is first investigated and the probability of "split" occurrence is related to the measurement parameters (i.e., observation time and frequency resolution). After solution of this basic problem the effect of different resonance peak bandwidths in an ELF spectrum (i.e., not white noise) on the frequency of occurrence of "split" peaks is investigated. The numerical results confirm that the frequency of occurrence of "split" peaks is inversely proportional to the length of the data sample and is directly proportional to the width of the resonance peak. The number of "split" occurrences in experimentally determined spectra was also found to be close to that predicted by an approximate computation. Thus it appears that observed "split" peaks are not a property of the earth-ionosphere cavity, but are the consequence of the unavoidable statistical error produced by the use of a data sample of finite length.

III. 1-8 SPECTRAL ANALYSES OF IONOSPHERIC-DOPPLER TIME SERIES. Kurt Toman, Ionospheric Physics Laboratory, Air Force Cambridge Research Laboratories, Hanscom AFB, Massachusetts, 01731

For assessing the dynamic behavior of periodicities between 5 and 100 minutes due to wavelike perturbations in the ionosphere, a conventional Fourier analysis method was previously applied to time series derived from mid-latitude ionospheric Doppler measurements, and random numbers. For selected ionospheric events, these results can now be compared with those obtained from the high-resolution maximum-entropy method. While the dynamics of spectral behavior is verified, truncation effects, inherent in the Fourier analysis of relatively short data samples, required caution in the physical interpretation of spectral peaks shifting

in time and frequency. For an appropriate number of auto-correlation-lag values Burg's unconventional maximum-entropy method reveals temporal changes in the spectrum distributions that appear to result from actual changes in the period of wavelike ionospheric perturbations.

SATELLITE BEACON EXPERIMENTS

T. A. Seliga, Chairman

- III. 2-1 SIMULATION AND MEASUREMENT OF EXOSPHERIC ELECTRON CONTENT. D. A. Poletti-Liuzzi, K. C. Yeh and C. H. Liu, Department of Electrical Engineering, University of Illinois, Urbana, Illinois, 61801; and M. Y. Youakim, MYY Systems, Champaign, Illinois, 61820

The ATS-6 beacon experiments are capable of measuring the value of electron content by using the Faraday effect, the differential group delay and the differential Doppler effect. Since the Faraday effect is weighted by the Earth's magnetic field, this method is insensitive to electrons in the exosphere, while both the differential group delay and the differential Doppler are equally sensitive to all electrons regardless of their location along the radio path. Therefore, by combining these methods the exospheric content can be measured and studied. In this paper we present some results of computer simulation to show the sensitivity of the technique to various ionospheric parameters. Some preliminary results of the measurements both for normal days and during magnetic storms will also be presented.

- III. 2-2 OBSERVATIONS OF A TRAVELING IONOSPHERIC DISTURBANCE WITH THE ATS-6 RADIO BEACON. K. Davies, R. B. Fritz, J. E. Jones, Space Environment Laboratory, NOAA/ERL, Boulder, Colorado, 80302; and G. Hartmann, J. P. Schödel, Max-Planck Institut, Lindau/Harz, West Germany

Closely spaced and widely spaced receivers are used to record radio signals from the ATS-6 radio beacon. The closely spaced Faraday receivers are located at the corners of an approximately equilateral triangle of side  $\approx 120$  km in Colorado. The other receivers are at Bozeman, Montana and at Dallas, Texas. From the time displacements the horizontal motions of ionospheric irregularities are deduced.

A particular event which occurred on October 14, 1974, and which moved toward the southwest with a speed of around 75 m/s is discussed. The total electron contents in Colorado increased suddenly and the "front" was followed by a region of strong spread F which produced enhanced radio scintillations.

III. 2-3 IONOSPHERE/PLASMASPHERE COLUMNAR ELECTRON CONTENTS MEASURED WITH THE ATS-6 RADIO BEACON. K. Davies, R. B. Fritz, A. K. Paul, Space Environment Laboratory, NOAA/ERL, Boulder, Colorado, 80302; G. K. Hartmann, G. Schmidt, Max-Planck Institut, Lindau/Harz, West Germany; and R. Leitinger, University of Graz, Graz, Austria

An attempt is made to determine the columnar total electron content along the path from Boulder (40°N, 105°W) to the ATS-6 satellite (0°, 94°W). The ATS-6 data include modulation phase and Faraday rotation. The content up to 1100 km is measured by phase observations of the orbiting NNSS satellites at Boulder and at Las Vegas, N.M., which enables the latitudinal gradient to be determined. These data are supplemented by profiles from topside and bottomside ionograms. Phase and Faraday measurements indicate that at night the plasmasphere content (above about 2000 km) is about 30 to 40% of the ionospheric content and by day it is about 10%.

The ATS-6 data are in general agreement with the NNSS, topside, and bottomside measurements. The largest discrepancies occur when the radio raypaths differ most in geographical direction.

Marked changes in the ionosphere and plasmasphere contents occur during storms when the plasmasphere content usually decreases. During prolonged quiet the plasmasphere content becomes roughly independent of time whereas the ionosphere content exhibits the usual diurnal variations.

III. 2-4 ATS-6 OBSERVATIONS OF THE IONOSPHERIC EFFECTS OF SOLAR FLARES. R. F. Donnelly, R. B. Fritz, D. N. Anderson, K. Davies, and R. N. Grubb, Space Environment Lab, NOAA ERL, Boulder, Colorado, 80302

X-ray and EUV (extreme ultraviolet) bursts of solar flares cause SITECs (sudden increases in total ionospheric electron content). Several SITECs were observed with high time resolution (1 sec) by the ATS-6 radio beacon experiments, including the white-light flare event of 1356 UT July 4, 1974. An empirical model of solar flare X-ray and EUV radiation was fitted to satellite X-ray measurements and other flare observations for each SITEC. The ionospheric effects of the flare radiations were computed and compared with the SITEC observations. During the early impulsive phase of the flare, the time dependence of the time-rate-of-change of the total electron content ( $dN_T/dt$ ) closely follows the bursts of photoionization caused by the impulsive flare bursts of EUV radiation. Frequency deviations derived from radio beacon experiments agree well with ground-based SFD observations during this portion of a flare. High time-resolution SITEC observations are therefore useful as broadband detectors of impulsive EUV radiation. During the later slow coronal component of the solar

flare, the E region approaches photoionization equilibrium and the SITEC is dominated by the F-region ionization enhancement, where electron loss rates are small and transport processes are significant.

III. 2-5 INITIAL POLARIZATION TRANSMITTED AT VHF FROM GEO-STATIONARY SATELLITE BEACONS. John A. Klobuchar, Air Force Cambridge Research Laboratories, Bedford, Massachusetts

Measurements of Faraday polarization rotation of VHF radio waves transmitted from geostationary satellites have been made for several years by many workers at various locations throughout the world to study the Total Electron Content (TEC) of the earth's ionosphere. In order to determine the absolute amount of total Faraday rotation a knowledge of the initial plane of polarization as transmitted from the satellite with respect to a known reference is necessary. A knowledge of this initial polarization angle is particularly important when the total Faraday rotation is small, such as at near-equatorial regions, and at all locations during nighttime, particularly under solar minimum conditions.

By using a VHF lunar radar at a time when the moon passed nearly behind each satellite this initial polarization has been determined with respect to the satellite spin axis for eight different satellites. These results are of use to all groups who intend measuring total Faraday polarization rotation. Problems in polarization measurements from geostationary satellite VHF signals and the resultant accuracy of the TEC determination will be discussed.

III. 2-6 A COMPARISON OF TOTAL ELECTRON CONTENT AS DETERMINED FROM GROUP PATH DELAY AND FARADAY MEASUREMENTS. John A. Klobuchar, Air Force Cambridge Research Laboratories, Bedford, Massachusetts

Using VHF and UHF radio waves transmitted from the geostationary satellite ATS-6 two different methods of measuring the total electron content along the path from the satellite have been used. The group path delay technique allow the measurement of  $\int N dl$  along the path, called the true TEC. The Faraday measurement of  $\int B \cos\theta N dl$ , called by some, IEC, or Ionospheric Electron Content, is a measure of the number of electrons in the first 2000-4000 km. of vertical height. Before the launch of ATS-6 virtually all TEC measurements from radio waves from geostationary satellites were made using the Faraday effect. Measurements of differences between these two experimental quantities will be discussed.

SCINTILLATION AND IRREGULARITY

E. A. Mechtly, Chairman

- III. 3-1 ANALYSIS OF THE BACKSCATTER SPECTRUM IN AN IONOSPHERIC MODIFICATION EXPERIMENT. H. Kim, F. W. Crawford, and K. J. Harker, Institute for Plasma Research, Stanford University, Stanford, California, 94305

The purpose of this study is to compare predictions of the backscatter spectrum, including effects of ionospheric inhomogeneity, with experimental observations of incoherent backscatter from an artificially heated region.<sup>1</sup> Our calculations show that the strongest backscatter echo received is not from the reflection level, but from a region some distance below (about 900 m for an experiment carried out at Arecibo<sup>1</sup>). By taking the standing wave pattern of the pump into account properly, the present theory explains certain asymmetrical features of the up-shifted and down-shifted plasma lines in the backscatter spectrum, and the several satellite peaks typically accompanying them.

1. I. J. Kantor, J. Geophys. Res., 79, 199-208 (1974).

- III. 3-2 A STUDY OF FREQUENCY AND SPATIAL CORRELATIONS OF TRANSIONOSPHERIC RADIO SIGNALS. C. H. Liu and K. C. Yeh, Department of Electrical Engineering, University of Illinois, Urbana, Illinois, 61801

The frequency and spatial correlations of transionospheric radio signals are studied using the parabolic equation method. Equations for the mutual intensity functions of the signal are derived that take into account the effects of multiple scattering. These equations are solved numerically. The solutions are then used to investigate the dependence of the correlation functions on the various ionospheric parameters such as the power spectrum of irregularities, their size, the slab thickness, the height, etc. Plots showing contours of constant correlation coefficients as functions of frequency and spatial separations will be given. Applications of the computed results to the characterization of transionospheric communication channels and to the frequency- and/or space-diversity schemes will be discussed.

III. 3-3 HIGH LATITUDE F LAYER IRREGULARITIES DURING THE  
MAGNETIC STORM OF OCT. 31 - NOV. 1, 1972.  
Jules Aarons, Ionospheric Physics Laboratory, Air  
Force Cambridge Research Laboratories, Hanscom Air  
Force Base, Massachusetts, 01731

Using the scintillation of radio beacons of satellites and of radio stars as a means of determining the intensity variations of the small scale F layer irregularities over large areas, observations of the high latitude effects of the magnetic storm of Oct. 31 - Nov. 1, 1972, were examined.

During the initial phase of the winter storm studied, the irregularity region at 63° invariant latitude was affected. Within minutes the scintillation intensities at latitudes of 60° increased but remained high for less than an hour. Within hours the 60° latitude was reached by the main phase of the storm and scintillation indices remained high for the night. At later times during the main phase of the storm lower latitudes (53° to 45°) showed increased irregularity intensity.

If the intense magnetic bay is considered as an impulse function the velocities of the equatorward source producing the irregularities vary from 300-600 meters per second in the region from 57° invariant latitude to 53°, slowing to 100-200 meters per second in the region 53°-45°.

The irregularity intensity at each site is strongly controlled by the intensity of the local magnetic variations.

A comparison with auroral photographs indicate that even 4° equatorward of the optical aurora, the irregularity intensities at F layer heights are considerable. High levels of scintillation activity are noted poleward of the diffuse aurora.

With the onset of very intense irregularities, a large percentage increase in total electron content was observed both at 53° and 60° invariant latitude for this storm; not all magnetic storms show this effect.

Heat conduction due to auroral current energy dissipation or from isotropic electric fields is postulated as the source for the production of F layer irregularities.

III. 3-4 IONOSPHERIC SCINTILLATION AT 1.5 and 4 GHz:  
SIMULTANEOUS RECORDING AT TANGUA, BRAZIL.  
R. R. Taur, COMSAT Laboratories

The data of simultaneously recorded 1.5 and 4 GHz scintillations at Tangua, Brazil, have been analyzed. It is found that the scintillation index varies approximately as  $\lambda$  (wavelength) between 1.5 and 4 GHz. The amplitude distributions, especially

that of the 1.5 GHz data, are somewhat irregular in shape and cannot be represented by a simple mathematical expression.

The power spectra of the amplitude fluctuations show a slope of  $-3$  and have low wave number roll-offs near  $10^{-2} \text{ m}^{-1}$ . Some possible implications of this findings are discussed. Half of the 4 GHz power spectra show the minima which are predicted by the thin-screen, weak scattering theory. The  $1/e$  fall offs of the auto-correlation correspond to sizes between 100 and 200 m. The cross-correlations between the 1.5 and 4 GHz scintillations are about 0.3.

---

This abstract is based upon work performed in COMSAT Laboratories under the sponsorship of the International Telecommunications Satellite Organization (INTELSAT). Views expressed in this abstract are not necessarily those of INTELSAT.

III. 3-5 SCATTERING FROM A TURBULENT PLASMA IN A MAGNETIC FIELD. K. Sivaprasad, R. Swift, M. Yildiz, College of Technology, University of New Hampshire, Durham, New Hampshire

Considerable theoretical work on the calculation of radar cross-sections from the weakly ionized wakes of reentry vehicles illuminated by a monochromatic wave have been reported in the literature. The radar cross-sections are expressed in terms of the spatial autocorrelation of the random electron density distribution in the vehicle wake. In this investigation, the scattering cross-sections from an electron plasma in a magnetic field illuminated by a plane wave is treated using the method of random phase approximation from quantum field theory. In both the classical and semi-classical limits,  $\hbar \rightarrow 0$ , the well-known Bernstein modes are obtained from the general results.

COMMISSION III

0900 Thursday, June 5

280 MRL

E-REGION AND BELOW

E. K. Smith, Chairman

- III. 4-1 RADIO EVIDENCE FOR INTERMITTENT MESOSPHERIC TURBULENCE.  
P. K. Rastogi and S. A. Bowhill, Aeronomy Laboratory,  
Department of Electrical Engineering, University of  
Illinois, Urbana, Illinois, 61801

Strong intermittency of coherent VHF radio echoes from 70-80 km height, observed at Jicamarca, Peru, suggests the existence of sudden bursts in the energy dissipated per unit mass by turbulence. The detailed complex autocorrelation function of these echoes is analyzed to show the presence of discrete layers of turbulence. It is estimated that these layers have a thickness of the order of 1 km or less. Horizontal size of these layers is estimated from echoes observed simultaneously from mesospheric regions separated by ~4.5 km, and is compared with the horizontal scale of gravity waves observed in the mesosphere. The conclusion that the turbulence in the mesosphere is intermittent in time and space is discussed in the context of gravity wave instabilities.

- III. 4-2 ELECTRON-DENSITY MEASUREMENTS IN THE D REGION BY A DIFFERENTIAL-PHASE PARTIAL-REFLECTION METHOD.  
D. S. Wratt, Aeronomy Laboratory, Department of  
Electrical Engineering, University of Illinois,  
Urbana, Illinois, 61801

From the complex correlation between ordinary and extraordinary signals partially reflected from heights within the D region, a number of electron-density profiles were calculated. The deduced electron densities for heights near 74 kilometers were consistent with the results of simultaneous differential-absorption measurements. It was found that for a transmitter frequency of 2.4 MHz the complex correlation differential-phase technique was suitable for determining the electron density only below 80 km altitude.

- III. 4-3 HORIZONTAL STRUCTURE OF MIDLATITUDE SPORADIC-E LAYERS OBSERVED BY INCOHERENT SCATTER RADAR. K. L. Miller and L. G. Smith, Aeronomy Laboratory, Department of Electrical Engineering, University of Illinois, Urbana, Illinois, 61801

An investigation of the horizontal structure of sporadic-E layers has been made using the incoherent scatter radar at the Arecibo

Observatory. Data are presented for two experiments, timed to coincide with the presence of sporadic-E layers on an ionosonde; one with the radar beam held in a vertical position, another with the beam scanning in azimuth across a sporadic-E layer. The first experiment was made at sunset and shows the passage of a large region of ionization, about 150 km in extent, having little small-scale horizontal structure. The second, at mid-day, shows considerable variation in the value of the maximum electron density in the vertical variation in the value of the maximum electron density in the vertical cross-section of an intense sporadic-E layer. The horizontal dimensions of the features range in size down to the resolution of the radar (300 m). By considering the data statistically it is shown that small patches, 300 m or less in horizontal extent, exist in the sporadic-E layer with densities great enough to account for the maximum frequency of the echo recorded on the ionosonde located at the observatory.

- III. 4-4 THE INTERMEDIATE LAYER OF THE NIGHTTIME E REGION.  
H. D. Voss, L. G. Smith and M. A. Geller, Aeronomy  
Laboratory, Department of Electrical Engineering,  
University of Illinois, Urbana, Illinois, 61801

Ionograms and rocket observations show the presence of a layer in the upper E region near midnight. This intermediate layer is formed by redistribution of ionization under the influence of neutral winds. The descent of the layer between midnight and sunrise shows the effect of the (2, 4) mode of the semi-diurnal tide. The source of this ionization near midnight is shown to be strongly dependent on geomagnetic activity. It is suggested that, even under rather quiet geomagnetic conditions, energetic electrons are an important source of this ionization.

- III. 4-5 SPECTRAL ANALYSIS OF E-REGION "DRIFT" MEASUREMENTS  
IN EGLIN, FLORIDA. K. Bibl and B. W. Reinisch,  
Lowell Technological Institute Research Foundation,  
450 Aiken Street, Lowell, Massachusetts, 01854;  
and W. Pfister, Formerly--Air Force Cambridge  
Research Laboratories, Now--16 Reed Street,  
Lexington, Massachusetts, 02173

Complex ionospheric echo amplitudes have been measured at three spaced antennas and different frequencies and ranges during several days of observation periods in the Spring of 1972 and 1973. Spectral analysis determines Doppler frequency and angle of arrival of the echo returns. One of the tools used for the interpretation of the data is a sky map where the reflection areas for each Doppler component observed in a 2.2 minute period are presented in an overhead horizontal plane. The observations can be classified into three categories. The first one corresponds to a virtually specular reflection from a smooth ionosphere with very narrow Doppler spread and almost negligible Doppler

shift appearing not far from zenith. The second category ideally is described by a straight line in the sky map with equally distributed spacings of Doppler frequency. This is produced by a drift motion of small scale structure in a horizontal or inclined ionosphere. In the third category the line in the sky map is definitely curved and the distribution of Doppler frequencies is more complicated. This requires the presence of a large scale structure in the order of tens of kilometers (or more) in addition to the moving fine structure. Frequently periods of the large scale structure in the order of 40 minutes can be detected from a sequence of sky maps even in the case of category one.

III. 4-6 NONLINEAR PROPAGATION OF INTENSE ELECTROMAGNETIC PULSES THROUGH THE D-REGION OF THE IONOSPHERE.  
Dr. William A. Seidler, II, Capt., USAF, Air Force Weapons Laboratory

The effects of the nonlinear plasma of the D-Region on high energy propagating EM pulses is examined using the high frequency approximation to Maxwell's Equations in retarded time.<sup>1</sup> The nonlinear coupling of the EM pulse to a January-noon D-Region plasma is predicted using the moments of the Boltzmann Equation in the earth's magnetic field. Energy is predicted to be absorbed from the pulse from frequency components up to 20 MHz. This energy absorption causes electron temperatures to increase from 0.02 ev to 100.0 ev, enhancing the electron-neutral collision processes. Collision frequencies are increased by three orders of magnitude, causing the absorption of from 92% to 96% of the pulses energy.

1. Karzas, W. J. and R. Lather, Detection of the Electromagnetic Radiation from Nuclear Explosions in Space, Phys. Rev., Vol. 137-3B, B1369, March 8, 1965.

COMMISSION VI

RADIO WAVES AND TRANSMISSION OF INFORMATION

Aharon A. Ksienski, Chairman

<u>Session</u>	<u>Page</u>
1. HIGH FREQUENCY DIFFRACTION (1400 Tuesday, June 3, 136 Physics) Chairman: T. B. A. Senior University of Michigan	56
2. OPTICS (0900 Tuesday, June 3, 143 Physics) Chairman: C. Yeh University of California	62
3. TRANSIENTS I (0900 Wednesday, June 4, 141 Physics) Chairman: D. L. Moffatt The Ohio State University	67
4. ARRAYS (0900 Wednesday, June 4, 144 Physics) Chairman: V. Galindo Jet Propulsion Laboratory	73
5. ANTENNAS (1400 Wednesday, June 4, 144 Physics) Chairman: K. F. Casey Kansas State University	79
6. ELECTROMAGNETIC THEORY (0900 Thursday, June 5, 151 Physics) Chairman: Chen To Tai University of Michigan	86
7. NUMERICAL METHODS (1400 Thursday, June 5, 144 Physics) Chairman: G. Thiele The Ohio State University	93
8. BIOLOGICAL EFFECTS (0900 Thursday, June 5, 136 Physics) Chairman: C. C. Johnson University of Utah	99

<u>Session</u>	<u>Page</u>
9. TRANSIENTS II (1400 Thursday, June 5, 151 Physics) Chairman: D. G. Dudley University of Arizona	105
10. /AP-S 17. RAY TECHNIQUES IN ELECTROMAGNETICS - A STATE-OF-THE-ART-REVIEW (0900 Wednesday, June 4, 151 Physics) Chairmen: P. L. E. Uslenghi University of Illinois L. B. Felsen Polytechnic Institute of New York	110
11. /AP-S 19. ELECTROMAGNETIC PULSE AND RELATED TOPICS (1400 Wednesday, June 4, 151 Physics) Chairmen: F. Tesche Science Applications, Inc. A. Poggio Lawrence Livermore Laboratory C. E. Baum Air Force Weapons Laboratory	111

## HIGH FREQUENCY DIFFRACTION

T. B. A. Senior, Chairman

- VI. 1-1 CREEPING WAVES ON A PERFECTLY CONDUCTING CONE.  
 K. K. Chan, L. B. Felsen, A. Hessel and J. Shmoys,  
 Department of Electrical Engineering and Electro-  
 physics, Polytechnic Institute of New York,  
 Farmingdale, New York, 11735

When an electromagnetic dipole source is located on the surface of a perfectly conducting cone, the induced currents below the horizon of the source are established by creeping waves provided that source and observation points are situated in regions where  $kR \gg 1$ . Here,  $k$  is the wavenumber descriptive of the time-harmonic oscillations and  $R$  is the cross sectional radius of the cone at the point in question. To establish the propagation characteristics of the creeping waves, we employ a characteristic Green's function formulation in spherical  $(r, \theta, \phi)$  coordinates, with  $\phi$  regarded as a variable in an infinitely extended angular space. In the resulting double integral representation, approximations are made that eliminate reflections from the cone tip. Also, in the Legendre functions  $P_{\nu}^{-\mu}(x)$  that occur in the integrand, attention is confined to large values of the integration variables  $\nu$  and  $\mu$ . In this range, relevant for the extraction of creeping waves, the Legendre functions can be replaced by uniform asymptotic Airy approximations. After evaluation of the  $\mu$  integral by residues and the  $\nu$  integral by the method of saddle points, one obtains an asymptotic formula that can be interpreted in terms of ray-optical propagation along a geodesic path on the cone surface. The formula also contains launching and detachment coefficients dependent on the source and observation point locations, respectively. When the apex is removed to infinity so that the cone degenerates into a circular cylinder, the results obtained are shown to reduce to the known formulas for conventional creeping waves.

The cone configuration provides an important canonical prototype which can be used to check the validity of GTD results postulated for general convex surfaces. The formulas are also relevant to the calculation of mutual coupling between apertures on the cone surface.

- VI. 1-2 ON THE DYADIC SLOPE DIFFRACTION COEFFICIENT.  
Y. M. Hwang, Antenna Department, WDL Division,  
PHILCO-FORD, Palo Alto, California, 94303  
(Formerly with The Ohio State University); and  
R. G. Kouyoumjian, The Ohio State University,  
Columbus, Ohio, 43210

The dyadic diffraction coefficient for an edge derived by Kouyoumjian and Pathak(1) is valid only if the field incident on the edge is slowly varying. Recently an additional term in the dyadic edge diffraction coefficient was reported(2); this is referred to as the dyadic slope diffraction coefficient. It relates the diffracted field to the spatial derivatives of the incident field, and it is important because it ensures that the derivatives of the diffracted field are continuous at shadow and reflection boundaries.

In the present paper the slope diffraction coefficient is derived by a new method. The field incident at the edge is decomposed into a sum of inhomogeneous plane waves, the edge diffraction for each of these waves is determined, and the diffracted field is then synthesized from these components. The new expression for the slope diffracted field is compared with that reported earlier. Examples involving significant slope diffraction effects are presented which are different from those reported earlier(2).

(1) R. G. Kouyoumjian and P. H. Pathak, "A Uniform Geometrical Theory of Diffraction for an Edge in a Perfectly-Conducting Surface," IEEE Proc., 62, p. 1448 (1974).

(2) Y. M. Hwang and R. G. Kouyoumjian, "A Dyadic Coefficient for an Electromagnetic Wave which is Rapidly-Varying at an Edge," URSI 1974 Annual Meeting, Boulder, Colorado.

- VI. 1-3 SPECTRAL THEORY OF DIFFRACTION--A NEW APPROACH FOR SOLVING HIGH FREQUENCY DIFFRACTION PROBLEMS.  
R. Mittra, Y. Rahmat-Samii and W. L. Ko,  
Electromagnetics Laboratory, Department of  
Electrical Engineering, University of Illinois,  
Urbana, Illinois, 61801

The geometrical theory of diffraction (GTD) is known to provide a convenient and powerful means for constructing asymptotic solutions to scattering from bodies whose characteristic dimensions are large compared to the wave length. It is well known, however, that in the application of GTD, special treatments are required in the neighborhood of shadow boundaries and caustics where the GTD solution for the diffracted fields diverge to infinity. A number of techniques have been suggested for alleviating this difficulty in the neighborhood of shadow boundaries. Most of these modify the

GTD diffraction coefficients in some manner, e.g., by introducing multiplicative transition region functions,<sup>1</sup> or additive compensating functions<sup>2,3</sup> that cancel out the undesirable and fictitious infinities in the GTD diffracted field at shadow boundaries. However, limitations exist in the use of these functions when there is a confluence of the caustic direction and the shadow boundary. Moreover, difficulties may arise in the accurate numerical computation of the fields in the neighborhood of the shadow boundaries because of the limiting procedure by which the infinities are canceled. Also, the transition function approach requires further correction when the incident wave at the point of edge diffraction is not locally plane.

In this paper we present a new formalism, henceforth referred to as the "Spectral Theory of Diffraction" or STD, which is capable of providing a uniform representation of the diffracted fields without any correction terms or factors. The spectral diffraction coefficients are readily constructed using the conventional form of GTD and are inserted into a field representation introduced in the paper that provides continuously valid results in the entire range of observation angles, including the shadow boundary and caustic directions even when these are close to each other. The simplicity and usefulness of the STD technique are illustrated in the paper for both two- and three-dimensional scatterers and the results are compared with those derived from other techniques.

1. R. G. Kouyoumjian and P. H. Pathak, "A uniform geometrical theory of diffraction for an edge in a perfectly-conducting surface," Proc. IEEE, vol. 62, pp. 1448-1461, 1974.

2. R. M. Lewis and J. Boersma, "Uniform asymptotic theory of edge diffraction theory," J. Math. Phys., vol. 10, pp. 2291-2305, 1969.

3. S. W. Lee and G. A. Deschamps, "A uniform asymptotic theory of electromagnetic diffraction by a curved wedge," Electromagnetics Laboratory Scientific Report No. 74-18, University of Illinois.

VI. 1-4 A NEW METHOD FOR IMPROVING THE GTD SOLUTION VIA THE INTEGRAL EQUATION FORMULATION. R. Mittra, W. L. Ko and Y. Rahmat-Samii, Electromagnetics Laboratory, Department of Electrical Engineering, University of Illinois, Urbana, Illinois, 61801

The usefulness of the GTD technique for solving high frequency diffraction problems has been adequately demonstrated, and the limitation of the moment solution of the integral equation for the same problems is also well understood. To date, no proof has been advanced towards demonstrating that the diffracted field

derived from the ray optical approach indeed satisfies the self-consistent formulation described by the integral equation. It will obviously be desirable to know how well the GTD solution satisfies the integral equation, and to systematically improve this solution when the necessity for such improvement is clearly indicated. The fundamental difficulty in combining the GTD and the integral equation approaches appears to stem from the fact that the GTD generates the far field solution for a given direction of incidence, whereas the moment solution of the integral equation approach yields the unknown surface current on the scatterer for an arbitrary angle of incidence. It is shown in this paper that these two approaches could be brought together by using the integral equation formulation in the Fourier transform domain<sup>1</sup> where the transform of the surface current solution can be directly related to the diffracted field far from the scatterer. The transformed version of the integral equation allows one to perform a convenient test on the solution derived by GTD, or its more recent version, the Spectral Theory of Diffraction<sup>2</sup> (STD), to see how well these solutions satisfy the transformed integral equation in which the Fourier transform of the current distribution is replaced by the approximate expressions for the far field that have been derived via the asymptotic techniques mentioned above. It is also possible to derive an iterative form of the transformed integral equation that can generate higher order solutions with the GTD or STD solution as the starting point. Examples have been included in the paper to illustrate the systematic improvement of the GTD solution using the procedure outlined in this paper.

1. R. Mittra and T. S. Li, "A Spectral Domain Approach to the Numerical Solution of Electromagnetic Scattering Problems," (to appear AEU).
  2. R. Mittra, Y. Rahmat-Samii and W. L. Ko, "Spectral Theory of Diffraction--A New Approach for Solving High Frequency Diffraction Problems," (to appear).
- VI. 1-5 A SURVEY OF PASSIVE REFLECTORS USED IN RADIO LINKS.  
Nhu Bui-Hai, Thomson-CSF/Division Faisceaux  
Hertziens, France

The use of higher and higher frequencies for radio links brings into light a certain number of factors whose importance have, until the present time, been underestimated. It is thus that the use of a periscope system, which associates an antenna at ground level with a passive reflector mounted on a mast, can offer increasingly evident advantages.

In effect, when an antenna must be mounted above ground and when using relatively low frequencies (below 2 GHz), an acceptable solution is to mount the antenna at the top of a mast, using a feeder line for connection to the radio equipment at ground level, feeder losses remaining low at these frequencies.

On the contrary, at higher frequencies (above 4 GHz), feeder attenuation becomes too great rendering its utilization less and less attractive. This is increasingly true at higher and higher frequency, such that the use of periscope system becomes more and more viable. It thus appears opentime to investigate all the possibilities of such system.

In the first place, we analyze the behavior of a periscope consisting of a passive reflector placed in the near field of the antenna by illustrating the gain and radiation performance as a function of passive reflectors forms and dimensions (rectangular, elliptic, curved).

In the second, we will treat far field passive reflector behavior. We shall indicate the principal configurations of utilization for each case and give the means of calculations the overall propagation performance.

Finally, we shall indicate the possibilities of periscope systems for two viewpoints: compatibility for high capacity radio links (very high performance periscope system) and simultaneous operation in several frequency bands (multiband periscope system).

- VI. 1-6 A COMPARISON OF GEOMETRICAL AND PHYSICAL DIFFRACTION TECHNIQUES FOR BACKSCATTERING FROM A CYLINDRICALLY CURVED PLATE. M. A. Plonus, Department of Electrical Engineering, Northwestern University, Evanston, Illinois; and R. Williams, Hallicrafters Company, Rolling Meadows, Illinois

Geometrical and physical optics techniques supplemented by their respective extensions, geometrical and physical diffraction are applied to the problem of a finite, cylindrically curved plate. Numerical calculations of the radar backscattering cross sections were made and a graphical comparison of these methods with experimental results is made. Keller's and Ufimtsev's Theories are discussed and compared as they apply to this problem.

- VI. 1-7 THEORETICAL AND EXPERIMENTAL STUDY OF SHADOWING PHENOMENA. S. S. Locus and K. M. Mitzner, Northrop Corporation, Aircraft Division, Hawthorne, California

A theoretical and experimental study was made of far-field backscatter from a conducting body which is partially shadowed by a body composed of absorbing material. On the basis of general theoretical considerations, it was predicted that shifting or deforming the shadow boundary would not significantly affect the scattering unless the shadow boundary passed near a point scattering center or an extended scattering center, that is, a line or area which scatters almost in phase. This prediction is based on

indications that the near-discontinuity in surface current across the shadow boundary does not produce any significant contribution to the backscatter unless it perturbs the current distribution near a scattering center. The theory was checked by measurements on a rectangular plate with its vertical edges normal to the line of sight. For line of sight far enough off normal to the plate, the two vertical edges act as extended scattering centers. Data for this case confirm the theoretical predictions that (1) the backscatter is not changed significantly by shadowing a strip down the middle of the plate, but (2) shadowing one vertical edge produces a backscattered field which can be recognized as that of the other vertical edge acting as an isolated scatterer.

- VI. 1-8 SURFACE WAVE CONTRIBUTIONS TO HIGH FREQUENCY BACK-SCATTERING FROM INHOMOGENEOUS DIELECTRIC SPHERES.  
C. L. Brockman, Jr., Hughes Aircraft Company, Canoga Park, California, 91304; and N. G. Alexopoulos, Electrical Sciences and Engineering Department, University of California, Los Angeles, California, 90024

In an earlier paper, the geometrical optics contributions to backscattering by inhomogeneous dielectric spheres were obtained by performing a Watson Transformation on the exact solution. The dependence of the dielectric constant treated was the ratio of the radial position to the radius of the sphere raised to an arbitrary power. The results were consistent with those obtained by geometrical optics, and were more accurate.

Surface wave contributions to backscattering can also be extracted from the exact solution with the Watson Transformation. Three types of surface wave contributions are described in this paper.

First, creeping waves, or waves that circulate around the outside of the sphere, were identified. These were shown to be very weak contributions compared to geometrical optics. A set of whispering gallery modes was also identified. These modes circulate around the inside surface of the sphere. It is postulated here that a large phase advance term in the result is actually a caustic correction factor. These modes only exist when the dielectric constant at the surface is less than that of the surrounding media, and they are very weak contributors. The third category is the partial surface waves, which consist of a combination of surface wave and geometrical optics behavior. These can compete with geometrical optics returns for some values of the parameters. For all three types, a phase difference between the contributions due to  $TE_r$  and  $TM_r$  excitations is identified, which vanishes for the homogeneous sphere or for the optical limit.

## OPTICS

C. Yeh, Chairman

- VI. 2-1 LEAKY WAVES IN INTEGRATED OPTICAL CIRCUITS. C. Yeh, Electrical Sciences and Engineering Department, University of California, Los Angeles, California, 90024

The development of low-loss fibers in recent years has spurred interest in the study of optical-fiber communication lines as well as the construction of optical integrated circuits. One of the very basic configurations for optical integrated circuits is the deposition of a layer of material of thickness  $2\alpha$  and dielectric constant  $\epsilon_2$  on a substrate whose dielectric constant is  $\epsilon_3$ . Optical waves may be supported along and within this layer. It is well known from electromagnetic theory that in order that this type of structure may support a surface guided wave, the dielectric constant of the three different regions must be such that  $\epsilon_1 < \epsilon_2$  and  $\epsilon_3 < \epsilon_2$ ,  $\epsilon_1$  is the dielectric constant of the region above the thin layer. However, in many important physical situations such as the deposition of ZnS ( $\epsilon/\epsilon_0 = 5.48$ ) or ZnSe ( $\epsilon/\epsilon_0 = 6.66$ ) on GaAs ( $\epsilon/\epsilon_0 \approx 15$ ) the dielectric constant of the substrate is higher than that of the layer. Hence, the ordinary surface guided wave cannot exist in this structure. The purpose of this presentation is to consider the problem of wave propagation along a structure where  $\epsilon_1 < \epsilon_2 < \epsilon_3$ . It will be shown that when the thickness of the layer is large compared with a wavelength of light, low-loss leaky modes may exist. Experimental results verifying the existence of these modes will also be shown. The case in which the  $\epsilon_2$  layer is nonuniform will also be discussed.

- VI. 2-2 EXCITATION OF AN OPTICAL FIBER BY A GAUSSIAN BEAM. M. Mostafavi, T. Itoh, and R. Mittra, Electromagnetics Laboratory, Department of Electrical Engineering, University of Illinois, Urbana, Illinois, 61801

To date, the excitation problem of optical fibers has been studied by neglecting the reflection from the fiber end and there has been no attempt to directly calculate the radiated power.

In this paper, we present the results of an in-depth analysis of the problem of Gaussian beam excitation of optical fibers at normal incidence. The first step involves the derivation of the eigenvalues and eigenfunctions of the guided modes as well as the

radiation spectra of the fiber. The second step entails the application of the continuity conditions at the interface containing the fiber end using Gaussian beams with different spot sizes as our excitation source. Next, the simultaneous equations derived from the continuity conditions are numerically solved for the reflected, guided and radiated modal coefficients and corresponding powers.

It is found that for a practical fiber with core permittivity of  $2.25 \epsilon_0$ , the reflected power is usually about 4 percent of incident power and that the most efficient single-mode excitation is possible by adjusting the spot size of the incident Gaussian beam to be the same as the core diameter of the fiber. Numerical results for other choices of parameters are also included in the paper.

VI. 2-3 A CRYSTAL OPTICS THERMOMETER PROBE FOR MEASURING ELECTROMAGNETICALLY INDUCED HEATING. T. C. Cetas, Heat Division, National Bureau of Standards, Washington, D.C., 20234

A thermometer has been developed which uses the optical activity of a Y-cut single crystal of  $\text{LiTaO}_3$  as the temperature sensitive element. Polarized light is rotated by the crystal through an angle which depends on the crystal thickness. The temperature coefficient of the rotation is approximately  $0.3 \text{ rad/mm} \cdot ^\circ\text{C}$ . The intensity of light passed through a sandwich composed of a sheet polarizer, the crystal and an analyzer is a function of this rotation and hence is temperature dependent also. A thermometer probe was constructed by bonding this sandwich to a bundle of optical fibers (along with a dielectric mirror so that the sensor would be at the probe tip). Half of the fibers conduct light from a light emitting diode (LED) to the sensor tip while the other half conduct light from the sensor to a photodiode detector. Both the LED output and the photodetector circuits were stabilized since drifting from both sources is equivalent to a changing temperature calibration. The proto-type uses a crystal 0.1 mm thick. A temperature range of  $50^\circ\text{C}$  with a  $0.1^\circ\text{C}$  resolution is attained. A slow drift equivalent to  $0.5^\circ\text{C}/16 \text{ hr}$  (i.e.,  $1\%/16 \text{ hr}$  in output signal) also resulted and was associated with photodiode drifting.

VI. 2-4 MICROWAVE MODAL STUDY OF DIELECTRIC OPTICAL WAVEGUIDES. S. W. Maley, Hussain Haddad, D. C. Chang, University of Colorado, Boulder, Colorado, 80302

A model study of an optical thin-film waveguide in the microwave frequency range can provide more precisely-controlled measurements for the purpose of confirming the validity of corresponding theoretical solutions. An experimental study using 9.4 GHz was conducted. Such a signal is fed into a rectangular waveguide horn which flares from a standard X-band waveguide to a 25.4 cm by

0.95 cm multimode rectangular waveguide in order to provide controlled excitation at one end of a dielectric slab which is placed between two metallic parallel plates. The dielectric slab is made of polystyrene foam, which has a relative permittivity close to 1.03. By compressing foam slabs of different initial volumes into slabs of the same volume, a different refractive index for each slab can be achieved. Slabs with slightly higher refractive index can then be used as the dielectric guides, as in the optical guiding structures. Experimental studies, such as power coupling between two guides, scattering pattern of curved guides at the bend, power loss due to continuous and scattering radiation in a curved section, etc., can be measured with a physical model closely identified with the theoretical one. Measurement of the field distribution was made with a miniature probe protruding from a slotted line placed on one of the metal plates, thus providing additional information on the detailed coupling mechanism in each case.

VI. 2-5 MULTIPLE SCATTERING EFFECTS ON COHERENT BANDWIDTH AND PULSE DISTORTION IN DISCRETE SCATTERERS. Akira Ishimaru and S. T. Hong, Department of Electrical Engineering, University of Washington, Seattle, Washington, 98195

This paper presents (1) formulation of integral equation for two-frequency correlation function in stationary and moving discrete scatterers, (2) approximate solutions for coherent bandwidth of an optical wave in fog, and (3) numerical calculations of the pulse shape in fog and cloud.

The integral equation is an extension of Twersky's integral equation to include the relationship with the two-frequency specific intensity and the average and the fluctuating velocities of the particles. The effect of size distribution is also included.

The coherent bandwidth is obtained both for weak and strong fluctuation cases. For weak fluctuation when the optical distance is much smaller than unity, the coherent bandwidth is substantially the same as in free space. For strong fluctuation when the optical distance is much greater than unity, the diffusion phenomena becomes dominant and the coherent bandwidth is proportional to  $(D\lambda^{-2} \rho^{-1/2} z^{-3/2})$  where  $D$  is the particle diameter,  $\rho$  is the number density and  $Z$  is the distance, and the delay is proportional to  $(\rho Z^2 \lambda^2)$ .

As an example, numerical calculations are given for a nano-second optical pulse through fog, and when the fog density is  $10^8 \sim 10^9 \text{ m}^{-3}$ , the pulse delay and spread are shown to be  $3.03 \mu \text{ sec}$  and  $1.28 \mu \text{ sec}$  respectively. This is in agreement with experimental data.

VI. 2-6 THE EFFECTS OF BEAM WANDER ON THE SCINTILLATION CHARACTERISTICS OF A MATCHED FILTER OPTICAL RECEIVER.  
C. S. Gardner, Department of Electrical Engineering,  
University of Illinois

In a previous paper<sup>1</sup> we described a spatial filtering technique for reducing scintillation noise in optical receivers. It was shown that under conditions of weak scattering scintillation noise can be completely removed if the optical signal is processed through a spatial filter which is matched to the unscattered field. Since beam wander is a strong scattering phenomenon it was not included in the weak scattering theory. In this paper we consider the effects of beam wander on the receiver performance. When beam wander is present the axis of the received beam will be randomly tilted and displaced with respect to the receiver axis. We assume that the angular tilt and the two orthogonal components of the transverse displacement are statistically independent and Gaussian distributed. The scintillation in the receiver output due to beam wander is calculated as a function of the receiver parameters and the beam wander statistics. It is shown that the effects of beam wander can be minimized by minimizing the transmitter and receiver aperture Fresnel numbers. However, in practice, the magnitude of beam wander may be so large that the receiver may be required to actively cancel beam wander to maintain low scintillation. The results indicate that a receiver employing spatial filtering and wander tracking may present an effective method for reducing scintillation noise in optical communication systems.

---

1. C. S. Gardner, "A spatial filtering technique for reducing scintillation noise in optical receivers," URSI Symp. Digest, June 1974, p. 8.

VI. 2-7 THE DETERMINATION OF THE JOINT PHOTOCOUNT STATISTICS.  
Gerard Lachs, Sharad Laxpati, and James A. Quarato.

The quantum mechanical theory of coherence and its relations to the detection statistics for laser communication and radar systems has been of considerable interest in recent years. Many of these systems utilize photocount detection (photon bucket) systems and the detection statistics for these systems are essentially the photocount statistics.

One important aspect of these systems is the joint photocount statistics. The joint photocount statistics yield information about the higher order correlation functions for the field and in a more practical vein yield information about the tendency of errors to occur in bursts in laser binary communication systems. Thereby the need for utilizing burst error correction codes in communication systems can be determined.

In this paper we shall present a method for computing the joint photocount statistics for incident radiation which is an arbitrary superposition of coherent and chaotic radiation. This is equivalent to laser light superimposed upon background radiation. The method of calculation is based upon a recurrence formula derived from the generating function for the single interval photocount statistics. Some specific data will be presented and discussed.

TRANSIENTS I

D. L. Moffatt, Chairman

- VI. 3-1 OBJECT DISCRIMINATION VIA POLE EXTRACTION FROM TRANSIENT FIELDS.\* F. J. Deadrick, H. G. Hudson, E. K. Miller, J. A. Landt, and A. J. Poggio, Lawrence Livermore Laboratory, Livermore, California

Development of the singularity expansion method (SEM) was fostered by the observation that pulse excited antennas and scatterers exhibit a behavior of the form  $\sum R_{\alpha} e^{s_{\alpha} t}$ . The  $R_{\alpha}$  are the amplitudes with which each of the structure's temporal modes of complex frequency  $s_{\alpha}$  has been excited. While the  $R_{\alpha}$  are thus source dependent, the  $s_{\alpha}$  are structure dependent only, offering the potential of greatly reducing the data required to characterize its transient response. In addition, the  $s_{\alpha}$  offer a possible mechanism for providing target sorting or classification, the subject of this paper.

Results are presented for the  $s_{\alpha}$  sets of various simple wire targets, obtained by use of Prony's method from computed and measured transient waveforms (R. Mittra, and M. Van Blaricum, "A Novel Technique for Extracting the SFM Poles and Residues of a System Directly from its Transient Response," USNC/URSI 1974 Annual Meeting, Boulder, Colorado). Data is shown for distinctly different targets (e.g., straight and crossed wires), as well as where a structure is smoothly deformed from one shape into another (e.g., a straight wire into a circular loop) to exhibit the possibilities for target discrimination. The effects of noise in the transient waveform on the  $s_{\alpha}$  calculation is shown, and a simple discrimination algorithm is described.

\*This work was performed under the auspices of the U.S. Energy Research and Development Administration.

- VI. 3-2 COMPLEX NATURAL RESONANCES OF RADAR TARGETS VIA PRONY'S METHOD. C. W. Chuang and D. L. Moffatt, The Ohio State University ElectroScience Laboratory, Department of Electrical Engineering, Columbus, Ohio, 43212

It has been shown that extraction of complex natural resonances and residues from true transient responses via Prony's method is both efficient and accurate.<sup>1</sup> However, in the art of radar

interrogation the true transient response is difficult to obtain and we must be content with an approximate one. Knowing the complex natural resonances of objects is essential to one type of radar target discrimination.<sup>2</sup> In this paper we consider the use of Prony's method in extracting complex natural resonances from approximate backscattering ramp responses of radar targets.

A ramp waveform is used in radar target discrimination because a good approximation to the time domain response can be obtained with only a few harmonically related frequency domain responses via Fourier synthesis. The backscattering ramp response  $F_R(t)$  can be approximated as

$$F_R(t) + \frac{1}{T} \left. \frac{G(\omega)}{\omega^2} \right|_{\omega=0} \approx \sum_{n=1}^N -\frac{T}{2\pi^2 n^2} \left| G\left(\frac{2\pi n}{T}\right) \right| \cos\left(\frac{2\pi n}{T}t + \phi_n\right),$$

where  $G(\omega)$  is the backscattering response at frequency  $\omega$  and  $\phi_n$  is the phase of  $G(2\pi n/T)$ . The value of  $T$  is chosen to be large enough such that the ramp response decays to a negligible value after a time interval  $T$ . Due to the weighting factor  $1/n^2$ , high frequency contribution is small. Therefore, typically  $N$  is set to 10. By applying Prony's method to this approximate ramp response, a few dominant resonances which are close to the origin of the complex frequency plane can be extracted. This is quite encouraging because for the purpose of radar target discrimination only a few dominant modes are needed. Objects considered are spheroids, simple wire aircraft models and some realistic aircraft models.<sup>3</sup> The accuracy of this method is found to be good when compared to the results obtained by other techniques.

1. VanBlaricum, M. and R. Mittra, "A Novel Method for Extracting the Sem Poles and Residues of a System Directly From its Transient Response," 1974 USNC/URSI-IEEE Meeting, Boulder, Colorado, October, 1974.

2. Mains, R. K. and D. L. Moffatt, "Complex Natural Resonances of an Object in Detection and Discrimination," Report 3424-1, June 1974, The Ohio State University ElectroScience Laboratory, Department of Electrical Engineering; prepared under Contract F19628-72-C-0203 for Air Force Systems Command.

3. Lin, Y. T., "Computation of Low Frequency Scattering from Airplanes," Report 2768-9, September 1972, The Ohio State University ElectroScience Laboratory, Department of Electrical Engineering; prepared under Grant AFOSR-69-1710 for Air Force Office of Scientific Research.

- VI. 3-3 ON THE DETERMINATION OF THE SEM NATURAL FREQUENCIES FOR THE RECTANGULAR PLATE. L. W. Pearson and R. Mittra, Electromagnetics Laboratory, Electrical Engineering Department, University of Illinois, Urbana, Illinois, 61801

The results of an initial investigation in determining the Singularity Expansion Method (SEM) natural frequencies for a rectangular plate are reported. The plate is modeled by way of the coupled, Hallen-type integral equations for thin plates, as given by Rahmat-Samii and Mittra.<sup>1</sup> The equations are discretized by means of a conventional method of moments formulation after extending them to the complex wavenumber case. The relationship between the symmetries of the two current components on the plate is derived and these symmetry conditions are used to obtain a significant reduction in the number of unknowns that have to be dealt with. This, in turn, allows one to derive a matrix equation which takes a "sparsely coupled" form and results in significant computational economy. Pole trajectories as calculated by this method for the first four symmetry modes on the plate are presented. It is shown that the subsectionally constant zoning is inadequate to accurately model the size of the plate. The shortcoming relates to Meixner's edge conditions which the currents must satisfy. Means of circumventing this shortcoming are discussed.

---

1. Y. Rahmat-Samii and R. Mittra, "Integral Equation Solution and RCS Computation of a Thin Rectangular Plate," IEEE Trans., vol. AP-22, pp. 608-610, July 1974.

- VI. 3-4 BROADBAND COLLECTION OF ENERGY FROM TRANSIENT FIELDS BY WIRE ANTENNAS.\* J. A. Landt, E. K. Miller, F. J. Deadrick and H. G. Hudson, Lawrence Livermore Laboratory, Livermore, California

Understanding energy collection by wire antennas is essential in predicting the likelihood of component burnout in equipment attached to the antennas. Although the CW and transient behavior of linear systems are related by Fourier transform, responses in one domain are difficult to estimate from the other without actually performing the transform. Furthermore, some concepts suitable for application in one domain are not useable in the other. A case in point demonstrated in this paper is the frequency domain theorem on maximum power transfer. This paper explores energy collection under pulsed conditions and presents representative data for the EMP response of linear dipoles and other antenna types. The energy collected by a dipole and the energy delivered to a load are found numerically and/or experimentally as functions of load value, load position, dipole length and radius, and angle of incidence of the EMP wave. It is found that virtually all of the energy (>99%) collected by a dipole from the incident wave can be delivered to a purely

resistive load, and that the optimum load value is approximately equal to the input resistance of an infinite cylindrical antenna, which is in most cases, substantially more than the input resistance of the dipole at resonance. The utility of a short-pulse transient range for obtaining such data experimentally is also demonstrated, and a contour plot format for data presentation is shown.

\*This work was performed under the auspices of the U.S. Energy Research and Development Administration.

- VI. 3-5 ON THE RADIATION OF AN ELECTROMAGNETIC PULSE FROM A LOOP ANTENNA. Ronald F. Blackburn, Air Force Weapons Laboratory, Kirtland AFB, New Mexico, 87115; and Clayborne D. Taylor, Mississippi State University, Mississippi State, MS, 39762

A resistively loaded loop antenna used in the simulation of the nuclear electromagnetic pulse is studied. Because of the width of the pulse frequency spectrum the response of the antenna is analyzed separately for three specific frequency regimes. Also the pulse-power source interaction with the antenna is considered. After the frequency response of the antenna is determined, Laplace transform theory is utilized to obtain the pulse response.

Experimental data from time domain field measurements are compared with theoretical predictions. Also corresponding frequency domain comparisons are made. In all cases good agreement is obtained.

- VI. 3-6 TRANSIENT RESPONSE OF A LOG-PERIODIC ANTENNA COMPUTED FROM FREQUENCY DOMAIN MEASUREMENTS. Werner J. Stark, Harry Diamond Laboratories, Adelphi, Maryland, 20783

Log-periodic antennas are frequently used for broadband communications in the frequency range of 2 to 120 MHz. The broadband characteristics of specific antennas can be determined from measurements of their response to a measured incident field over the frequency range of interest. Once the broadband characteristics of an antenna have been adequately described, it is a simple matter to determine the transient response by employing Fourier transform methods.

This paper describes the application of an automated CW Test Facility to the measurement of the broadband characteristics of a typical log-periodic antenna operating in the frequency range of 30 to 76 MHz. These characteristics are used to compute the antenna response to a transient electromagnetic pulse polarized parallel to the antenna elements and propagating in the plane of the antenna. The accuracy of this method of computing the transient response is evaluated by comparing the computations to corresponding time-domain measurements.

VI. 3-7 ANTENNA TRANSIENT RESPONSE MEASUREMENTS UTILIZING A TEM HORN. D. H. Schaubert and A. R. Sindoris, Department of the Army, Harry Diamond Laboratories, ATTN: AMXDO-RAE, 2800 Powder Mill Road, Adelphi, Maryland, 20783

The time-domain receive transfer function of an antenna is the normalized time-dependent voltage induced across the antenna's load by an incident electric field with a  $\delta$ -function time behavior. This transfer function is characteristic of an antenna and can be convolved with an arbitrary incident waveform to obtain the antenna's response to the incident signal. Here an experimental technique for determining an antenna's receive transfer function is considered. The technique consists of measuring the induced voltage when the antenna under test is illuminated by an impulse electric field radiated from a TEM horn. The TEM horn was chosen because it radiates a single pulse of very wide bandwidth when excited by a voltage step. This allows observation of the antenna's response over a long time interval and insures that minimum data processing will be required to compensate for the finite bandwidth of the pulse radiated by the TEM horn. The experimental technique permits observation of any anomalous behavior that may be missed in a purely analytic treatment of the antenna's transient response. As a part of the discussion the radiation characteristics of the TEM horn will be discussed.

VI. 3-8 TIME DOMAIN RESPONSE OF WIRE ANTENNA ARRAYS.\*  
Fred John Solman, III, Massachusetts Institute of Technology, Lincoln Laboratory, Lexington, Massachusetts, 02173; and Walter L. Weeks, Purdue University, West Lafayette, Indiana, 47907.

A numerical technique for solution of a time domain integro-differential equation for antenna arrays of thin parallel wires is developed. This technique permits the solution of arrays with resistive loading and transmission line interconnections. Additional restrictions are defined on the choice of time steps when resistive loading or transmission line interconnections are used.

The technique was used to find the approximate impulse response of several types of wire antenna arrays with a view towards synthesis of structures with a time limited impulse response. Such structures are potentially wideband antennas. The antenna models studied included a dipole, a two element receiving array of dipoles, a three element array with each element driven at the same time, a two element array with elements driven from a common transmission line, and a five element log periodic dipole array. The results of these models were compared with measurements and other calculations and found to be in good agreement.

Based on these models, a non-dispersive version of the five element log periodic dipole array was synthesized and modeled by using this solution technique. The results indicate substantially non-dispersive radiation of the incident pulse and useful pattern and impedance characteristics over a 5:1 frequency range.

---

\*This work was done in partial fulfillment of the requirements for the degree of Doctor of Philosophy at Purdue University.

ARRAYS

V. Galindo, Chairman

- VI. 4-1 THE DOME ANTENNA - CONCEPT AND ANALYSIS. P. A. Valentino, J. J. Stangel, and L. Schwartzman, Sperry Gyroscope, Sperry Rand Corporation, Great Neck, New York

This paper presents an innovative concept in phased array technology, a phased array fed lens known as the Dome Antenna. The concept employs a uniquely designed passive lens or dome to alter the scan characteristics of a planar phased array. The phased array thus modified is capable of generating beam patterns whose characteristics (e.g., gain, beamwidth, etc.) with scan angle conform optimally to a given operational requirement. That a single planar phased array can be modified by a passive lens to scan a full hemisphere is indicative of the flexibility of this concept. The lens efficiently transforms the scan characteristics of the planar "feed array" into the desired hemispheric coverage requirement with a minimal number of active components (i.e., phase shifters) realizing a significant reduction and cost savings compared to corresponding conventional multifaced phase array antenna designs.

The lens acts as a transformation device transforming the gain envelope of the feed array into the required gain contour. For a lossless system energy is conserved, and from Stangel's Theorem it can be shown that the integral of the gain envelope over all space for any gain contour generated is a constant. This explains the trade-off between gain and scan coverage utilized by a Dome Antenna to realize a specified requirement with a minimum number of active components. Detailed analysis have been conducted to evaluate design trade-offs and antenna performance. Results show that this type of antenna system will yield high quality performance over an entire hemisphere (or greater) while providing a significant cost savings due to the efficient use of only a single active planar array.

- VI. 4-2 THE DOME ANTENNA - EXPERIMENTAL IMPLEMENTATION. F. J. Esposito, L. Schwartzman, and J. J. Stangel, Sperry Gyroscope, Sperry Rand Corporation, Great Neck, New York

This paper describes the implementation and experimental evaluation of the Dome Antenna concept in a three-dimensional electronically scanned antenna at C-Band.

An extensive test program evaluating the performance of the antenna has been conducted. Representative data and interpretation will be presented. This data will encompass the following characteristics:

- Antenna Gain
- Radiation Patterns
- Monopulse Error Slope Linearity
- Pointing Accuracy
- Polarization Characteristics
- Back Lobe Radiation
- Signal Bandwidth
- Sidelobe Cancellation Effectiveness
- Active Reflection Coefficient

Two gain/scan variations (corresponding to lens embodying different refractive properties) were evaluated.

VI. 4-3 LOW SIDELOBES IN LENS FED ARRAYS. David T. Thomas, Raytheon Company, Goleta, California, 93017

Low sidelobe arrays are essential to the operation of (1) communications systems in the presence of environment (clutter, multipath, etc.), RF noise or jamming, and (2) radar systems in the presence of environment or jamming. Lens fed arrays are advantageous because of (1) instantaneous electronic scanning, (2) their wide instantaneous frequency bandwidths (typically octave or more), (3) frequency independent beam positions (no beam squint), and (4) ease of simultaneous multibeam implementation.

Taylor distributions<sup>1</sup> and Dolph-Chebyshev arrays<sup>2</sup> have long been used for efficiently producing low sidelobes. In conventional phased arrays, the corporate feed unequally divides (or sums) the power to provide amplitude distributions closely approximating ideal Taylor or Chebyshev distributions. In lens-fed arrays,<sup>3</sup> a different approach for achieving low sidelobes is used - the multiple beam port feed. Three port feeds are capable in theory of 40 dB sidelobes, and four or five port feeds even better. The lens design for this type of lens-fed phased array should have beam ports spaced  $57.3 (\lambda/D)$  degrees apart, where D is the array length.

Amplitude distributions obtained, using three port feeds, closely approximate a Taylor 40 dB distribution. Aperture efficiency is within a few per cent of ideal Taylor distribution efficiency. Practical bandwidths for low sidelobe lens-fed arrays are about 10%, although the usual octave bandwidths of lens-fed arrays can be utilized if higher sidelobes are acceptable at the band edges. Techniques for broadbanding low sidelobe lens-fed arrays also exist at some cost in gain and hardware.

Achievable low sidelobe levels depend on the random phase and amplitude errors present. Simulated patterns based on measured lens data indicate that 31 dB sidelobe levels should be achievable using three-port feeds in lens-fed arrays. Theoretical sidelobe levels for this case were 37 dB, indicating that some degradation due to random errors should be expected.

1. T. T. Taylor, "Design of Line Source Antennas for Narrow Beamwidth and Sidelobes," IRE Trans., Vol. AP-4, pp. 16-28, Jan. 1955.
2. C. L. Dolph, "A Current Distribution for Broadside Arrays which Optimizes the Relationship between Beamwidth and Sidelobe Levels," Proc-IRE, Vol. 34, pp. 335-348, June 1946.
3. D. H. Archer, "Lens Multibeam Arrays," Electronic Progress - Raytheon Company.

W. Rotman and R. F. Turner, "Wide Angle Lens for Line Source Applications," IEEE Trans. Vol. AP-11, 1963, pp. 623-632.

- VI. 4-4 FINITE TRAVELLING-WAVE RECEIVING ARRAY OF PARALLEL WAVEGUIDE-BACKED SLOT ANTENNAS: THEORY AND EXPERIMENT. D. P. Nyquist and M. A. Scott, Department of Electrical Engineering and Systems Science, Michigan State University, East Lansing, Michigan, 48824; and H. H. Lai, Department of Electrical Engineering, Solid-State Electronics Group, University of Illinois, Urbana, Illinois, 61801

Reception characteristics of a finite, travelling-wave, parallel array of  $N$  transverse, rectangular slots cut in an infinite ground plane, excited by an incident plane wave, and backed by a rectangular waveguide are investigated analytically and experimentally. Received power is delivered to one of two load impedances (of arbitrary reflection coefficients) at either end of the backing waveguide. Standing-wave content of the waveguide field is controlled by adjustment of these reflection coefficients. The incident plane wave of arbitrary polarization has its plane of incidence normal to the ground screen and parallel to the array axis while the angle of incidence is the arbitrary angle between its wave vector and the array axis.

A coupled system of Hallen-type integral equations for the slot fields excited in the array elements by the incident wave is formulated based on the boundary condition for tangential magnetic fields at the slot apertures. This system is solved numerically by the method of moments to evaluate the slot voltage distribution in each array element. In terms of these slot voltages, the amplitude of the dominant mode excited in the backing waveguide and the power delivered by it to the load impedance are evaluated for various incidence angles to determine the reception pattern of

the array. Previous investigations have considered primarily infinite arrays using an approximate variational formulation with assumed slot fields.

Slot fields and reception patterns are investigated for various array and backing-waveguide dimensions. Voltages along each slot element closely approximate a shifted-cosine distribution of the type expected on an approximately complementary parasitic-element dipole array. Slot voltages along the array exhibit a progressive, linear phase delay and thus constitute a travelling-wave aperture field. The phase velocity of this wave can be varied from less to greater than the speed of light by adjustment of backing-waveguide width. Scanning of the reception beam from endfire to near broadside is consequently achieved by appropriate width variations. Experimental results confirm all theoretically determined aperture field phase velocities and reception patterns.

- VI. 4-5 RADIATION CHARACTERISTICS OF FLANGED PARALLEL-PLATE WAVEGUIDE ARRAY. Kohei Hongo, Electromagnetics Laboratory, Department of Electrical Engineering, University of Illinois, Urbana, Illinois, 61801, on leave of absence from Shizuoka University, Hamamatsu, Japan

Radiation characteristics of a flanged parallel plate waveguide array of  $N$  elements are studied using the Weber-Schafheitlin discontinuous integral technique. The electro-magnetic fields in an exterior half-space are expanded as the linear combination of  $N$  expressions which satisfy the required boundary conditions on the conducting flange. The fields in each waveguide region are expanded in terms of the normal mode expression of the waveguide. Matching each expression at the aperture develops determinantal equations for the expansion coefficients in a matrix form. When the separation between the elements is large compared with the wavelength, the asymptotic solutions for the matrix elements which represent the coupling between the waveguide are derived. Using the solutions for single flanged parallel plate waveguide, the radiation characteristics of the array can be readily calculated by applying an iteration procedure. Some numerical results for physical quantities such as reflection coefficients, coupling coefficients, radiation pattern, etc., are obtained and a part of them are compared with those calculated based on other methods.

- VI. 4-6 THE PERFORMANCE OF DOUBLE RIDGED WAVEGUIDE ELEMENT IN A PHASED ARRAY. S. S. Wang, The Bendix Corp., Communications Division, Baltimore, Maryland; and A. Hessel, Polytechnic Institute of New York, Department of Electrical Engineering and Electrophysics, Farmingdale, New York

Double ridged waveguide is known for its broadband guiding characteristics and thus constitutes a potentially wide-band

linearly-polarized phased array element. In addition, the reduction of the size due to ridge loading makes this element attractive for wide-angle scanning applications (in view of the compact lattices that may be realized).

This paper examines the double ridged waveguide element performance in an infinite phased array. Galerkin's method is used twice, first to obtain the ridged waveguide dispersion relation and modal fields and later in matching aperture fields to free space in a unit cell.

Design procedure and a number of wide-band array designs for quarter hemisphere scan and different nominal (feed guide) bandwidths will be discussed. In addition, one narrow-band design for H-plane scan will be considered. In all cases examined, maximum VSWR occurs at the high end of the band in H-plane scan.

An examination and comparison of element performance in these designs reflects the capabilities of the double ridged waveguide element in a phased array.

VI. 4-7 THE ORGANIZATION OF RADIOMETRIC ARRAYS. C. A. Lewis, T. K. Lai, and H. C. Lin, ElectroScience Laboratory, Department of Electrical Engineering, The Ohio State University, Columbus, Ohio, 43212

The sensitivity of radiometric arrays depends strongly on the attenuation and noise introduced between the elements and the final detector. The properties of general reciprocal combinatorial circuits are used to show that sensitivity considerations favor location of the active devices as close to the antenna elements as possible when a given class of low-level amplifying or frequency-converting active elements is specified. This leads to complicated structures which also tend to be very expensive, especially at the higher frequencies. Some examples of this tradeoff will be presented.

An alternate approach, which appears to offer promise for millimeter-wave radiometers, is the use of large subapertures. Calculations of piecewise linear and piecewise uniform approximations to continuous distributions show that grating lobes are cancelled by element nulls when the subapertures are contiguous; otherwise they depend on the ratio of element spacing to subaperture dimension. They can be kept small by minimizing the unfilled space between subapertures. Further control by multi-channel data processing is being investigated.

VI. 4-8 DESIGN OF WIDEBAND RF BIAS INSERTION UNITS CAPABLE OF PASSING VIDEO PULSES. Gerald W. Renken, Honeywell, 1625 Zarthan, Minneapolis, Minnesota

Construction of wideband, RF bias units, capable of passing video pulses to an active device in an RF system is simple if ferrite choke material is used in the bias unit. A 200 MHz to 10 GHz RF bandwidth precludes the use of discrete components to realize the bias unit design, since most discrete circuit elements lose their ideal, lumped models around 3.0 GHz.

Proof that a bias unit designed and built with discrete circuit elements would not perform in a predictable fashion over the entire 200 MHz to 10 GHz bandwidth was verified experimentally. Analysis of this discrete component bias unit provided theoretical curves for comparison with the measured RF insertion loss and RF path isolation data. The RF data followed the theory until approximately 3.0 GHz. Self resonances of the discrete elements seriously perturbed both types of RF response at that frequency, and its higher harmonics.

Replacing the discrete circuit elements with a ferrite choke resulted in a bias unit, that when experimentally tested, gave smooth and predictable RF data over the bandwidth.

Both bias insertion units pass a video pulse with an 80 nanosecond risetime from the bias/video input port to the active device.

## ANTENNAS

K. F. Casey, Chairman

- VI. 5-1 ANTENNA NEAR FIELD PATTERN COMPUTATION BY PLANE WAVE SPECTRUM INTEGRATION. Alexander C. Brown, Jr., Atlantic Research Corporation, Alexandria, Virginia

Recently, antenna near fields of a circular symmetric antenna were computed by R. C. Rudduck, D. C. F. Wu and M. R. Intihar (IEEE, Trans. A. P., Mar. 1973) using the plane wave spectrum (PWS) integration method. More recently, the on-axis near field of a rectangular aperture antenna were computed by A. Brown, Jr. (URSI Oct. 1974) using the PWS integration method. Although a double integration was required, computation times were reduced considerably by restricting integration to some smaller region in wavenumber space than that region corresponding to all visible wavenumbers. This region of significant contribution was enclosed by the wavenumber bandwidth contour.

The idea of a significant wavenumber bandwidth contour is also found to be valid for computing antenna near field patterns as well as for computing on axis fields. For example, in the case of a 50 wavelength ( $\lambda$ ) diameter ( $D$ ) circularly symmetric aperture, at a distance of  $.125(2D^2/\lambda)$ , and at off axis angles exceeding  $11.5^\circ$ , the significant wavenumber bandwidth contour is an annular region  $17.5^\circ$  (.3 in normalized wavenumber units) wide. The field point is on the center ring of this region. One notes that the significant wavenumber bandwidth contour need not always contain the main lobe.

- VI. 5-2 SOME RESULTS ON EFFECTS OF COMPLEX SCATTERING STRUCTURES IN THE NEAR FIELD OF DIRECTIVE ANTENNAS. C. E. Ryan, Jr. and F. L. Cain, Radar Division, Engineering Experiment Station, Georgia Institute of Technology, Atlanta, Georgia, 30332

Recent investigations of problems occurring in the selection of radar antenna sites on ships<sup>1</sup> have required techniques for the estimation of the effects of complex scattering structures in the near field of antennas. The particular structures of interest are tower-like masts of tubular construction with either rectangular or triangular cross sections as viewed from the vertical axis. These structures affect the gain and sidelobe levels of the radar antenna when the antenna boresight axis is scanned close to or through the mast structure. Since neither

specific theoretical models nor measured data for such near-field complex scatterers were available, a series of measurements was performed and utilized to derive and verify a simple theoretical model. This simple theoretical model is based upon the standard aperture blocking analysis method<sup>2</sup> and has been found to be adequate for percentage blockages of less than 30 percent for relatively short antenna/obstacle separation distances. As the antenna/obstacle separation increases, the near-field pattern characteristics of the antenna<sup>3,4</sup> can be used, in connection with the approximate physical optics techniques<sup>5</sup> to derive useful results. Although such physical optics methods have been computer implemented for space-frame radome supports,<sup>6</sup> the computations are lengthy. The model used here permits relatively rapid assessment of the blockage effects. The experimental data have also been used to develop a set of curves which are useful for rapid assessments of the antenna gain loss and sidelobe levels resulting from scattering by the complex structures.<sup>7,8</sup>

The investigations discussed above indicate that additional theoretical and experimental efforts are required to fully account for the effects of complex scatterers in the near field of a directive antenna. However, the relatively simple models and the empirically derived curves which have been developed are useful engineering tools for first-order assessment of many practical configurations.

1. C. E. Ryan and R. D. Nevels, "Final Report on Consulting Services in Support of the Patrol Frigate Electromagnetic Effectiveness Analysis Program," Engineering Experiment Station, Georgia Institute of Technology, Atlanta, Ga., Subcontract No. A2MV-568343 to Prime Contract No. N00024-72-C-1444, August 1973.
2. C. L. Gray, "Estimating the Effect of Feed Support Member Blocking on Antenna Gain and Sidelobe Level," Microwave Journal, March 1964, pp. 88-91.
3. T. S. Saad, R. C. Hansen, and G. J. Wheeler, Editors, MICROWAVE ENGINEERS HANDBOOK - VOLUME 2, Artech House Inc., Dedham, Mass., 1971, pp. 36-37.
4. F. L. Cain, E. E. Weaver, and E. F. Duffy, "Prediction of Near-Field Coupling between Misaligned Antennas," 1974 IEEE International Symposium on Electromagnetic Compatibility, July 1974.
5. R. F. Harrington, TIME HARMONIC ELECTROMAGNETIC FIELDS, McGraw-Hill Book Co., Inc., New York, 1961.
6. J. R. Collier, "Digital Calculation of E.M. Diffraction from Aperture Blocking," Report No. 1180-5, The Ohio State University Antenna Laboratory (now Electro-Science Laboratory), Columbus, Ohio, 15 Sept. 1961 (AD-266310).

7. F. L. Cain, C. E. Ryan, C. P. Burns, and B. J. Cown, "Near-Field Obstacle Effects and Phased-Array Studies," Final Report, Engineering Experiment Station, Georgia Institute of Technology, Atlanta, Ga., Contract No. N00024-71-C-1120, 31 January 1972.

8. F. L. Cain, B. J. Cown, E. E. Weaver, and C. E. Ryan, "Phased-Array Studies and Near-Field Effects of Metallic and Dielectric-Coated Structures on Antenna Performance," Final Engineering Report, Georgia Institute of Technology, Atlanta, Ga., Contract N00024-74-C-1215, January 1975.

VI. 5-3 SLOT-UNIPOLE ANTENNA SYSTEM FOR ENERGY DENSITY RECEPTION AT UHF. Kiyohiko Itoh, Ryuichi Watanabe, and Tadashi Matsumoto, Department of Electronic Engineering, Hokkaido University, Sapporo, Japan

Radio signal received by moving vehicles in cities with high buildings may exhibit violent amplitude fluctuations, because of the existence of not only unsensible area, but also a standing-wave pattern owing to an interference between multi-reflected waves or direct and reflected waves, which high buildings cause in urban environments. In order to reduce the effect of signal fading caused by the standing-wave, a new type of the energy density antenna has been proposed by one of the authors as a slot-unipole energy density antenna system (SUA), which receives the E-field with a unipole and H-fields with orthogonally crossed slots for a vertically polarised wave. For the purpose of mounting on the mobile, 1) the shallow cavity backed slot antenna is the most suitable for the slot section in SUA, 2) the unipole, having a rectangular cavity at its base, can be easily designed as a loaded unipole, considering the cavity as a reactance element. Based on these results, this paper deals with techniques for a trial manufacture and experimental results of SUA in the UHF band, particularly 800-1000 MHz, where the land mobile telephone will be in practical use in the near future, and discusses the usefulness of SUA, which gives quite encouraging results.

VI. 5-4 ELECTRICALLY SMALL COMPLEMENTARY PAIR (ESCP) WITH INTER-ELEMENT COUPLING. K. G. Schroeder, The Aerospace Corporation, El Segundo, California

Whenever available installation height is limited, a monopole antenna can be foreshortened so as to fit into the limited space. This causes the monopole impedance to become very reactive and hence narrow band and its efficiency is reduced by losses occurring in the circuits required to tune the antenna. Typical performance results are: 1 to 10 percent bandwidth and 70 to 30 percent efficiency, respectively, for an antenna length (height) of 0.05 wavelengths. (Ref. 1)

An alternate approach for tuning a short monopole consists of using two of the antennas which are mutually-coupled, and match the input reactance of one with the reactance of the other after it has gone through an inversion circuit. This inversion circuit is realizable in the form of an externally complementarized hybrid feed circuit similar to the one described previously for resonant-height antennas. (Ref. 2) Mutual-coupling can be adjusted in a constrained design volume by varying the length to diameter ratio of the elements.

The net gain of the pair can be roughly estimated from the individual small radiator pattern gain (1.75 dB + 3 dB for ground plane) plus the pair directivity gain (Ref. 3), minus the matching losses.

1. J. A. Seeger, R. L. Hamson, A. W. Walters, "Antenna Miniaturization," Electronic Design, March 4, 1959, pp. 64-69.
  2. K. G. Schroeder, "A New Class of Broadband Antennas Using Complementary Pair Element Groups," 1965 IEEE International Convention Record, Vol. 5.
  3. R. M. Foster, "Directive Diagrams of Antenna Arrays," Bell System Technical Journal, Vol. 5, 1926, pp. 292-306.
- VI. 5-5 SOME FAR-FIELD STUDIES OF AN OFFSET LAUNCHER.  
M. J. Gans, R. A. Semplak, Bell Laboratories,  
Crawford Hill Laboratory, Holmdel, N.J., 07733

An offset paraboloidal reflector illuminated by a balanced feed horn constitutes an efficient launcher for coupling microwaves into quasi-optical beams. Measurements on a launcher with low blockage show low cross polarization. The amplitude, phase and polarization characteristics are predicted by two Gaussian beam modes, and the resulting formulas are found to agree well with measurements at 19 and 28 GHz. For example, with increasing offset angles, radiation pattern to the on-axis co-polarized signal is observed to vary from -44 to -37 dB, within 1 dB of the predicted variation.

- VI. 5-6 AN INTENSITY INTERFEROMETER FOR RADIO ASTRONOMY WITH IMPROVED SIGNAL-TO-NOISE PERFORMANCE.  
Robert H. MacPhie, Electrical Engineering  
Department, University of Waterloo, Waterloo,  
Ontario, Canada

A new type of intensity interferometer (involving fourth-order correlation products) is introduced which is suitable for use in long baseline interferometry in radio astronomy.

There are independent local oscillators (not necessarily ultra stable) at each end of the baseline, oscillators whose narrow band outputs are mixed with the wideband RF signal plus noise voltages from the RF amplifiers at each antenna. Two pairs of IF outputs are obtained which are brought together by IF (no phase stability problem) transmission lines and two conventional second-order correlation products are formed. However, due to the independence of the local oscillators at each end of the baseline, neither of these cross products contains a dc component. Nevertheless each does have a narrow band "signal" embedded in wide band noise. Band pass filters are used to eliminate most of this noise before the fourth-order correlation product is formed. This fourth-order output does have a dc (signal) component which enjoys a far better signal-to-noise ratio than the corresponding outputs from other types of intensity interferometers.

- VI. 5-7 SCATTERING BY A SLOTTED CIRCULAR CYLINDER.  
K. Hongo (on leave from Shizuoka University, Japan), T. Itoh, S. Safavi-Naini, Electromagnetics Laboratory, Department of Electrical Engineering, University of Illinois, Urbana, Illinois, 61801

A slotted circular cylinder is a useful model of an important engineering problem of aperture coupling. In this paper a new efficient method is presented for analyzing the scattering by a hollow cylinder with a rectangular slit on the wall.

In contrast to many conventional numerical techniques, the formulation in the present method is carried out in the spectral, or the Fourier transform domain. Field expressions for both inside and outside of the cylinder are Fourier transformed and the interface conditions on the slit are imposed directly in the transform domain. These steps lead to a set of algebraic equations for the transform of the unknown aperture field. These equations are subsequently solved by Galerkin's method which is adopted for use in the transform domain. The desired quantities, e.g., the aperture and scattered fields, are readily derived from the knowledge of the solution of the matrix equation referred to above. The technique is illustrated in the paper by considering the problem of an infinitely long slit, although the finite slit case can also be attacked using the same technique.

An advantage of the present method is that the transformed equation is of algebraic rather than convolution form. This feature allows one to solve the problem more efficiently to form the numerical point of view as compared to the conventional moment solution of the integral equation in the space domain. Another advantage is that the accuracy of the solution

can be systematically improved by increasing the size of the matrix, although in many cases, the required matrix size is as small as  $2 \times 2$  or even  $1 \times 1$ .

- VI. 5-8 VARIATIONAL SOLUTION FOR THE ADMITTANCE OF A FINITE CYLINDRICAL DIELECTRIC-COATED ANTENNA. T. C. K. Rao and M. A. K. Hamid, Antenna Laboratory, Department of Electrical Engineering, University of Manitoba, Winnipeg, Canada R3T 2N2

A variational expression for the admittance of a dielectric coated conducting cylinder of finite length when the conductor is excited by a delta function generator at the centre is obtained by following the method developed by Hurd for a hollow conducting tube. The integral equation and the resulting expression are formulated with the tangential electric field in the outermost surface extending from the antenna ends to  $+\infty$  as unknown. The corresponding admittances of the infinite antenna which is needed for the evaluation of the admittance of the finite structure is derived following the procedures suggested by Duncan, Kunz, Ting and Schelkunoff. Suitable trial field is chosen and the resulting integrals are evaluated asymptotically for long antennas. Numerical results are presented to show the effects of variation of the dielectric shell thickness and permittivity on the input admittance and radiation pattern of the antenna.

- VI. 5-9 THE INFLUENCE OF A CIRCULAR DISC ON THE ELECTROMAGNETIC FIELD OF A HORIZONTAL DIPOLE PLACED OVER A LOSSY DIELECTRIC HALF-SPACE. A. V. Lugovoy and V. G. Sologub, Institute of Radiophysics and Electronics, Academy of Sciences of the Ukrainian SSR, Kharkov, USSR

As is known, the electromagnetic field radiated by a horizontal electric dipole over a dielectric half-space is essentially determined by the properties of the latter. In many cases of practical interest, however, it is desirable to reduce the influence of the dielectric to a minimum. For this purpose a conducting screen can be placed between the dipole and the dielectric. The present paper is dedicated to an analysis of the screening effect of a thin circular disc. Power characteristics of the dipole field are analyzed in dependence of the position and size of the disc.

Using the results of (1) and (2) the problem of finding the scattered field can be reduced to solving a system of two second-kind Fredholm integral equations with rather simple nuclei. The simplicity of the nuclei allows numerical methods to be effectively employed for seeking the solution. If the

size of the disc is small compared with both the wavelength and separation from the dielectric, the successive approximation method can be applied.

These methods are used for analyzing the cases of a dipole co-axial with the disc and of a plane wave normally incident on the interface. Note some of the most essential features: First, it turns out that the screening effect of the disc only slightly depends on the properties of the dielectric and its separation from the disc. A substantial dependence exists on the size of the disc and the distance between the screen and the dipole. The screening effect is weaker when this distance is increased. E.G., a disc  $2\lambda$  in diameter ( $\lambda$  is the wavelength) placed at  $\lambda/4$  from the dipole provides the same amount of screening as a  $4\lambda$  disc at  $\lambda/2$ .

For wavelengths larger than the double diameter of the disc the latter can be substituted by an equivalent electric dipole whose moment depends on the position and size of the disc. As the diameter of the disc approaches  $\lambda/2$ , the amount of the energy radiated in the free half-space changes sharply whereas the field pattern remains almost unchanged. The magnitude of this variation depends on the position of the disc and is pronounced the better, the higher is the conductivity of the medium. The effect is related to a "plunger" type standing wave excited between the disc and the dielectric. It disappears when the disc is laid on the dielectric.

---

1. L. N. Brazhnikova and V. G. Sologub. Akustichesky Zhurnal, 1971, vol. 19, No. 2, pp. 280-283.

2. A. V. Lugovoy and V. G. Sologub. Zh. Tehn. Fiz. (Sov. Phys.-Techn. Phys.) 1973, vol. 43, No. 3, pp. 678-681.

## ELECTROMAGNETIC THEORY

Chen To Tai, Chairman

- VI. 6-1 ALTERNATIVE REPRESENTATIONS OF THE DYADIC GREEN'S FUNCTION FOR A RECTANGULAR CAVITY.\* C. -T. Tai, Radiation Laboratory, Department of Electrical and Computer Engineering, The University of Michigan, Ann Arbor, Michigan, 48104

The different representations of the dyadic Green's function of the electric type will be presented in this paper. The work supplements the incomplete version previously discussed by Morse and Feshbach. In one of the representations, the construction of the dyadic Green's function is based on the modal functions for a cavity; in another representation use is made of the waveguide modes. The equivalence between the different representations can be proved by means of some not too well known series. The relationship between the dyadic Green's function of the electric type and that of the vector potential type will also be pointed out.

\*The work reported here was supported by the Harry Diamond Laboratories.

- VI. 6-2 DETERMINATION OF RADIATED POWER IN THE PRESENCE OF SOURCE-SCATTERER INTERACTIONS. W. V. T. Rusch, Department of Electrical Engineering, University of Southern California, consultant, Jet Propulsion Laboratory; and P. Cramer, Jet Propulsion Laboratory, Pasadena, California, 91103

When a localized electromagnetic source illuminates a passive scatterer, the resulting field distribution is sometimes characterized by quantities which are normalized by the total radiated power,  $P_T$ . Examples are directivity, beam efficiency, antenna temperature, etc. Normalization will be in error if it is assumed that  $P_T$ , the total power radiated in the presence of the scatterer, is equal to  $P_S$ , the total source power in the absence of the scatterer. In the case of an electric current distribution,  $\vec{J}$ , which is held fixed as a perfectly conducting scatterer is placed in its proximity

$$P_T = P_S - \frac{1}{2} \text{Re} \int \vec{E}_s \cdot \vec{J}^* dv$$

where  $\vec{E}_g$  is the scattered field radiated by the currents induced on the scatterer. The integral can be interpreted as a mutual impedance term which effectively changes the source input impedance so that the total power changes although the input current remains constant.

Examples are presented to illustrate conditions under which this effect is particularly significant, and a technique is described whereby source multipoles can be used to evaluate the correction term.

VI. 6-3 A SURFACE FORMULATION FOR CHARACTERISTIC MODES OF MATERIAL BODIES. Yu Chang, Union College, Schenectady, New York; and R. F. Harrington, Syracuse University, Syracuse, New York

A theory of characteristic modes for material bodies is developed using equivalent surface currents. This is in contrast to the alternative approach using induced volume currents. The mode currents form a weighted orthogonal set over the material body surface, and the mode fields form an orthogonal set over the sphere at infinity. The characteristic modes of material bodies have most of the properties of those for perfectly conducting bodies. Formulas for the use of these modes in electromagnetic scattering problems are given. A procedure for computing the characteristic modes is developed, and applied to two-dimensional bodies. Illustrative examples of the computation of characteristic currents and scattering cross sections are given for cylinders of different material constants.

An additional approach for computing the scattering cross sections is also given, based on the method of moments. In terms of this method, the operator equations are reduced to matrix equations, and the current is found by matrix inversion. The computation of scattering cross sections corresponds to an additional matrix multiplication with a measurement matrix. The matrix inversion solution is compared to the modal solution using characteristic modes.

VI. 6-4 JUNCTION CONDITIONS FOR ELECTRICALLY THIN CONDUCTORS. R. W. P. King, Harvard University, Cambridge, Massachusetts and The University of Mississippi, University, Mississippi

An important step in the determination of the distributions of current and charge on metal radiating and scattering structures that include confluent wires is the correct specification of these quantities at the junctions. Of particular interest are the parasitic crossed conductors used to simulate an aircraft exposed to an electromagnetic field of high intensity.

The junction conditions imposed in the literature include Kirchhoff's current law, continuity of the surface density of charge (i.e., the charge per unit length divided by the radius of the wire), continuity of the charge per unit length, continuity of the scalar potential and of components of the vector potential. Most numerical methods rely on the currents extrapolated to the junction to satisfy Kirchhoff's current law and impose no condition on their derivatives.

From a study of the charge distributions in (1) the coaxial line with a change in the radius of the inner conductor, and (2) the spheroidal antenna with a sinusoidal current and two confocal sections with different eccentricities, it is concluded that at the junction of electrically thin conductors Kirchhoff's current law and the continuity of charge per unit length (not the charge divided by the radius) are the correct zero-order conditions. Since the potentials are always continuous everywhere except across double layers (delta-function generators), conditions on the potentials are redundant and insufficient to specify the currents and their derivatives at a junction.

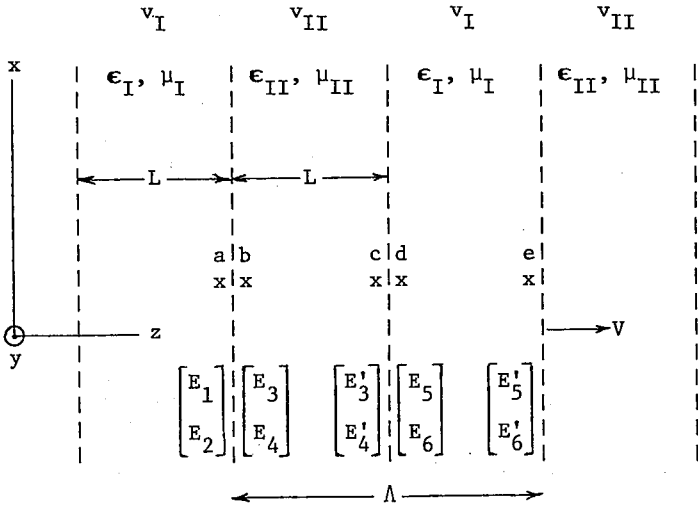
- VI. 6-5 ACCURATE NETWORK REPRESENTATION OF NEAR FIELDS AND FAR FIELDS SCATTERED BY DISCONTINUITIES IN WAVEGUIDE.  
T. E. Rozzi, Electromagnetics Laboratory, Electrical Engineering Department, University of Illinois, Urbana, Illinois, 61801, on leave of absence from Philips Research Laboratories, Eindhoven, Holland

It is currently assumed that equivalent networks of waveguide discontinuities be approximate, far-field representations, as contrasted to field solutions, yielding the accurate details of the near field as well as of the far field. In fact, at any distance from the discontinuity, it is possible to construct broad-band multiport equivalent networks of the scattering problem from a rigorous Rayleigh-Ritz variational approach. Voltage and currents at the ports, then, reproduce the details of the field. The approach is based upon the observation that for lossless reciprocal structures, the frequency dependence of the Green's operator must satisfy a generalized form of Foster's theorem. Furthermore, if the reference planes are placed at a finite distance away from the discontinuity, the number of ports in the equivalent network can be taken as finite. The application to transverse iris and obstacle-type discontinuities will be treated in detail.

VI. 6-6 SCATTERING OF NORMALLY INCIDENT ELECTROMAGNETIC WAVES BY A MOVING SQUARE WAVE MODULATION OF THE PERMITTIVITY. Kaiser S. Kunz, Arts and Sciences Research Center, New Mexico State University, Las Cruces, New Mexico; and B. K. Singaraju, National Research Council Resident Research Associate, Air Force Weapons Laboratory, Electronic Division, Kirtland Airforce Base, Albuquerque, New Mexico

An acoustical square wave produces a change in the density of a medium and this in turn varies the number of polarizable dipoles per unit volume and hence the permittivity  $\epsilon$ . One can also produce such a modulation of permittivity, in principle, by an electromagnetic pump wave in a nonlinear material (e.g., a ferroelectric crystal), see Tsai and Auld.<sup>1</sup>

We idealize the physical situation as in the above reference, by assuming a square wave modulation of the permittivity  $\epsilon$  of an infinite medium, without dispersion, by a pump wave moving to the right with a velocity  $V$  (may be taken as positive or negative). The situation is sketched in the following figure.



A small electromagnetic wave traversing the medium parallel or antiparallel to the pump will experience reflections at the moving discontinuities of the pump wave. This results in a composite signal wave made up of forward and backward components in the stationary medium between these discontinuities. The doppler shifts of these components and the wave matrix relating the electric fields across a discontinuity are those given by Tsai and Auld.<sup>1</sup>

We obtain a wave matrix A relating the forward wave ( $E_5'$ ) and backward wave ( $E_6'$ ) at the point "e" in the figure to those one pump wavelength  $\Lambda$  earlier, point "a". It is given by

$$\begin{bmatrix} E_5' \\ E_6' \end{bmatrix} = \begin{bmatrix} A_{11} & A_{12} \\ A_{21} & A_{22} \end{bmatrix} \begin{bmatrix} E_1 \\ E_2 \end{bmatrix}, \quad (1)$$

where

$$A_{11} = \frac{1}{2} \left[ (1 + \beta_+) e^{ik_3 L} + (1 - \beta_+) e^{-ik_4 L} \right] e^{ik_1 L} \quad (2a)$$

$$A_{12} = -\frac{1}{2} \beta_- \frac{1 + \frac{v}{v_I}}{1 - \frac{v}{v_I}} \left( e^{ik_3 L} - e^{-ik_4 L} \right) e^{ik_1 L} \quad (2b)$$

$$A_{21} = \frac{1}{2} \beta_- \frac{1 - \frac{v}{v_I}}{1 + \frac{v}{v_I}} \left( e^{ik_3 L} - e^{-ik_4 L} \right) e^{-ik_2 L} \quad (2c)$$

$$A_{22} = \frac{1}{2} \left[ (1 - \beta_+) e^{ik_3 L} + (1 + \beta_+) e^{-ik_4 L} \right] e^{-ik_2 L} \quad (2d)$$

and

$$\beta_{\pm} = \frac{1}{2} \left( \frac{\eta_{II}}{\eta_I} \pm \frac{\eta_I}{\eta_{II}} \right), \quad (3)$$

$\eta_I$ ,  $\eta_{II}$  being the impedances of the two regions. Here  $k_1$ ,  $k_3$  are the propagation constants of the forward waves and  $k_2$ ,  $k_4$  those of the backward waves in regions I and II, respectively.

The nature of composite wave in the infinite medium is determined by the eigenvalues of A which are of two distinct types, depending on whether or not their magnitudes are equal to unity. We look at the various cases using some of the methods proposed for treating instabilities.<sup>2,5</sup>

To properly interpret the modulated composite wave, which has segments of different amplitudes, frequencies, and wave numbers, one applies a type of Fourier analysis to obtain a Floquet-type expansion.<sup>3,4</sup> These can then be compared to the well-known case of a sinusoidal pump wave.

One finds, for example, that the frequency spectrum of the composite wave is discrete with a separation between components that is equal to the fundamental frequency of the pump wave.

For a small modulation of the medium the forward wave component usually dominates with only a small backward wave component. For proper choices of the parameters one obtains a resonance condition in which the backward wave is of the same order of magnitude as the forward wave. The propagation constants  $k_1$  and  $k_2$  of the forward and backward components are then related to the propagation constant  $K$  of the pump wave by

$$k_1 = \frac{n}{2} K + \frac{V}{v} K \quad (4)$$

and

$$k_2 = \frac{n}{2} K - \frac{V}{v} K. \quad (5)$$

Here  $n$  is a positive integer and

$$v = \frac{v_I + v_{II}}{2} \cong v_I \cong v_{II}. \quad (6)$$

Eqs. (4) and (5) are just the Bragg conditions for the case of normal incidence.

It is, of course, doubtful if these conditions can be met experimentally. The case of oblique incidence, however, involves the consideration of two separate transmitted waves at each moving discontinuity and this makes the treatment very much more difficult.

1. C. S. Tsai and B. A. Auld, Wave interactions at moving boundaries, *J. Appl. Phys.* 38, No. 5, 2106-2115 (April, 1967).
2. R. Briggs, *Electron-Stream Interaction with Plasmas*, MIT Press, Cambridge, Mass., 1964.
3. D. E. Holberg and K. S. Kunz, "Parametric properties of fields in a slab of time-varying permittivity," *IEEE Trans. on Antennas and Propagation*, AP-14, 183-194 (March, 1966).
4. D. E. Holberg and K. S. Kunz, "Parametric properties of dielectric slabs with large permittivity modulation," *Radio Science* 3 (new ser.), 273-286 (March, 1968).
5. Ronald L. Fante, Optical propagation in space-time-modulated media using many-space-scale perturbation theory, *J. Opt. Soc. Amer.* 62, No. 9, 1052-1060 (Sept., 1972).

- VI. 6-7 NEAR FIELD COUPLING BETWEEN TWO SECTORAL HORNS USING THE GENERALIZED SCATTERING MATRIX TECHNIQUE.  
M. F. Iskander and M. A. K. Hamid, Antenna Laboratory,  
Department of Electrical Engineering, University of  
Manitoba, Winnipeg, Canada R3T 2N2

The generalized scattering matrix technique applies to evanescent as well as propagating waveguide modes and has been employed to solve many waveguide discontinuities as well as various diffraction and scattering problems. The approach in this paper is to employ Schwarz's method of overlapping regions to derive the individual scattering matrix at the waveguide-horn junction, and that at the aperture of the H-plane transmitting sectoral horn in the presence of the H-plane receiving horn. The generalized scattering matrix approach is then employed to combine the scattering matrices of the successive junctions using the appropriate shifting matrix. This results in the response at the output of the receiving horn for a given fundamental TE mode in the feed line of the transmitting horn. The results for the behaviour of the multiply scattered fields and coupled power are presented to show the effect of the separation distance as well as the geometrical dimensions of the horns.

The accuracy of the solution is varified by comparison with a numerical solution based on the method of moments. It is also shown that the method has specific geometrical advantages since the dimensions of the overlapping regions can be related to all the geometrical parameters as well as the scattering matrix parameters of each corresponding junction.

- VI. 6-8 TOWARDS UNIQUENESS IN INVERSE EM PROBLEMS.  
L. B. Dean, NOAA Post-Doctoral Fellow, U.S.  
Department of Commerce, National Oceanic and  
Atmospheric Administration, Environmental  
Research Laboratories, Boulder, Colorado, 80302

The question of uniqueness is examined for the problem of determining the spatial variation of the complex conductivity within a volume. Physical arguments concerning macroscopic electromagnetics are combined with the Poynting's vector and the Maxwell's stress tensor relations of frequency domain electromagnetics to determine uniqueness properties of the conductivity. The arguments presented are analogous to those presented in the usual uniqueness theorem of electrodynamics.

## NUMERICAL METHODS

G. Thiele, Chairman

- VI. 7-1 INCORPORATION OF EDGE CONDITIONS INTO MOMENT METHOD SOLUTIONS. D. R. Wilton and S. Govind, University of Mississippi, University, Mississippi, 38677

Singular currents at edges pose numerical problems in moment method solution procedures. Badly behaved or slowly converging solutions along with poorly satisfied boundary conditions are often encountered. This paper reports the results of an investigation on the convergence of the current on an infinite strip with respect to the choice of expansion functions for TM illumination. For this problem, the current is entirely parallel to and singular at the edges. It is found that pulses seem to be superior to piecewise linear expansion functions in representing the current near the edge. This was further verified by considering an analogous static problem for which the solution is known exactly. However, by suitably incorporating the edge singularity into the expansion functions, the rate of convergence can be significantly enhanced. Furthermore, the anomalous behavior of solutions using piecewise linear expansion functions is eliminated. In addition, it is found in the static analog case that a correction factor can be used a posteriori to correct the edge behavior when pulses are used. A similar correction factor is being tested for the dynamic case.

A similar approach is being considered for the case of the TE polarization wherein the current is non-singular at the strip edge, but satisfies a similar edge condition.

- VI. 7-2 ON STATISTICAL ELECTROMAGNETIC THEORY OF A LARGE SYSTEM. R. M. Bevensee, Lawrence Livermore Laboratory, Livermore, California, 94450

We discuss the problem of inverting the matrix equation  $V = Z \cdot I$  for an antenna or scattering problem to obtain the currents, when the  $Z$ -matrix is statistical (i.e., ill-defined or uncertain). For a large system with many statistical parameters the direct solution would be prohibitively time consuming. We consider instead using a Markov chain to estimate the statistical moments of a single current of interest. Each state of the chain is evaluated by a secondary Markov process which can be truncated when the accuracy is sufficient. We shall discuss

conditions by which all this is possible and try to estimate the computing time required for a large system with many statistical parameters.

- VI. 7-3 APPLICATION OF STABILITY PARAMETERS IN THIN-WIRE ANTENNA MODELING. C. A. Klein, Philco-Ford Corporation, 3939 Fabian Way, Palo Alto, California, 94303; and R. Mittra, Electromagnetics Laboratory, Electrical Engineering Department, University of Illinois, Urbana, Illinois, 61801

As is well known, solutions of integral equations derived by the method of moments sometimes are highly sensitive to minor changes in data. When these ill-conditioned situations occur it is an advantage to have a simple numerical guide to the severity of this difficulty. This paper will compare such stability parameters as the normalized determinant, spectral radius, condition number and two new parameters, viz., the a posteriori condition number and the pivot ratio. The comparison will be made on the basis of reliability and computational ease. Briefly discussed will be how scaling the matrix can affect the stability and the distribution of error.

These stability concepts will be applied to thin-wire modeling of antennas. Considered will be using Pocklington's versus various implementations of Hallen's integral equations, the effect of changing the radius of the antenna, and results from unequal segmentation of antennas and from antennas with junctions.

- VI. 7-4 TRANSIENT BEHAVIOR OF A CAVITY-BACKED SLOT APERTURE. D. K. Cheng and C. A. Chen, Electrical and Computer Engineering Department, Syracuse University, Syracuse, New York

Induction theorem is used to formulate the problem of transient electromagnetic excitation of a rectangular cavity through an aperture which is not necessarily small. The governing second-order differential equation is converted into a set of first-order equations by the introduction of appropriate new variables. These first-order equations correspond to normalized state equations, and the conversion will result in faster convergence in the numerical solution. Moment method is employed to solve the equations subject to specified boundary conditions. Cavity fields are expressed in terms of subsectional expansion functions with time-dependent coefficients and external fields are represented as superpositions of plane waves. These fields are properly matched at the aperture, and the effect of cavity-wall reflections is included in the formulation. The expansion coefficients are evaluated by the singularity-expansion method in terms of natural frequencies, natural modes, and coupling coefficients. Some numerical results for the transient excitation of a cavity-backed slot aperture will be presented.

VI. 7-5 RADIATION EFFICIENCY CHARACTERISTICS OF SINGLE AND MULTI-WIRE BEVERAGE ANTENNAS.\* E. K. Miller, D. L. Lager, and R. J. Lytle, Lawrence Livermore Laboratory, Livermore, California, 94550

Previous studies (Lytle, et al., "Beverage Antenna, A Multi-conductor Antenna that Significantly Interacts with the Ground," 1974 URSI Symposium on Electromagnetics Wave Theory, London, July 1974.) have indicated that the radiation efficiency of Beverage antennas could be increased by using multiple, closely-spaced wires. These results, although in qualitative agreement with experimental measurements, were of uncertain validity because they were derived using an approximate image theory to determine the antenna-ground interaction.

In this paper, results are presented concerning the radiation efficiency of single and multi-wire Beverage antennas obtained from calculations based on rigorous Sommerfeld theory. The dependence of the Beverage antenna's efficiency upon the ground and antenna parameters is developed, and the indications of the approximate theory are shown to be confirmed. Of perhaps greatest interest is the finding that the radiation efficiency is most sensitive to the effective antenna diameter, and increases in direct proportion to the rate at which the antenna sheds energy, a phenomenon relatively independent of the ground's presence.

---

\*This work was performed under the auspices of the U.S. Energy Research and Development Administration.

VI. 7-6 RADAR CROSS SECTIONS OF ARBITRARY, MULTI-LAYERED, LOSSY DIELECTRIC CYLINDERS. T. K. Wu and L. L. Tsai, Electrical Engineering Department, University of Mississippi

The scattering properties of TM illuminated lossy dielectrical cylinders are analyzed by surface integral equation techniques. The method involves first moment method solutions for the surface fields at the interface, and then from these the scattered fields in the far zone.

For a homogeneous circular cylinder of lossy dielectric ( $\epsilon_r=4$ ) radar cross section (RCS) is plotted over  $k_0 a = .62$  to  $2.48$ , a range over which many resonances exist, with the conductivity  $\sigma$  as parameter. The numerical solution results show excellent agreement with the exact eigenfunction expansion results. It is interesting to note that when the dielectric cylinder becomes slightly lossy, the resonances are more significant than the lossless case. As the conductivity  $\sigma$  is further increased, the previous resonances become reduced finally approaching the perfectly conducting cylinder trends.

RCS for homogeneous lossless and lossy elliptical cylinders are next considered. For the lossless elliptic cylinder good agreement is also obtained with results available in the literature. One additional example considered is a wedge-semicircle cross sectioned cylinder, which may model airplane wings or re-entry vehicle plumes.

For multi-layered cylinders, consideration is first for a circular conducting cylinder coated with a circular dielectric sheath, where comparison with the exact solution is shown. Applications to the case of the cylinder with a plume sheath is finally also studied.

VI. 7-7 RECENT CAPABILITY EXTENSIONS FOR WIRE CODES.\*  
A. J. Poggio, R. W. Adams, and E. K. Miller,  
Lawrence Livermore Laboratory, Livermore,  
California, 94550

Several topics pertaining to the enhancement of the capabilities of wire codes are considered, namely, the treatments of end caps, discontinuous radii, kernel approximations near the singularity, and an overlapping sinusoidal interpolation scheme for collocation algorithms.

Using a method based on the exact integral representations for fields due to sources on open surfaces, a general basis function for end caps and the annular region at the intersection of two cylinders of differing radii is derived. This basis is mathematically attractive in that it does not require a surface integration for field evaluation, satisfies all physical constraints on current density, and leads to a simple relation between current and its derivative at the join region.

The kernel approximation based on the work of Tesche is extended to allow for the effects of variations in the radius to wavelength ratio ( $ka$ ) while requiring little further computational effort.

A current basis employing sinusoidal interpolation functions and an overlap scheme for a collocation solution is presented. Continuity of current and its derivative is enforced with little additional penalty in computation time while the treatment of junctions is greatly simplified.

In all cases, results are presented to illustrate the advantages afforded by these approaches.

\*This work is performed under the auspices of the U.S. Atomic Energy Commission.

- VI. 7-8 AN ITERATIVE-SOLUTION ANALYSIS OF THE BENT-WIRE SCATTERER. Chalmers M. Butler and James O. Prewitt, Department of Electrical Engineering, University of Mississippi, University, Mississippi, 38677; and Ronald W. P. King, Department of Engineering and Applied Physics, Harvard University, Cambridge, Massachusetts, 02138

A technique for determination of currents induced on a bent-wire scatterer by a specified incident plane wave is developed, and expressions amenable to iterative solution techniques are derived for the wire currents. There is a significant difference in the iterative solution procedure applied to the bent-wire problem from that applied to either the straight wire or to perpendicular crossed wires. This difference is explained in detail. Sample results are presented for calculated currents induced on the bent-wire in free space as well as over a ground plane. Finally, the authors show that, in many cases, the zero order solution is a good approximation to the actual current, and they point out that such solutions can be calculated with ease (slide rule or pocket calculator).

- VI. 7-9 A GUIDE TO CHOOSING BASIS AND TESTING FUNCTIONS IN THE METHOD OF MOMENTS. William A. Davis, Department of Electrical Engineering, Air Force Institute of Technology, Wright-Patterson Air Force Base, Ohio, 45433

During the past decade, the method of moments has become one of the primary methods for solving EM scattering problems. The basis and testing functions used in this method have typically been chosen to obtain a well-behaved matrix with elements of relatively simple form for computation. In addition, several authors have considered the effects of the above choices on near field behavior in EM problems. These ideas may be drawn together to form a guide for choosing the basis and testing functions in the method of moments.

The equation to be solved is given by  $Lf = g$ . Approximate  $f$  by  $f_a$ , a finite sum of the functions  $f_i(x) = f(x-x_i)$ . Let the testing functions be given by  $w_i(y) = \tilde{w}(y-y_i)$ . Thus the moment method consists of taking the inner product of  $w_i$  with the equation  $Lf_a = g$  to obtain a set of simultaneous equations for the coefficients of the  $f_i$ . Only the functions  $\tilde{w}$  and  $f$  have to be specified to complete the formulation of the problem.

To obtain a guide for choosing  $\tilde{w}$  and  $f$ , define the function  $\rho(y) = \langle \tilde{w}(x-y), g(x) \rangle$  and  $\rho_f(y) = \langle \tilde{w}(x-y), Lf_a(x) \rangle$ . ( $\langle \cdot \rangle$  represents an inner product),  $\tilde{w}$  is chosen such that  $\rho$  is well-behaved in the sense that  $\rho$  is slowly varying about the  $y_i$ . For example,  $\rho$  may be a series of pulse functions if the  $y_i$

sample points are chosen about the pulse centers. To choose  $\tilde{f}$ , one notes that the moment method consists of approximating  $\rho$  by the interpolating function  $\rho_f$ . It is thus clear that  $f$  be chosen such that  $\rho_f$  is a reasonable approximation  $\rho$ . This latter part is not as difficult as it might seem in EM scattering problems since the local behavior of  $Lf$  can often be reasonably approximated by the local behavior of  $f$ .

The implication of this guide is to say that  $g$  and  $Lf_a$  are approximately equal as defined by integration with the testing functions. This is consistent with the forms of equality that occur in both the theories of calculus and of distributions, where equality is defined by integration with testing functions.

COMMISSION VI

0900 Thursday, June 5

136 Physics

BIOLOGICAL EFFECTS

C. C. Johnson, Chairman

- VI. 8-1 HEATING PATTERNS OF ENCLOSED AND DIRECT CONTACT MICROWAVE DIATHERMY APPLICATORS. Gideon Kantor, Mays L. Swicord and Murray J. Blair, Division of Electronic Products, Bureau of Radiological Health, FDA, Rockville, Maryland, 20852

Spaced applicators with enclosures of shielded absorbing material as well as direct contact applicators were developed to minimize scatter radiation at 2450 MHz. The applicators were loaded with a multilayered planar phantom of simulated fat and muscle tissues and heating patterns in the midplane of the phantom were obtained with an infrared thermographic camera. Temperature profiles across the fat-muscle interface as well as inside the muscle tissue were measured to compare heating patterns with and without enclosures. Heating patterns of direct contact applicators using waveguides, loaded with dielectric slabs, and truncated horns, lined with absorbing material, were investigated. Near field measurements of the unloaded applicators were obtained to evaluate the influence of the longitudinal electric field component (perpendicular to the applicator aperture) on the heating pattern for all the applicator designs. The scattered field was found to be less than  $5 \text{ mW/cm}^2$  (equivalent plane wave power density) for a microwave diathermy output of 130 watts.

- VI. 8-2 INDUCED CURRENTS IN BIOLOGICAL MEDIA WITH IMPLANTED METALLIC CONDUCTORS. D. P. Nyquist and K. M. Chen, Department of Electrical Engineering and Systems Science, Michigan State University, East Lansing, Michigan, 48824

The response of a biological medium with implanted metallic conductors to an impressed electromagnetic field is investigated. Implanted prosthetic devices, e.g., the cardiac pacemaker, constitute such a system. Induced high-frequency currents can damage the device, while intense local fields constitute a biological hazard. To assess the potential radiation hazards produced by these effects, fields excited in the conducting medium and currents induced on the metallic body are determined in terms of the system dimensions, the conductivity and permittivity of the biological medium (modelled as those of the human torso), and the frequency of the impressed field.

A model consisting of a metallic cylinder sheathed by a conducting cylinder of biological medium is initially considered. The impressed field consists of either an incident, plane EM wave or a uniform E-field having either TE (axial H-field) or TM (axial E-field) polarizations. Significant potential hazards are evident only with plane incident waves having TE polarization. Existence of these effects is dependent upon the presence of a magnetic field associated with the spatially-changing incident electric field. At frequencies of 100 MHz and 915 MHz, the surface current induced on a metallic cylinder of 3 cm radius sheathed by a biological cylinder of 30 cm radius can be as great as twice the amplitude of that induced on the same cylinder in vacuum. This significant induced current is associated (at 2.45 GHz as well) with a normal electric field at the cylinder surface which exceeds that existing in its absence.

Investigation of currents and fields associated with metallic objects immersed in finite biological media of varying shapes is presently in progress.

VI. 8-3 CALIBRATION OF MINIATURE MICROWAVE ELECTRIC FIELD DETECTOR FOR IMPLANTATION MEASUREMENT WITHIN BIOLOGICAL TISSUES. Augustine Y. Cheung, Institute for Fluid Dynamics and Applied Mathematics, University of Maryland, College Park, Maryland, 20742

A miniature, broadband, isotropic microwave probe has been developed by the Bureau of Radiological Health for radiation detection in the near field.<sup>1</sup> The objective of this paper is to describe the calibration of the probe for quantitative measurements within biological tissues. The probe consists of three mutually orthogonal colinear dipole elements supported by an alumina substrate. In practical applications, it is immersed within muscular tissues bounded by fat and bone on the outside. The procedures developed by Galejs for the calculation of impedance of a strip antenna submerged within a multilayer dielectric is followed.<sup>2</sup> Numerical integrations are carried out by a UNIVAC 1108 computer. The results indicate that the dielectric properties of the muscle which varies significantly with temperature, dominates the impedance under most conditions for frequencies ranging from 1-12 GHz. There is also a geometry dependence governed by the antennas' length (or frequency) and the dimensions of the substrate. Experimental calibration are carried out within an infinite slab (Dimension  $\gg \lambda_0(\epsilon)^{1/2}$ ) of simulated muscle<sup>3</sup> irradiated by a known field within an anechoic chamber. The temperature of the slab is monitored by a non-perturbing thermometer to keep track of the temperature variation of its dielectric properties. Experimental and theoretical results of the calibration are discussed.

1. H. Basser, M. Swicord and J. Abita, "A Broadband Miniature Electric Field Probe," Proceedings of the New York Academy of Sciences Conference on Biological Effects of Nonionizing Radiation (in press, Feb. 1974).

2. J. Galejs, "Driving Point Impedance of Linear Antennas in the Presence of a Stratified Dielectric," IEEE Trans. Antennas and Propagation, AP-13 (Sept. 1965).

3. A. Y. Cheung and D. W. Koopman, "Experimental Development of Simulated Biomaterials for Dosimetry Studies of Hazardous Microwave Radiation," Journal of Microwave Power (to be published, 1975).

VI. 8-4 MEASURE OF ENZYMATIC ACTIVITY COINCIDENT WITH 2550 MHZ MICROWAVE EXPOSURE. Thomas R. Ward, John W. Allis and Joe A. Elder, Experimental Biology Laboratory, National Environmental Research Center, Environmental Protection Agency, Research Triangle Park, North Carolina, 27711

Enzyme preparations were exposed to microwave radiation and enzymatic activity was simultaneously monitored spectrophotometrically with a crossed-beam exposure/detection system. To the authors' knowledge, this is the first time that enzymatic activity has been measured coincidentally with exposure to microwaves. The following enzymes were studied: glucose-6-phosphate dehydrogenase from human red blood cells, adenylate kinase from rat liver mitochondria, and rat liver microsomal NADPH cytochrome c reductase. Activities of these enzymes were determined at saturation with substrate where the rate of turnover was constant.

The apparatus consisted of a Cary 15 spectrophotometer fitted with a waveguide tuner and an applicator in the sample compartment. The waveguide was positioned so that the microwave beam (2450 MHz, continuous wave) was perpendicular to the light path and entered through the top of the open sample cuvette.

Enzymatic activities were determined at 25°C. The temperature of both the reference and sample solutions was measured with microthermocouples; in the latter, an implanted microthermocouple was positioned 1 mm above the light path of the spectrophotometer. Separate circulating water baths maintained constant temperatures in each compartment. From the magnitude of the temperature rise (5.2°C) due to absorption of microwave energy in the sample and the rate of sample cooling, the absorbed dose rate was calculated to be 45 mW/g. No difference was found between the specific activity of unirradiated and microwave-irradiated enzyme preparations.

- VI. 8-5 MICROWAVE EFFECTS ON HUMAN TISSUE CULTURE CHROMOSOMES. B. S. Guru and K. M. Chen, Department of Electrical Engineering and Systems Science, and Roger Hoopingarner, Department of Entomology, both at Michigan State University, East Lansing, Michigan, 48824

An experimental study has been conducted to investigate the chromosomal aberrations induced by a microwave in human amnion and lymphocyte tissue culture cells.

Human amnion cells were grown in Eagle's minimum essential medium (MBM), supplemented with 13% fetal calf serum, in plastic tissue culture bottles. Human lymphocyte cells were obtained from fresh human blood and grown in chromosome medium (GIBCO). The lymphocyte cells were stimulated by phytohemagglutinin to divide and the cells were exposed to microwave radiation at different growth stages.

A closed waveguide system was used in the experiment. The cell samples were placed inside of the waveguide and exposed to a S band microwave of a certain intensity and over a certain period. The waveguide system was driven by a high power microwave system which could provide 25 watts over the frequency range of 1 to 4 GHz. The power absorbed by the cell sample was carefully measured by monitoring the incident and reflected powers to the waveguide system. The actual electric field at the location of cells imbedded in a liquid medium was determined numerically based on a tensor integral equation.

Chromosomal aberrations were observed for these human cells when exposed to a microwave of 2.45 GHz at the level of 40 volts/m for less than 10 minutes or 20 volts/m for about 60 minutes. The induction of these chromosomal aberrations were non-thermal in nature as the temperature of the cell samples was kept below 37°C during the radiation exposure. The radiation exposure to these cells is substantially lower than the U.S. safety standard of 194 volts/m.

- VI. 8-6 A NUMERICAL STUDY OF MICROWAVE DOSE DISTRIBUTION IN THE HUMAN HEAD. Stanley M. Neuder, Bureau of Radiological Health, Rockville, Maryland, 20852; and R. Bruce Kellogg, IFDAM, University of Maryland, College Park, Maryland, 20742

A computer program has been written to calculate microwave scattering from a family of concentric spherical shells using the spherical harmonics expansions of Stratton<sup>1</sup> and Shapiro-Lutomirski-Yura.<sup>2</sup> The program utilizes a rigorous analysis for the number of terms in the series needed for a given accuracy. Comparisons of the number of terms required are made with heuristic rules developed by Kritikos-Schwan<sup>3</sup> and Joins-Spiegel.<sup>4</sup>

The program is applied to study the distribution of microwave radiation on the human head. As in (Ref. 2), the head is modelled by a family of concentric spheres, the inner sphere representing the brain cavity. Some numerical and graphical results are presented giving the maximum and average power deposition in the head as a function of frequency and of variations in the dielectric parameters. In addition, field polarizations are discussed with implications for implantable probes.

1. Electromagnetic Theory, McGraw-Hill, 1941.
  2. IEEE Trans. Microwave Theory Tech., Vol. MIT-19 (1971), p. 187.
  3. IEEE Trans. Biomedical Eng., Vol. BME-19 (1972), p. 53.
  4. IEEE Trans. Biomedical Eng., Vol. BME-21 (1974), p. 46.
- VI. 8-7 THE MICROWAVE HEARING EFFECT--A THEORETICAL ANALYSIS.  
Charles Cain and David Borth, Department of Electrical Engineering, University of Illinois, Urbana, Illinois, 61801

Several investigators have suggested that the audible "clicks" heard by people exposed to microwave radiation may be explained in terms of thermally generated acoustic transients in the head produced by pulsed microwave energy. To verify this hypothesis, a theoretical analysis of the stress gradients produced in materials irradiated with electromagnetic energy was conducted. For liquids confined to planar geometries, a one-dimensional non-homogeneous wave equation may be derived taking into account the volume forces due to both radiation pressure and thermal expansion, and the surface forces due to radiation pressure.

Closed-form solutions for both particle displacement and pressure waves were found for several different boundary conditions, as well as the Fourier transforms of these quantities. The closed-form solution was found to consist of both a stationary part, whose effect is important only in the immediate region of the incident electromagnetic wave, and a travelling part, which propagates unattenuated through an ideal liquid.

To quantify these results, a numerical example using physiological saline was considered. From this example, it became apparent that thermal expansion was approximately four orders of magnitude more effective than radiation pressure in converting electromagnetic energy to acoustic energy. For relatively moderate microwave pulse energies, acoustic transients that would be above the human threshold of hearing are generated.

VI. 8-8 ELECTROMAGNETIC TRANSIENT PROPAGATION IN MODELS OF MAN. James C. Lin and Chuan-Lin Wu, Department of Electrical Engineering, Wayne State University, Detroit, Michigan, 48202

The biological effects and potential hazards of exposure to electromagnetic radiation have been a concern in recent years. However, the literature on the interaction of nonionizing electromagnetic radiation with biological systems has for the most part been dealing mainly with the effects of continuous radiation. The consequences of pulsed wave radiation on the human body have only been recognized lately. Most recently, the biological effects of high amplitude electromagnetic pulse have been a concern. In fact, several federal and private organizations are considering promulgating a standard on exposure to electromagnetic pulses. Unfortunately, there is insufficient scientific information on which to base a realistic standard. In this paper, a theoretical analysis of the characteristics of transmitted electromagnetic pulse in homogeneous spheroidal models of human and animal bodies is made. Both Gaussian and triphasic transient waveforms are considered. Neglecting the displacement current, it is shown that the transmitted pulse can be expressed in closed-form which indicates that the transmitted electromagnetic field is related to the time derivative of the incident pulse. Numerical results are obtained for both types of incident waveforms and they are compared to indicate their relevance to electromagnetic pulse interaction with man.

TRANSIENTS II

D. G. Dudley, Chairman

- VI. 9-1 TIME DOMAIN VS. FREQUENCY DOMAIN SOLUTION OF EM SCATTERING PROBLEMS. C. L. Bennett and R. M. Hieronymus, Sperry Research Center, Sudbury, Massachusetts

With the advent of high-speed digital computers, the numerical solution of electromagnetic scattering problems became practicable. The frequency domain approach was the first to receive attention, in the early sixties, in the form of a solution of an integral equation for the currents on the surface of a scatterer at one frequency. In the late sixties when interest developed in wider band radar systems in particular, and transient electromagnetics in general, a direct time domain approach was developed. This consisted of the solution of a space-time integral equation for currents on the scatterer surface by a "marching on in time" procedure. This paper examines these complementary techniques and considers their relative advantages and disadvantages. Results will be presented and discussed. Particular attention will be given to the computer storage and running times required by these two approaches.

- VI. 9-2 APPLICATION OF THE IMPULSE RESPONSE AUGMENTATION TECHNIQUE TO SCATTERING BY A SPHERE-CAPPED CYLINDER. C. L. Bennett, Sperry Research Center, Sudbury, Massachusetts

The impulse response augmentation technique combines the known singular portion of the impulse response with the computed smoothed impulse response to yield an estimate of the target's total impulse response. Past results obtained using this technique for the case of the sphere have been shown excellent agreement with the exact sphere impulse response. Results have also been obtained for the case of a prolate spheroid that exhibits a polarization dependence in the impulse response. This paper describes the application of the impulse response augmentation technique to the case of a sphere-capped cylinder. The impulse response obtained contains a polarization dependence that is proportional to the difference in the principle curvatures at the specular point. This feature modifies the step portion and adds a ramp portion to the impulse response. Moreover, a portion of the impulse response return can also be attributed to the join region between the cylinder body and the

sphere caps. Results are presented and discussed for a number of incident angles and for both TE and TM polarizations.

- VI. 9-3 ELECTROMAGNETIC PENETRATION THROUGH TWO COUPLED RECTANGULAR APERTURES. Juang-Lu Lin, The Boeing Aerospace Company, P. O. Box 3999, Mail Stop 4A-41, Seattle, Washington, 98124

A theory of an electromagnetic diffraction by two coupled rectangular apertures on an infinite plane conducting screen is presented. The problem is solved in two different ways: one is by an integral equation method and the other is by a numerical method. The computed results based on these two methods are in very good agreement.

In the close form analysis, an approximate kernel appropriate to this problem is used. The aperture field distribution is also decomposed into symmetric and antisymmetric modes such that the two simultaneous integral equations for the aperture field distribution may be converted into two independent integral equations which can be solved separately.

In the numerical method, the problem is transformed into solving the complementary problem of the diffraction by two coupled rectangular plates modeled by a wire mesh, and the diffracted field due to apertures can be obtained by applying the Babinet's principle directly to this problem.

The numerical examples include the calculations of the transmission coefficient as a function of separation between the apertures, using the integral equation and the numerical methods, and they are in very good agreement. The aperture field distributions are also plotted as a function of separation between the apertures with incident angle as a parameter.

The outcome of this research should prove useful in determining the electromagnetic penetration through the apertures or holes in an aeronautical system.

- VI. 9-4 A SIMPLE WAY OF SOLVING TRANSIENT THIN-WIRE PROBLEMS. Lennart Marin and T. K. Liu, The Dikewood Corporation, Westwood Research Branch, Los Angeles, California, 90024

So much has been said about scattering from thin wires that one more paper about this topic is hard to justify. Almost all work done in recent years involving scattering and radiation from thin wires has been based on numerical calculations on a computer. These numerical calculations tend to become very complicated and there are many cases where a simplified analysis yields sufficiently accurate results. In this paper, approximate analytical expressions for the time history of the current induced on a thin wire are obtained when the wire is either excited by an incident step-function

plane wave or by a slice generator whose output voltage is a step function in time.

The method is based on an expansion of the induced current in terms of the natural modes. In this expansion the induced current is expressed as a sum of exponentially damped sinusoidal oscillations whose current distribution is a standing wave in space. The natural modes are found from the nontrivial solutions of the Maxwell equations together with the approximate boundary conditions on the structure and the outgoing wave condition at infinity. When the scattering body is a straight wire, approximate asymptotic expressions for the natural modes can be found in terms of the "antenna parameter"  $\Omega = 2 \ln$  (wire length/wire radius). A comparison between the results obtained from the asymptotic theory and those obtained by solving the time-domain integral equation on a computer is made and good agreement is found. The advantage with the asymptotic method lies in the fact that all expressions are of simple analytic form and can be computed using a desk calculator. This method has also been used to study the currents induced on the following structures: a wire bent into an L shape, crossed wires (a simplified model of an aircraft), two parallel wires (staggered and nonstaggered) and a wire bent into a ring. The exciting field can be that of an incident plane wave, a slice generator, or a moving charged particle.

VI. 9-5 COMMON MODE-INDIVIDUAL WIRE MODEL FOR COMPLEX CABLE SYSTEMS. W. L. Curtis and J. M. Carter, Boeing Aerospace Company, Seattle, Washington; M. L. Vincent and G. L. Maxam, Boeing Aerospace Company, Albuquerque, New Mexico

Study of EMP (Electromagnetic Pulse) effects on electronic circuitry such as in aeronautical systems often involves the analysis of complex multiconductor cables. In theory, it is possible to analyze such systems in detail but because of the complexity, the large number of circuits to be evaluated, and a broadband transient analysis requirement, simple approximate models for the cable systems must be used.

The common mode-individual wire model was developed to meet this necessity. The multiconductor branched cable system is first modeled as a single conductor excited at one or more points or, if appropriate, by a continuously distributed source. The common mode currents are calculated using standard transmission line equations. The individual wires in the cable bundle are assumed to couple to the common mode current producing voltage excitations at the terminations of the wire under investigation. The individual wire model with voltage sources at the terminations of the wire is used to calculate a Thevenin voltage and impedance. Calculated common mode currents and Thevenin voltages and impedances are compared with laboratory

measurements. Calculated and measured time domain open circuit voltages for an aircraft cable system with a pulse excitation are compared.

- VI. 9-6 PENETRATION OF EM WAVES THROUGH LAYERS OF EXTREMELY THIN METAL FOIL. Yu-Ping Liu and W. Dennis Swift, IRT, Box 80817, San Diego, California, 92138

For some particular cases, the amount of EM energy which penetrates through one or more layers of extremely thin metal plate or foil is of major concern. Here, an extremely thin plate is defined as a plate whose thickness is much smaller than a skin depth. For a designer, the knowledge of the transmission ratio of an EM wave passing through one or more layers of thin foil is valuable. In this paper, solutions for several such problems are given.

First, the penetration ratios of EM wave passing through copper and aluminum are presented for several different frequencies and thickness. Then, the equations for the penetration through two parallel layers are derived. The difference between the results of the double layer problem and that of the equivalent single layer is discussed. The distance parameter between the layers is included in the discussion. Finally, the general extension of the conclusion to many layer problems is reached.

- VI. 9-7 SGEMP COUPLING THROUGH APERTURES. Bharadwaja K. Singaraju, John K. Little, and Carl E. Baum, Air Force Weapons Laboratory, Albuquerque, New Mexico

The problem of the coupling of a system generated electromagnetic pulse (SGEMP) through an aperture in a perfectly conducting infinite plane is studied in this paper. Neglecting the nonlinear effects, an electric charge 'Q' is assumed to travel at a velocity by the aperture in a straight line. Using the Babinet's principle, the equivalent problem is deduced to be a magnetic charge traveling by a disc. General theory is developed to include SGEMP coupling through an arbitrary aperture. Coupling through a slot is studied by calculating the currents induced on an equivalent wire by a magnetic charge. Singularity expansion method is used for this purpose. Extensive numerical results for the currents induced on the wire and the aperture fields are presented.

- VI. 9-8 TRANSITION RADIATION AT A DIFFUSE DIELECTRIC INTERFACE. K. F. Casey, Department of Electrical Engineering, Kansas State University, Manhattan, Kansas, 66506

When a charged particle moves in a continuously or discontinuously inhomogeneous medium, transition radiation is emitted. Cerenkov radiation is also produced if the particle moves in or near a region in which the phase speed of light is less than

the speed of the particle. In this paper we consider the Cerenkov and transition radiation produced when a charged particle passes through an inhomogeneous layer separating two semi-infinite homogeneous media.

It is found that the transition-radiation field consists of two components. The first, which dominates the low-frequency behavior of the field, is a spherical wave centered at the point of first impact on the inhomogeneous layer. This is the only contribution to the transition-radiation field present when the interface between the homogeneous media is abrupt. The second component of the transition-radiation field is a family of cylindrical waves resulting from the transition-radiation modes of the inhomogeneous layer which are refracted into the homogeneous media. At high frequencies or at early times, this component dominates the total field.

If the particle speed exceeds the speed of light in any of the three regions, then Cerenkov radiation will also be present in addition to the transition radiation components.

COMMISSION VI

0900 Wednesday, June 4

151 Physics

Session VI-10 (Joint AP-S 17)

RAY TECHNIQUES IN ELECTROMAGNETICS -  
A STATE OF THE ART REVIEW

Organizers: S. W. Lee and R. Mittra, University of Illinois  
Chairman: P. L. E. Uslenghi, University of Illinois

A. Invited Papers

- 17-1. INTRODUCTION TO RAY TECHNIQUES  
(0900) G. A. Deschamps, University of Illinois
- 17-2. A UNIFORM GEOMETRICAL THEORY OF DIFFRACTION  
(0918) FOR AN EDGE IN A PERFECTLY CONDUCTING SURFACE  
R. G. Kouyoumjian, Ohio State University
- 17-3. A UNIFORM ASYMPTOTIC THEORY OF DIFFRACTION  
(0936) J. Boersma, Technical University of Eindhoven
- 17-4. PHYSICAL THEORY OF DIFFRACTION  
(0954) K. M. Mitzner, Northrop Corporation
- 17-5. THE EQUIVALENT CURRENT METHOD  
(1012) T. B. A. Senior, The University of Michigan
- (1030) COFFEE BREAK

B. Discussion

Chairman: L. B. Felsen, Polytechnic  
Institute of New York

(1100)

COMMISSION VI

1400 Wednesday, June 4

151 Physics

Session VI-11 (Joint AP-S 19)

A. ELECTROMAGNETIC PULSE AND RELATED TOPICS:  
SOURCE REGION

Organizer: C. E. Baum, Air Force Weapons Lab  
Chairman: F. Tesche, Science Applications, Inc.

- 19-1. ELECTROMAGNETIC PULSE GENERATED BY  
(1400) NUCLEAR EXPLOSIONS (Invited Paper)  
C. L. Longmire, Mission Research Corp.
- 19-2. EMP GENERATION NEAR OBJECTS WITH CYLINDRICAL  
(1430) SYMMETRY IN THE SOURCE REGION  
T. C. Mo, R & D Associates
- 19-3. A SIMPLE WAY OF SOLVING TRANSIENT THIN-WIRE PROBLEMS  
(1445) L. Marin and T. K. Liu, The Dikewood Corporation
- 19-4. TRANSIENT RESPONSE OF A THIN WIRE EXCITED  
(1500) BY A MOVING CHARGED PARTICLE  
T. K. Liu, L. Marin, and K. S. H. Lee,  
The Dikewood Corporation
- 19-5. REFLECTION OF PULSES AT OBLIQUE INCIDENCE  
(1515) FROM STRATIFIED DISPERSIVE MEDIA  
K. Sivaprasad and N. N. Susungi,  
University of New Hampshire
- (1530) COFFEE BREAK

B. ELECTROMAGNETIC PULSE AND RELATED TOPICS:  
NON-SOURCE REGION

Chairman: A. Poggio, Lawrence Livermore Laboratory

- 19-6. USE OF SINGULARITIES IN THE COMPLEX PLANE AND  
(1600) EIGENVALUES OF INTEGRAL EQUATIONS FOR TRANSIENT  
AND BROADBAND ELECTROMAGNETIC ANALYSIS AND  
SYNTHESIS (Invited Paper)  
C. E. Baum, Air Force Weapons Laboratory
- 19-7. TRANSIENT SOLUTION OF ANTENNAS WITH  
(1630) NONLINEAR LOADS USING FREQUENCY DOMAIN DATA  
F. M. Tesche, Science Applications, Inc., and  
T. K. Liu, The Dikewood Corporation

19-8. THEORETICAL AND EXPERIMENTAL INVESTIGATION OF THE  
(1645) IMPULSE RESPONSE OF A CYLINDRICAL SHIELD  
W. Croisant and D. J. Leverenz,  
U.S. Army Construction Engineering Laboratory; and  
J. T. Verdeyen, University of Illinois

19-9. ANALYSIS OF TRANSIENT RADIATION FROM AN ELECTRIC  
(1700) DIPOLE IN A SPHERICAL CAVITY IN A MEDIUM  
R. J. Pogorzelski, R. D. Nevels, and D. R. Wilton,  
University of Mississippi

(1900) COCKTAIL AND DINNER

(2030) C. PANEL ON FUTURE DIRECTIONS IN TRANSIENT AND  
BROADBAND ELECTROMAGNETICS

Chairman: C. E. Baum, Air Force Weapons Laboratory

Panelists:

C. L. Bennett, Sperry Research Center  
R. F. Harrington, Syracuse University  
E. Miller, Lawrence Livermore Laboratory  
R. Mittra, University of Illinois  
F. M. Tesche, Science Applications, Inc.  
D. Wilton, University of Mississippi

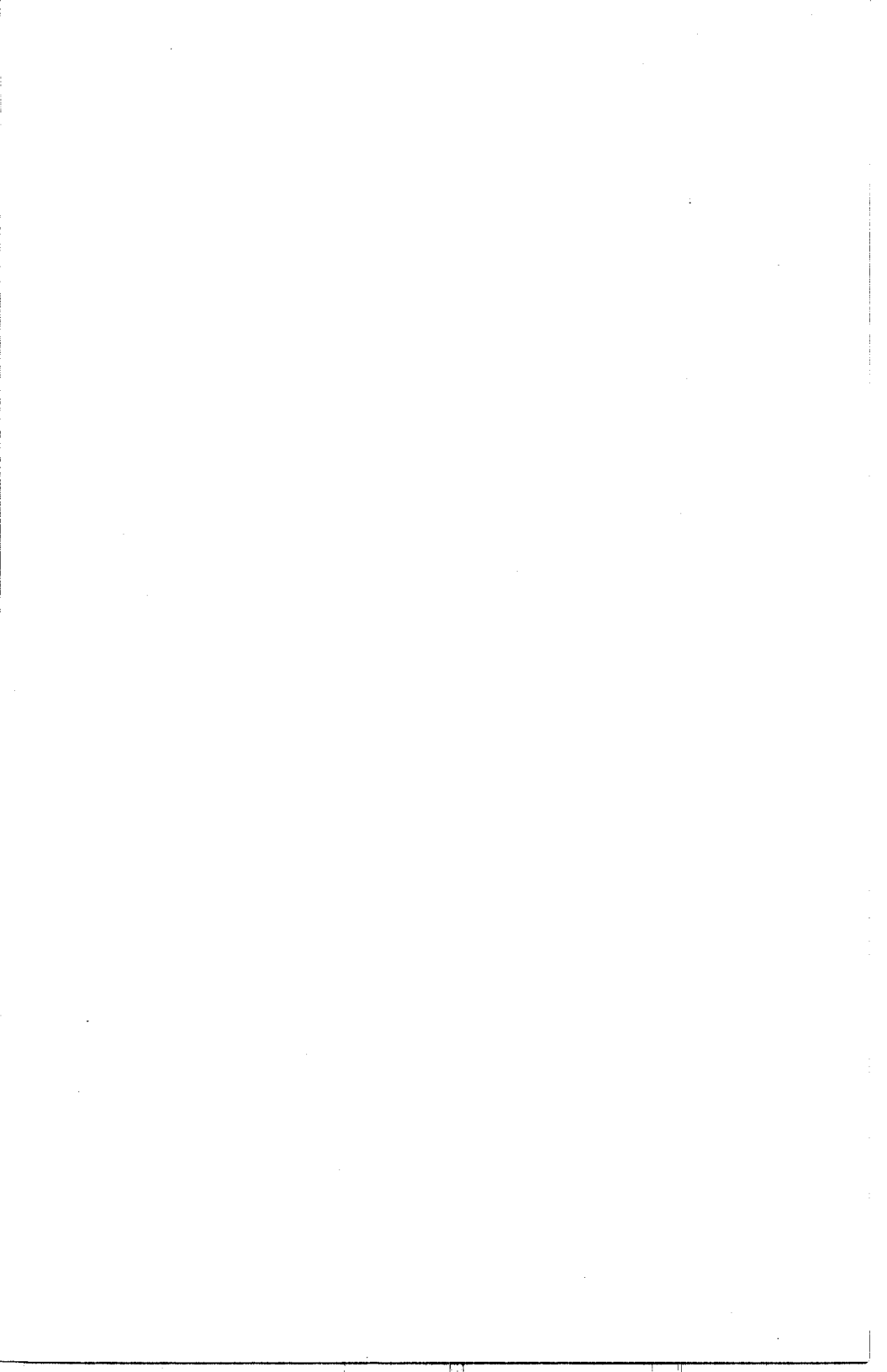
AUTHOR INDEX

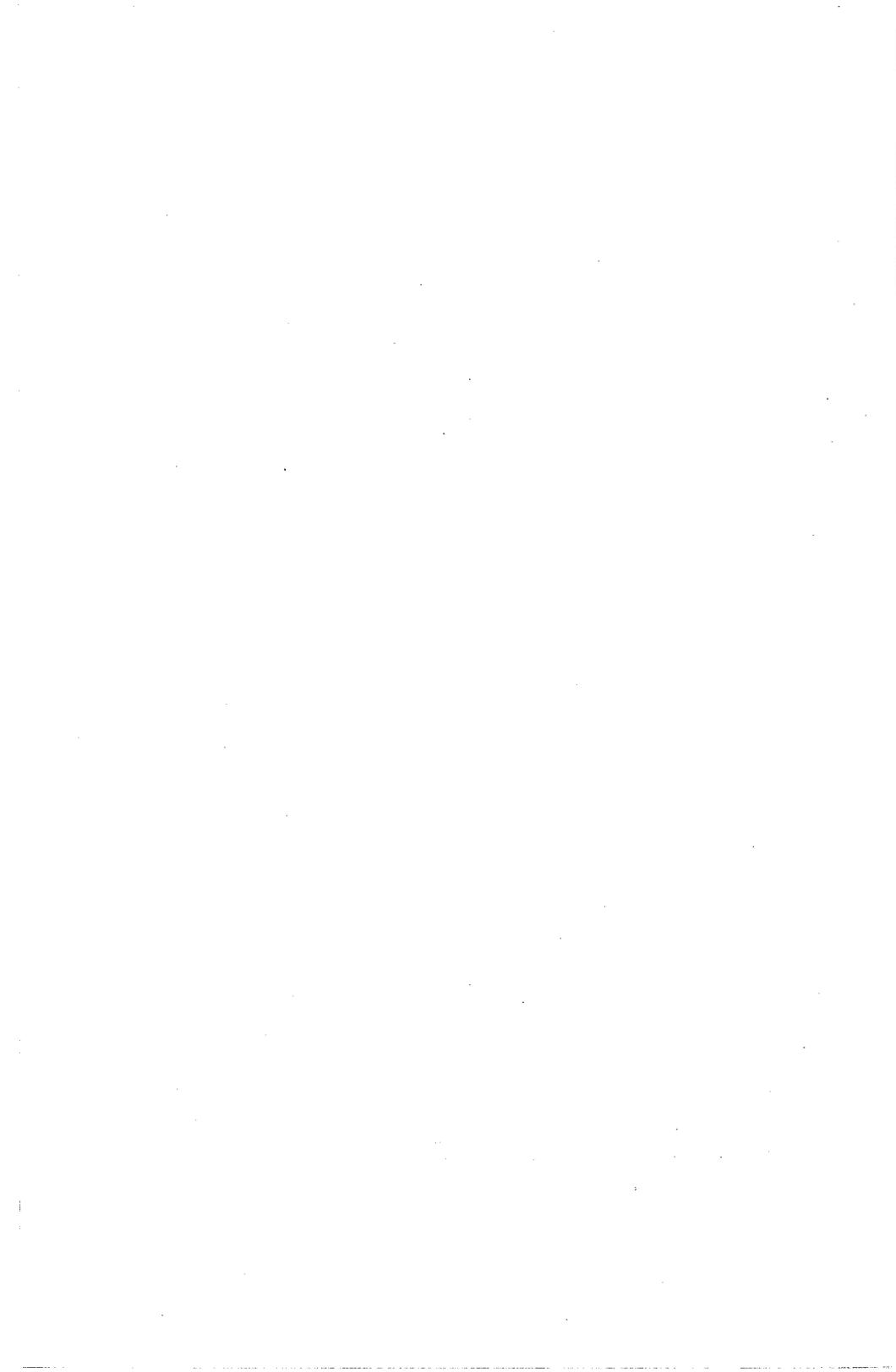
Aarons, J.	49	Chang, D. C.	63
Adams, R. W.	96	Chang, H-T	8
Ahn, S.	41	Chang, Y.	87
Alexopoulos, N. G.	61	Chen, C. A.	94
Allan, L. E.	30	Chen, K. M.	99,102
Allis, J. W.	29,101	Cheng, D. K.	94
Altshuler, E. E.	32	Cheung, A. Y.	100
Ament, W. S.	12	Christian, J. R.	4
Anderson, D. N.	46	Chu, R-S	14
Assis, M. S.	32	Chuang, C. W.	67
Baird, R. C.	5	Claassen, J. P.	19
Barrick, D. E.	19	Clifford, S. F.	23
Batlivala, P. P.	24	Coleman, P. D.	3
Baum, C. E.	108,111,112	Cooper, L. J.	5
Beal, J. C.	4	Cooper, W. K.	33
Beard, C. I.	22	Corcoran, V. J.	3
Bell, R. L.	41	Cramer, P.	86
Bennett, C. L.	105,112	Crawford, F. W.	48
Besieris, I. M.	15	Croisant, W.	112
Bevensee, R. M.	93	Curtis, W. L.	107
Bibl, K.	52	Dass, S. C.	4
Birnbaum, George	2	Davies, K.	45,46
Blackburn, R. F.	70	Davis, W. A.	97
Blair, M. J.	99	Daywitt, W. C.	5
Boerner, W. M.	23	Deadrick, F. J.	67,69
Boersma, J.	110	Dean, L. B.	22,92
Borth, D.	103	DeGauque, P.	11
Bostian, C. W.	30,34	Deschamps, G. A.	110
Bowden, C. M.	3	DeTemple, T. A.	3
Bowhill, S. A.	42,51	Dinger, R.	4
Brockman, C. L.	61	Donnelly, R. F.	46
Brown, A. C.	79	Dudley, D. G.	105
Brown, F.	3	Duff, B. M.	4,5
Brown, G. S.	17	Earnshaw, K. B.	23
Bui-Hai, N.	59	Einloft, C. M.	32
Bush, T. F.	25	Elder, J. A.	101
Butler, C. M.	97	English, W. J.	4
Cain, C.	103	Esposito, F. J.	73
Cain, F. L.	79	Fang, D. J.	35
Carter, J. M.	107	Fannin, B. M.	34
Carver, K. R.	20,33	Fante, R. L.	12
Casey, K. F.	79,108	Felsen, L. B.	56,110
Cauterman, M.	11	Fich, S.	4
Cetas, T. C.	63	Findlay, J. W.	5
Chan, K. K.	56		

Fitzjarrald, D. E.	26	Horie, K.	4
Fritz, R. B.	45,46	Hudson, H. G.	67,69
Fung, A. K.	19	Hules, F. T.	24
Furuhama, Y.	14	Hwang, Y. M.	57
		Hyde, G.	35,37
Gabillard, R.	11		
Galindo, V.	73	Ippolito, L. J.	30,34
Gallagher, J.	3	Ishimaru, A.	64
Gans, M. J.	82	Iskander, M. F.	92
Gardner, C. S.	12,65	Itoh, K.	81
Gassend, M. L. A.	23	Itoh, T.	62,83
Geller, M. A.	42,52		
Georges, T. M.	27	Janes, D. E.	29
Gillespie, E. S.	4	Jensen, D. R.	27,28
Goldhirsh, J.	31	Jeong, T. H.	1
Goldstein, J.	4	Jones, J. E.	45
Goubau, G.	4	Jordan, A. K.	41
Govind, S.	93	Jordan, E. C.	1
Gray, D. A.	30	Johnson, C. C.	99
Greene, G. E.	27	Johnson, R. C.	4
Grimoud, J.	11		
Grody, N. C.	32	Kanda, M.	5
Grossi, M. D.	8	Kantor, G.	99
Grubb, R. N.	46	Kasevich, R. S.	5
Gruner, R. W.	4	Katz, I.	6,16,22
Guru, B. S.	102	Kaul, A.	36
Gustafson, T. K.	3	Kay, I.	18
		Kellogg, R. B.	102
Haddad, Hussain	63	Kelso, J. M.	40
Hall, F. F.	26	Kim, H.	48
Hamid, M. A. K.	84,92	King, J. L.	37
Harker, K. J.	48	King, R. W. P.	1,87,97
Harrington, R. F.	87,112	Klein, C. A.	94
Harris, C.	5	Klobuchar, J. A.	47
Harris, J. M.	35	Ko, W. L.	57,58
Hartmann, G.K.	45,46	Konrad, T. G.	28
Hess, D. W.	4	Kouyoumjian, R. G.	57,110
Hess, G. C.	42	Ksienski, A. A.	54
Hessel, A.	56,76	Kunz, K. S.	89
Hieronymus, R. M.	105		
Hill, D. A.	7	Lachs, G.	65
Hodge, D. B.	36	Lager, D. L.	7,25,95
Hodges, D. T.	3	LaGrone, A. H.	7
Hollis, J. M.	5	Lai, H. H.	75
Hong, S. T.	64	Lai, T. K.	77
Hongo, K.	76,83	Laine, E. F.	7
Hood, C. G.	41	Lam, P. C.	12
Hooke, W. H.	27	Landt, J. A.	67,69
Hoopingarner, R.	102	Lang, R. H.	13

Laxpati, S.	65	Pappert, R. A.	10
Lee, K. S. H.	111	Parhami, P.	40
Lee, S. W.	110	Paris, J. F.	33
Leitinger, R.	46	Paul, A.	43
Lerfald, G. M.	23	Paul, A. K.	46
Leverenz, D. J.	112	Payne, J. M.	5
Lewis, C. A.	77	Pearson, L. W.	69
Lin, H. C.	77	Pfister, W.	52
Lin, J-L	106	Plant, W. J.	17
Lin, J. C.	104	Plonus, M. A.	60
Little, J. K.	108	Poggio, A. J.	67,96,111
Liu, C. H.	45,48	Pogorzelski, R. J.	112
Liu, T. K.	106,111	Poletti-Liuzzi, D. A.	45
Liu, Y-P	108	Polk, C.	43
Locus, S. S.	60	Prewitt, J. O.	97
Longmire, C. L.	111		
Lugovoy, A. V.	84	Quarato, J. A.	65
Lytle, R. J.	7,25,95		
		Rahmat-Samii, Y.	57,58
MacPhie, R. H.	82	Rao, N. N.	40
Maley, S. W.	10,63	Rao, T. C. K.	84
Manus, E. A.	30	Rastogi, P. K.	51
Marin, L.	106,111	Reinisch, B. W.	52
Marshall, R. E.	30	Reitz, J. R.	1
Matsumoto, T.	81	Renken, G. W.	78
Maxam, G. L.	107	Richards, P. L.	3
Mayer, P. A.	41	Richter, J. H.	27
McCormick, G. C.	30	Rocke, A. F. L.	5
Mechtly, E. A.	48	Ross, D. B.	42
Merrill, J. T.	27	Rouse, J. W.	26
Mink, J. W.	5	Rozzi, T. E.	88
Miller, E. K.	67,69,95,96,112	Rusch, W. V. T.	86
Miller, K. L.	51	Ryan, C. E.	79
Mittra, R.	12,57,58,62, 69,94,110,112	Safavi-Naini, S.	83
		Schaubert, D. H.	71
Mitzner, K. M.	60,110	Schmidt, G.	46
Mo, T. C.	111	Schödel, J. P.	45
Moffatt, D. L.	67	Schroeder, K. G.	81
Morland, D. K.	23	Schuler, D. L.	16
Moseley, B.	36	Schwartzman, L.	73
Mostafavi, M.	62	Scott, M. A.	75
		Seidler, W. A.	53
Naito, Y.	4	Seliga, T. A.	45
Nelson, R. F.	13	Semplak, R. A.	82
Neuder, S. M.	102	Senior, T. B. A.	56,110
Nevels, R. D.	112	Shmoys, J.	56
Newell, A. C.	4,5	Sindoris, A. R.	71
Noonkester, V. R.	28	Singaraju, B. K.	89,108
Nyquist, D. P.	75,99	Singarayar, S.	4,5

Sivaprasad, K.	50,111	Weber, R. L.	19
Smith, E. K.	40,51	Weeks, W. L.	71
Smith, L. G.	51,52	Wetzel, L.	9
Solman, F. J.	71	Wiley, P. H.	30
Sologub, V. G.	84	Williams, R.	60
Stangel, J. J.	73	Wilton, D.	93,112
Stankov, B.	27	Wratt, D. S.	51
Stark, W. J.	70,73	Wu, C-L	104
Stein, J.	37	Wu, T. K.	95
Steinhorn, J.	36,37		
Stoyer, C. H.	8	Yaghjian, A. D.	5
Straiton, A. W.	34	Yeh, C.	62
Stutzman, W. L.	30	Yeh, K. C.	45,48
Susungi, N. N.	111	Yildiz, M.	50
Swicord, M. L.	99	Youakim, M. Y.	45
Swift, R.	50		
Swift, W. D.	108	Zrnic, D. S.	24
Tai, C. T.	86		
Tamir, T.	14		
Taur, R. R.	49		
Taylor, C. D.	70		
Telford, L. E.	32		
Tesche, F.	111,112		
Theobald, D. M.	36		
Thiele, G.	93		
Thomas, D. T.	74		
Toman, K.	43		
Tou, C. P.	42		
Tsai, L. L.	95		
Ulaby, F. T.	24,25		
Uslenghi, P. L. E.	110		
Valentino, P. A.	73		
Vandament, C. H.	41		
Verdeyen, J. T.	112		
Vincent, M. L.	107		
Vogel, W.	34		
Voss, H. D.	52		
Wagner, N. K.	34		
Wait, J. R.	1,7,8		
Walsh, E. J.	20		
Wang, S. S.	76		
Wang, T-i	23		
Ward, T. R.	101		
Watanabe, R.	81		













*1975 USNC/URSI ANNUAL MEETING  
October 20-23, 1975  
University of Colorado  
Boulder, Colorado*

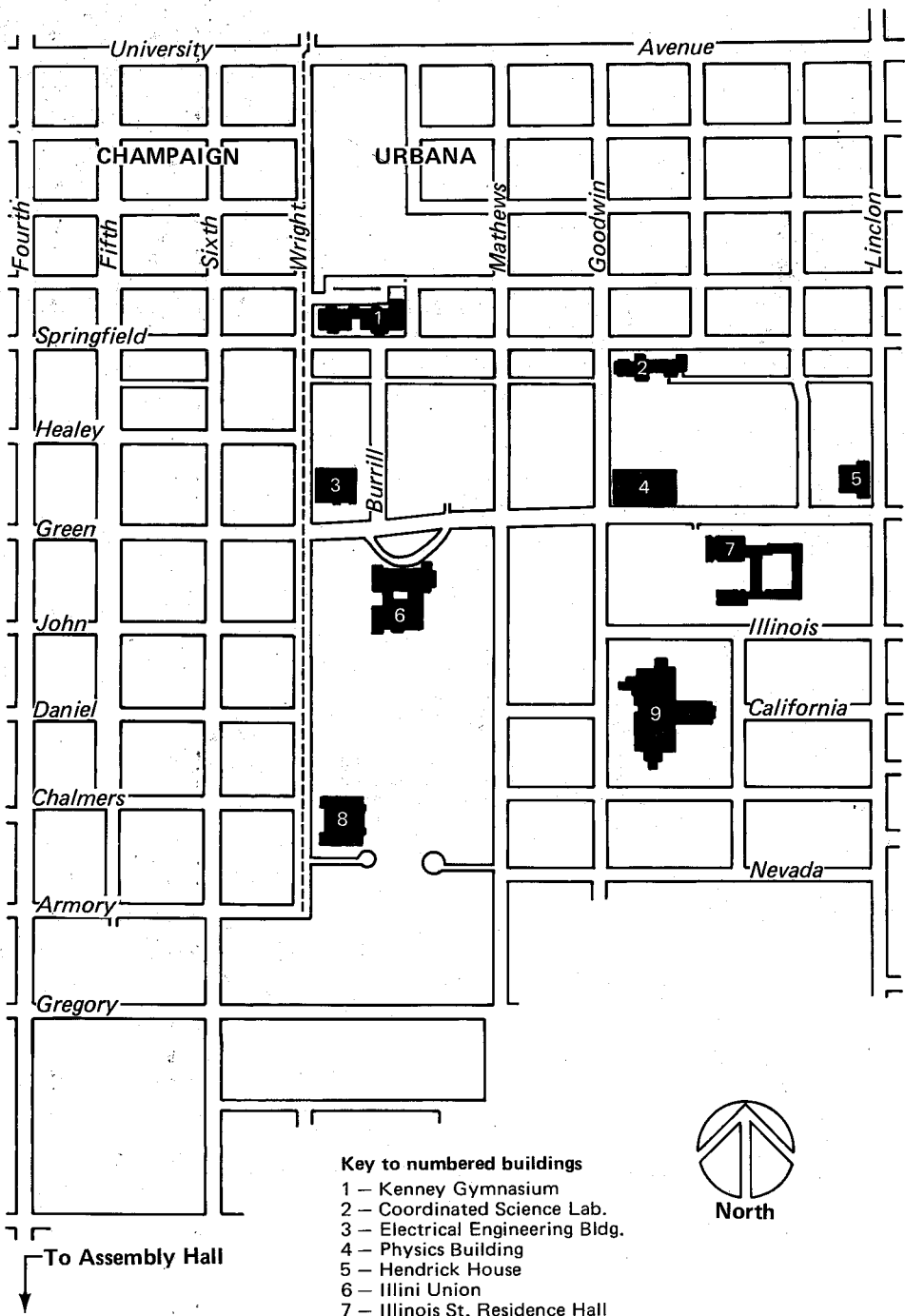
For information contact:

Richard Y. Dow  
National Academy of Sciences  
2101 Constitution Avenue  
Washington, D. C. 20418

*1976 INTERNATIONAL IEEE/AP-S SYMPOSIUM AND  
USNC/URSI MEETING  
October 10-15, 1976  
University of Massachusetts  
Amherst, Massachusetts*

For information contact:

Robert E. McIntosh  
Dept. of Electrical Engineering  
University of Massachusetts  
Amherst, Massachusetts 01002



**Key to numbered buildings**

- 1 – Kenney Gymnasium
- 2 – Coordinated Science Lab.
- 3 – Electrical Engineering Bldg.
- 4 – Physics Building
- 5 – Hendrick House
- 6 – Illini Union
- 7 – Illinois St. Residence Hall
- 8 – Lincoln Hall
- 9 – Krannert Center



**To Assembly Hall**